FACULTEIT INDUSTRIELE INGENIEURSWETENSCHAPPEN

CAMPUS GROUP T

Feasibility study of an additive manufactured support structure using the principles of topology optimization

Jelle VANTON
Michiel VLAEYEN

Promotor: Prof. dr. ir. Dewulf Wim

Co-promotoren: Ing. Jef Loenders
Ir. Fernand Vandeput
Ing. Koen Huybrechts

Masterproef ingediend tot het behalen van de graad van master of Science in de industriële wetenschappen: elektromechanica

Academiejaar 2016-2017

FOREWORD

First, we would like to thank the company S.A.B.C.A. and in particular our advisor ir. Fernand Vandeput to provide the subject and the knowledge throughout this Master's thesis. We are very grateful to him and the company to finance the designed topology optimized structure.

We would also like to thank ing. Koen Huybrechts from 3D Systems for the input about the production capabilities of selective laser melting. Without his passionate participation, the production of the support structure could not have been successfully conducted.

We would also like to acknowledge ing. Jef Loenders of KU Leuven to guide and support us during the whole thesis. The door to him was always open whenever we ran into a trouble spot. He steered us in the right direction whenever he thought we needed it.

Finally, we must express our very profound gratitude to our families and friends for their unfailing support and continuous encouragement during our years of study and through the process of researching and writing this thesis. This accomplishment would not have been possible without them. Thank you.

Jelle Vanton
Michiel Vlaeyen

ABSTRACT

The aim of this thesis is to investigate the feasibility of additive manufacturing as a manufacturing method for system support brackets in the aircraft industry. A technology demonstrator is produced by selective laser melting and designed using the principles of topology optimization. Finite element method is used to validate the outcome of the topology optimization.

The thesis proves that additive manufacturing can compete with the conventional methods from a mechanical perspective. The possiblities of additive manufacturing from an economic point of view are investigated with a trade-off study. The break-even analysis of the system support bracket calculates the situation when additive manufacturing is profitable.

The thesis points out that the question of whether additive manufacturing is more profitable than conventional methods, depends on the fuel price and consumption. The requirements for obtaining a profitable system support structure are also listed.

Key words: finite element method, selective laser melting, technology demonstrator, topology optimization, trade-off study

EXTENDED ABSTRACT

Additive manufacturing wordt reeds in vele uiteenlopende industrieën toegepast. In de commerciële luchtvaart is deze productiemethode echter nog weinig gebruikt. Vliegtuigfabrikanten onderzoeken de mogelijkheden om additive manufacturing toe te passen bij de productie van onderdelen. In dit kader is de thesis gevoerd. De thesis omvat het ontwerpen, het testen en een trade-off studie van een draagstructuur.

De thesis onderzoekt de haalbaarheid van additive manufacturing als productiemethode voor een draagstructuur in vliegtuigen. De structuur bevestigt elektrische kabels, brandstofpijpen, afsluitventielen en het bijhorend verdeelstuk aan het vliegtuig. De huidige structuur wordt geproduceerd met behulp van verschillende productietechnieken zoals frezen, vormgieten, smeden en plaatbewerkingen. Elk van deze technieken heeft zijn eigen beperkingen. Vormgieten heeft een hoge productiekost voor kleine oplages. Frezen brengt beperkingen in vormvrijheid mee en metalen platen kunnen slechts op een aantal manieren gevouwen worden. Additive manufacturing heeft deze beperkingen niet. Om deze reden heeft de vliegtuigindustrie interesse om complexe onderdelen te produceren met additive manufacturing.

De productiemethode voor de system support structure is selective laser melting. Selective laser melting is een additive manufacturing techniek waarbij een laser fijn metaalpoeder laagsgewijs aan elkaar smelt. Het gebruikte metaalpoeder is AlSi10Mg. Dit is één van de weinige beschikbare metaalpoeders waarmee selective laser melting kan uitgevoerd worden. Een nadeel van deze laagsgewijze productie zijn de anisotrope materiaaleigenschappen van het as-built geprinte materiaal. De materiaaleigenschappen hiervan zijn van mindere kwaliteit in vergelijking met wanneer conventionele technieken, zoals smeden, zouden gebruikt worden. Een ander nadeel is de noodzakelijkheid van ondersteuning voor overhangende elementen van het geprinte materiaal. In tegenstelling tot vormgieten heeft additive manufacturing geen mal nodig. Dit maakt de productie van kleine oplages goedkoper. Een ander voordeel is de vormvrijheid. Vrijwel elke vorm kan geproduceerd worden. Dit is niet het geval bij conventionele technieken. Deze vormvrijheid maakt additive manufacturing uitermate geschikt voor een topologische optimalisatie.

Topologische optimalisatie is de wiskundige theorie om de beste verdeling van materiaal in een beschikbaar volume te vinden. Software berekent de lichtste structuur aan de hand van gegeven belastingen en inklemmingen. De principes van topologische optimalisatie worden toegepast om een technologie demonstrator te ontwerpen. Deze demonstrator toont de mogelijkheden van additive manufacturing en topologische optimalisatie.

Om de topologische optimalisatie uit te voeren, is een ontwerpcyclus doorlopen. Dit is een iteratief proces.

De eerste stap is het bepalen van de vrije ruimte. Hierbij wordt de ruimte bepaald die de structuur mag innemen. Brandstofleidingen en andere aanwezige componenten mogen geen deel uitmaken van deze ruimte. Ook blindklinknagels, losse moeren en bouten worden uit de vrije ruimte verwijderd. De volledige vrije ruimte kan pas bepaald worden na enkele iteraties waarbij de optimale structuur berekend wordt.

In de volgende stap wordt een eindige elementen model van de vrije ruimte gemaakt. De vrije ruimte wordt gemesht en de verbindingspunten van de structuur met het vliegtuig worden ingeklemd. De belastinggevallen worden aangelegd op de gemeshte ruimte. Er zijn acht mogelijke belastingsgevallen. Dit zijn de verschillende acceleratie-richtingen van de aan de structuur bevestigde componenten bij een crash.

Bij de stap 'optimalisatie model' worden de constraints en het objectief ingesteld. Het objectief is de minimalisatie van de massa van de technologie demonstrator. De ingevoerde constraints zijn: een minimale staafdiameter, een vereiste stijfheid en een maximale Von Mises-spanning gelijk aan de laagste elasticiteitsgrens van het anisotropisch materiaal AlSi10Mg.

Tijdens de vierde stap voert *Altair HyperWorks* de topologische optimalisatie uit aan de hand van de ingestelde parameters uit de vorige stap. Het resultaat hiervan is een ruwe structuur. De massa hiervan is 0,616kg. Deze structuur wordt gebruikt als input voor de volgende stap.

De vijfde stap is het verfijnen van de ruwe structuur. Omdat de ruwe structuur overgedimensioneerd is, zorgt de verfijning voor een gewichtsbesparing. De verfijnde structuur wordt aangepast aan de orientatie tijdens het printen. Samen met de volgende stap, de validatie, is deze stap iteratief doorlopen. De massa van de verfijnde structuur in de laatste iteratie bedraagt 0,189kg. Dit is een significante gewichtsbesparing ten opzichte van de oorspronkelijke structuur die een massa heeft van 0,380kg.

De validatie controleert of de bekomen structuur voldoet aan de vereisten. Tijdens een crash moeten de Von Mises-spanningen onder de 172MPa blijven. Bij installatie van de structuur wordt deze mogelijk vervormd. De ontstane spanningen moeten onder de 50MPa blijven. De natuurlijke frequentie van de structuur moet boven de 25Hz liggen. Aan de hand van een eindige elementen analyse wordt dit gecontroleerd. De bekomen structuur van 0,189kg voldoet aan al deze voorwaarden. Na de validatiestap is de technologie demonstrator klaar om geprint te worden. Er is aangetoond dat via additive manufacturing een structuur kan ontwikkeld worden die lichter is dan de originele structuur en voldoet aan alle eisen.

Na het ontwikkelen en testen van een draagstructuur wordt een trade-off gemaakt. De totale kostprijs om de topologisch geoptimaliseerde structuur te ontwerpen en te installeren bedraagt €3 078. Aan de hand van een break-even analyse wordt de winstgevendheid van de technologie demonstrator vergeleken met de originele structuur. De totale kost van de originele structuur is €610. Omwille van de hoge kostprijs van de topologisch geoptimaliseerde structuur, is er geen break-even. De geoptimaliseerde structuur is lichter en verbruikt daardoor minder brandstof dan de originele structuur. Uit deze studie blijkt dan ook dat de topologisch geoptimaliseerde structuur winstgevend is als de brandstofprijs stijgt en het vliegtuig minimaal 55,6% van zijn totale reikwijdte vliegt gedurende elke vluchtcyclus.

Deze thesis toont met de technologie demonstrator aan dat additive manufacturing mogelijkheden biedt aan de luchtvaartindustrie. Op mechanisch vlak heeft deze technologie geen problemen om te concurreren met de huidige technieken. Het overtreft de state of the art productiemethoden in het ontwikkelen van lichte structuren. Vanuit economisch perspectief is additive manufacturing nog niet rendabel voor de ontwikkelde draagstructuur. De productiekost van additive manufacturing is te hoog. Het is mogelijk om deze kost naar beneden te krijgen en de technologie wel rendabel te maken. In de toekomst kan met behulp van een betere productiviteit van de machine, een groter bouwplatform om meerdere stuks per cyclus te bouwen of een grotere laagdikte de productiekost dalen. Ook wanneer de stijgende brandstofprijzen in rekening worden gebracht, wordt additive manufacturing winstgevend. Onderzoek naar deze nieuwe toepassing is zeker de moeite en biedt toekomstperspectief voor producenten van vliegtuigonderdelen.

Key words: finite element method, selective laser melting, technology demonstrator, topology optimization, trade-off study

SUMMARY

LIST OF FIGURES

LIST OF SYMBOLS

k	stiffness	[N/m]
u	displacement vector	[m]
x	displacement	[m]
C	Compliance	[m/N]
E	Young's modulus	[GPa]
F	Force	[N]
G	Gravitational acceleration	[9,81m/s²]
K	Stiffness matrix	[N/m]
P	Penalization factor	[\ ]
U	Strain energy	[J]
V	Volume	[m³]
δ	displacement	[m]
ε	strain	[\ ]
ζ	move limit	[\ ]
η	tuning parameter	[\ ]
ρ_e	relative density of an element	[%]
σ	tensile stress	[MPa]
Ω	Design space	[m³]

LIST OF ABBREVIATIONS

AM	Additive manufacturing
CAD	Computer-aided design
FEM	Finite element method
MS	Military Standard
NAS	National Aerospace Standard
RBE	Rigid body element
S.A.B.C.A.	Société Anonyme Belge de Constructions Aéronautiques
SIMP	Solid Isotropic Material with Penalization
SLM	Selective laser melting

INTRODUCTION

The aim of this thesis is to investigate the feasibility of additive manufacturing (AM) as a manufacturing method for system support brackets in the aircraft industry. The system support bracket is a structural part located at the second fuel tank. The function of the bracket is to support two pressure relief valves, the manifold for these two valves as well as the fuel pipe and electric cables. This investigation includes the design, testing and producibility of a system support bracket. This additive manufactured structure, named 'spider', will serve as a technology demonstrator. This technology demonstrator exhibits the possibilities of AM to replace the current system support bracket. AM is already used in space and medical industry for the production of implants and dentures. Civil aircraft manufacturers are investigating AM since AM is not commercially available in aviation. One of this projects is the A320neo project of Airbus.

The current system support bracket is produced by various manufacturing techniques, such as: milling, investment casting, forgings and assemblies. Each of these techniques has its own limitations. Casting has a high tooling cost. Milling has limited shape possibilities. Metal plates can be folded in limited ways. AM overcomes these limitations. Little or no tooling is required after the production of the spider. Almost every shape is producible with AM. This property makes AM perfectly suitable for topology optimization because topology optimization doesn't take account of the production method used.

The system support bracket is designed using the principles of topology optimization. This technique is a mathematical theory for finding the best material distribution in a volume. The result of topology optimization is a spider with the lowest possible weight to withstand all the load cases. With topology optimization it is possible to create a lighter structure than the original one. *Altair HyperWorks* is the software to run the topology optimization to design the spider.

AM has also a downside. It imposes some design rules on the spider before it is producible. Overhanging elements need to be supported and sharp corners have to be round off. The AM method used to produce the technology demonstrator is selective laser melting (SLM). In the SLM process, a component is build up by layers of powder that are locally melted by a laser beam. After melting and solidification of a part of the powder in the layer, the base plate moves down the distance of one layer thickness and a new layer can be applied. This process repeats itself until the entire component is finished.

The mechanical properties of parts produced by AM are poor compared to some convential manufacturing methods, like forging. The strength of the spider obtained by topology optimization is tested with a finite element method. The results of the finite element method must meet a required limit. When the spider passes these tests, it proves to be strong enough to work in the required circumstances.

A trade-off study between the spider and the current system support bracket is made to complete the feasibility investigation. All the aspects of the total cost of the two system support structures are discussed and compared. A break-even analysis is included in the trade-off study. The conditions at which the spider is more profitable than the current system support structure are calculated. After this part the feasibility investigation is finished. A producible and profitable spider gives opportunities to the entry of AM into the aircraft industry.

1 DESIGN

The thesis consists of two parts. The first part of the thesis is the design of a system support structure of a business jet. This structure is designed with use of topology optimization. Subsequently the structure will be produced with the 3D printing technology: selective laser melting. This part gives the theory behind topology optimization and selective laser melting. Next the system support structure and accompanying requirements are described. The followed workflow for the design of the structure is explained and finally a finite element analysis is performed on the design to check all the requirements.

1.1 Topology optimization

Topology optimization is the design method for the system support structure. The theory behind this method is briefly described in the following part. An example of this theory is made with *Altair HyperWorks*, the software to carry out the topology optimization.

1.1.1 Theory

Topology optimization is the theory for finding the best distribution of material in a design space [1]. This method is used to find the optimal load path for a structure under certain boundary conditions and particular loads. The result of this method is a structure optimised for a given objective, like minimal mass, with given constraints, like maximal displacement or maximal stress. Bendsøe and Sigmund were the first to develop this theory and made it an interesting engineering tool. The following description of the theory of topology optimization is based on the work of Eschenauer [2], Bendsøe and Sigmund [3].

The domain of the design space of the structure is Ω and the volume is V. This volume is divided in different element volumes V_e with domain Ω_e. The formulation of the topology optimization is a minimization of the strain energy of the volume, U. To use this method the equations of linear elasticity theory are assumed. One of these equations is Hooke's law for stiffness. These law states that the tensile stress, σ, is equal to the strain, ε, multiplied by the Young's modulus, E.

$$\sigma = E\varepsilon$$

The compliance of a material, C, is the inverse of the Young's modulus. Now Hooke's law becomes:

$$\varepsilon = C\sigma$$

Another law of Hooke is the spring law. The force, F, on the structure is equal to the displacement, x, multiplied by the structure's stiffness k.

$$F = kx$$

It is important to notice that the linear elasticity theory assumes that isotropic material is used. This is not the case with the aluminium for SLM. Later is explained why isotropic material might be assumed. The strain energy can be formulated as following:

$$U = \frac{1}{2}u^T K u = \sum_{1}^{N} \frac{1}{2}\int_{V_e} \varepsilon_e^T E_e \varepsilon_e dV_e$$

$$U = \sum_{1}^{N} \frac{1}{2}\int_{V_e} \sigma_e^T C_e \sigma_e dV_e$$

With u the displacement vector and K the stiffness matrix of the volume. The volume consists out of N different elements with each its own volume, V_e. The stress and strain on an element are denoted by ε_e and σ_e. E_e and C_e are the element elasticity and compliance matrices. This expression for the strain energy is subject to:

$$\sum_{i=1}^{N} \rho_i V_i \leq V$$

$$\rho_i = \begin{cases} 1\ if\ \Omega_i \in \Omega \\ 0\ if\ \ \Omega_i \in \mathbb{R}^3 \backslash \Omega \end{cases}$$

The relative density of an element is ρ_e. If the compliance is function of the relative density, then the relative density is the only variable of the problem. This can also be done for the stiffness and elasticity matrix of an element.

$$C_e = \rho_e C$$

The total compliance of a structure is C. Now the relative density is the only variable. The problem with this relative density distribution is that the variable of an element is zero or one. This will lead to mathematical problems. The result of such an optimization will look like a checkerboard and is visible in Figure 1-1b. To avoid this, intermediate values need to be introduced. This is done by a penalization method. The method used by *Altair HyperWorks* is confidential, instead the solid isotropic material with penalization (SIMP) method is discussed.

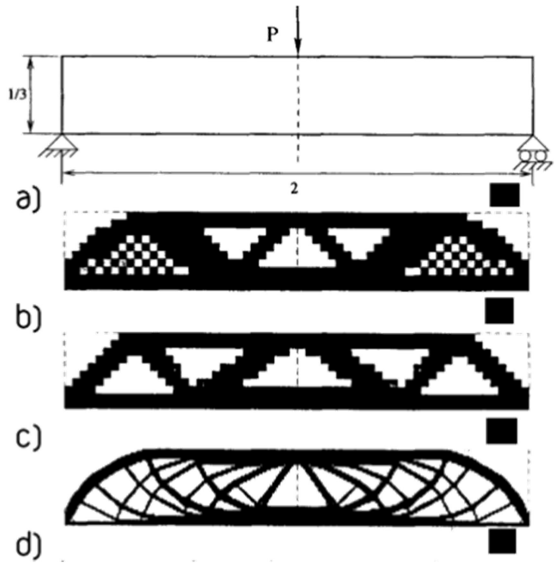

Figure 1-1: a) Design space b) Checkerboard c) SIMP solution with 600 elements d) SIMP solution with 5400 elements

SIMP is the most frequently used penalization method. A penalization factor, P, is used to generate values closer to zero or one. This reduces the computational efficiency and eases to integrate it in software. A greater penalization factor will bring the values closer to zero or one. This is shown in Figure 1-2.

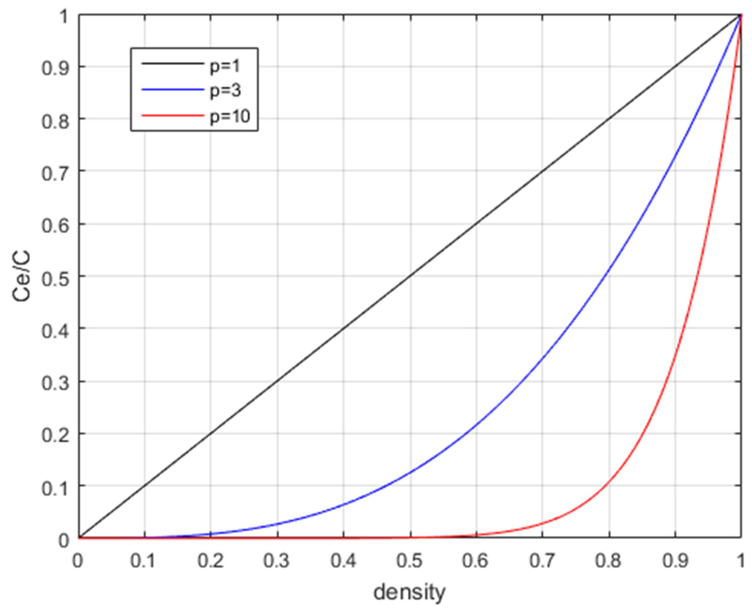

Figure 1-2: Influence of penalization factor

Usually a value greater than three is required as penalization factor. The compliance in function of the relative density becomes:

$$C_e = \rho_e^P C$$

It is important to know how the relative density is determined. Theoretically the relative density lies between zero and one. But a value of zero gives problems with singularities. Therefore a small minimal value for the relative density is introduced, ρ_{min}. Typically this value is 10^{-3}. The update scheme for the relative density after each step is given by:

$$\rho_{K+1} = \begin{cases} max\{(1-\zeta)\rho_K, \rho_{min}\} & if \quad \rho_K B_K^\eta \leq max\{(1-\zeta)\rho_K, \rho_{min}\} \\ min\{(1+\zeta)\rho_K, 1\} & if \quad min\{(1+\zeta)\rho_K, 1\} \leq \rho_K B_K^\eta \\ \rho_K B_K^\eta & otherwise \end{cases}$$

ρ_K is the relative density after step K. B_K is given by the expression:

$$B_K = \Lambda_K^{-1} p\rho(x)^{p-1} E_{ijkl}^0 \epsilon_{ij}(u_K)\epsilon_{kl}(u_K)$$

In this expression u_K is the displacement field at iteration step K. The variable η is a tuning parameter and ζ is a move limit. These values are commonly chosen to be respectively 0,5 and 0,2. Λ_K is a Lagrange multiplier for intermediate densities, ρ, between ρ_{min} and 1.

When $B_K = 1$, a local optimum is reached. This occurs when the strain energy of an element is equal to Λ. This element of the structure will not be modified. Material is added to a place where B_K is greater than one and removed when B_K is smaller than one. Regions with a low specific strain energy have a low relative density. A high relative density occurs when an element has high specific strain energy. The topology optimized structure consists of elements with a high relative density.

1.1.2 Example

A thin plate with an incision is subjected to two opposed forces. The objective of the topology optimization is to design a clip with a minimized mass. The constraints are displacement constraints. The places where the forces are applied, may move maximally a certain distance in the direction of the force. This load case is shown in Figure 1-3.

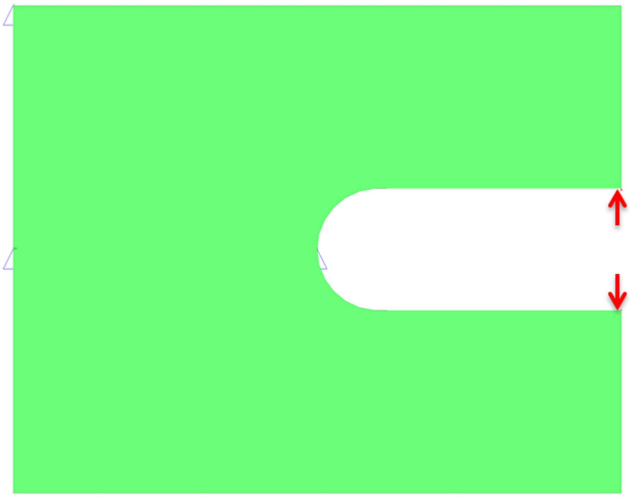

Figure 1-3: Load case of the thin plate

The results of the topology optimization are shown in Figure 1-4. After each iteration, the final solution becomes more visible. The iteration process stops when a constraint is met and when the total B_K is one. On the right side of Figure 1-4 the optimized structure is shown. It is possible that this solution still needs to be modified. This takes places in the post-processing. The post-processing will be discussed later.

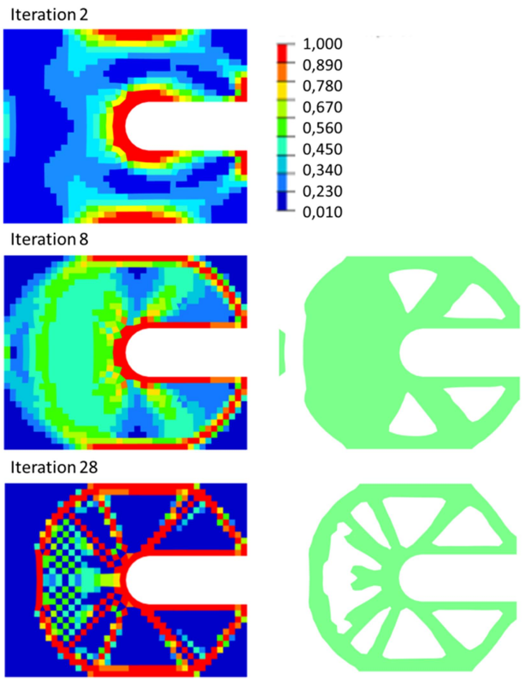

Figure 1-4: Left) The distribution of the relative densities Right) The optimized structure with densities above 0,3

1.2 Selective laser melting

Selective laser melting or SLM is an additive manufacturing (AM) process that allows the production of components with functionalities beyond the capabilities of any existing conventional technology. Complicated 3D-objects are produced using 2D cross sectional layer data as shown in Figure 1-5. [1, 4]

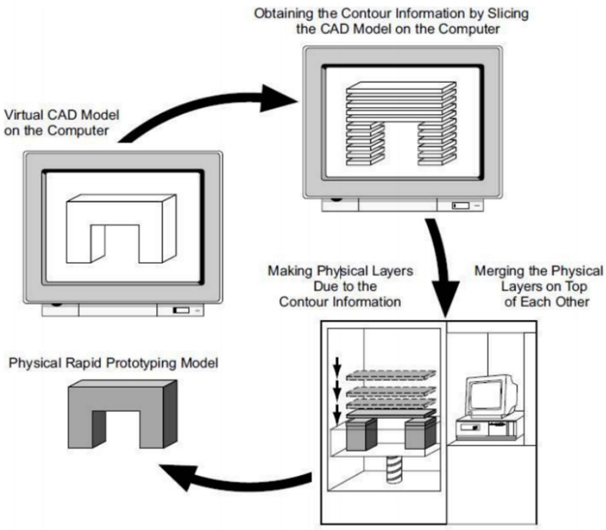

Figure 1-5: Topology optimization workflow

Abovementioned reasons make selective laser melting the suitable method for the production of topologically optimized parts. Where these parts formerly had to be assembled using conventional methods, they can now be made in a single piece. The SLM technique is therefore used in aerospace, medical and other high-technology industries.

In the SLM process, a component is build up by layers of powder that are locally melted by a laser beam. After melting and solidification of a part of the powder in the layer, the base plate moves down the distance of one layer thickness (20µm-100µm) in the z-direction. Now a new layer can be applied. This process repeats itself until the entire component is finished. The setup for an SLM process is indicated in Figure 1-6. [5]

Crucial parameters in the SLM-process are laser scanning speed, laser power, layer thickness and hatching distance. In order to fully melt the metal powder, the amount of energy produced by the laser, taking into account distance and speed, should be equal to the energy density for the specific processed material. [6]

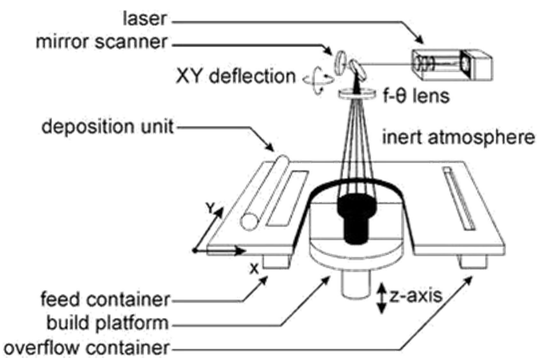

Figure 1-6: Selective laser melting

Sometimes the component needs to be supported by another structure (support structure) during the SLM process. Support structures are waste of material because they are removed after the process. Since the cost of transferring a material in powder form is rather high, it is important to reduce the amount of waste. Furthermore the support structures affect the tolerance errors and surface roughness. After the process, these support structures have to be removed either manually or with removal techniques like wire cutting. The powder that is not melted, can be recycled.

Although selective laser melting can produce very complex products, there are some design constraints. The first and most important design constraint is the orientation. A proper orientation will reduce the amount of waste and therefore the total cost of the final product. Software programs can determine the optimal orientation.

Even when the best possible orientation is chosen, there may still be a need for supports. They are used when there are overhanging elements or holes present in the structure. Overhanging elements need support below a certain α-angle. This angle is visible in Figure 1-7 [6]. If the angle is higher than 45°, no supports are needed.

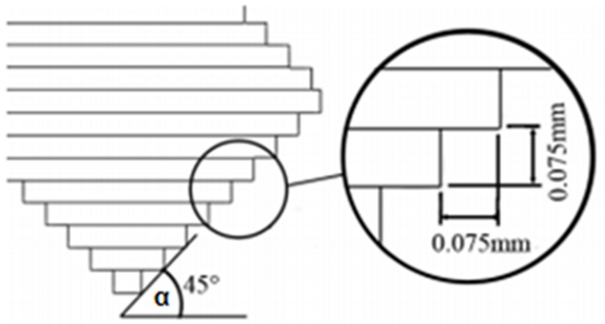

Figure 1-7: Influence of the angle on the amount of support structures needed

Stress concentrations by sudden geometrical changes in the workpiece must always be avoided. Therefore convex and concave fillets are used. The higher the ratio of the fillet, the greater the likelihood of curl. This is because the number of layers between the smallest angle and the self-supporting angle increases. Figure 1-8 shows the influence of the radius of fillets. [6]

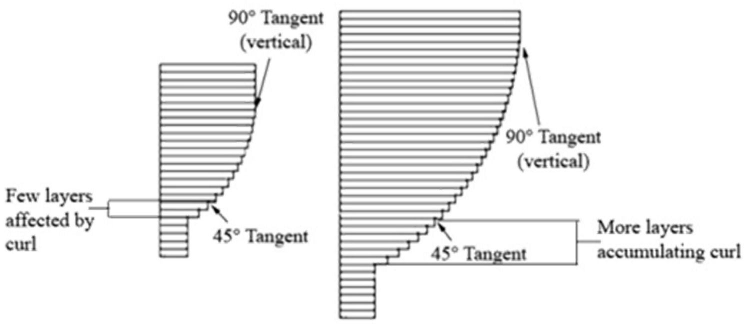

Figure 1-8: Influence of the fillet radius and chamfers on the amount of support structures needed

The non-design and the design space are connected using fillets. The transition is as gradually as possible to minimize the risk of stress concentrations. Special attention should be paid to the fixed clamping because the highest stresses are already naturally present here.

The main advantage of the SLM technique is the possibility of producing very complex products. Designers can search for the optimal solution without having to take too much account of the limitations of the production technique. Shapes and curvatures that cannot be carried out by conventional techniques are possible with the SLM-technique.

A disadvantage of the technique is that it is rather slow for large volume parts. It takes a lot of time to melt the powder for these products. Depending on the complexity and size of the end-product, the process can take days. Therefore lattices structure can be used. Dense volumes of material are replaced by lattices with the same stiffness and strength, but the processing time will reduce significantly.

Another disadvantage of the technique is the poor surface quality of the as-built part and the existence of some porosity in the bulk of the material. Additional processing is required to improve the part, resulting in additional production costs. The surface roughness is related to three important parameters:

- The orientation of the surface
- The particle size
- The layer thickness

Also the staircase effect contributes to the poor surface roughness of the as built structure. This effect is due to the layer by layer process of the SLM production method. The effect is shown in Figure 1-9 (Copyright ©2017 3D Systems. All rights reserved). The staircase effect can be limited by

- Decreasing the layer thickness
- Using a larger angle α

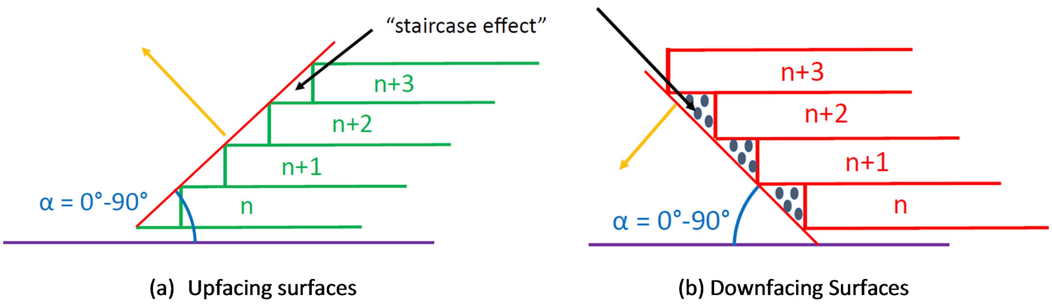

Figure 1-9: Staircase effect

The introduction of AM-produced parts in commercial aerospace industry is slow. This has a number of reasons of which the most important are the following:

- Inferior properties of AM-produced materials compared to sheet metal and machined or forged components
- The limited number of alloys available in powder form
- Airworthiness regulations (e.g. FAA rules) to be further developed

However, the weight savings that the technology can provide, makes SLM worthwhile to apply in the aerospace industry. [1, 7]

1.3 System support structure

This thesis deals with the design and manufacturing of a system support structure. This product is a structural part, known as the “spider” support assembly, to be used on board of a business jet. The function of the product is to support two pressure relief valves, the manifold for these two valves as well as the fuel pipe and electric cables.

The system support structure is located under the secondary fuel tank at the back of the aircraft (Figure 1-10). It is a secondary structure. This means that the forces applied to the structure are relatively low. However the structure is a critical structure as it is part of the fuel system and excessive deformation or rupture under crash landing conditions may cause fuel spillage leading to fire or explosions.

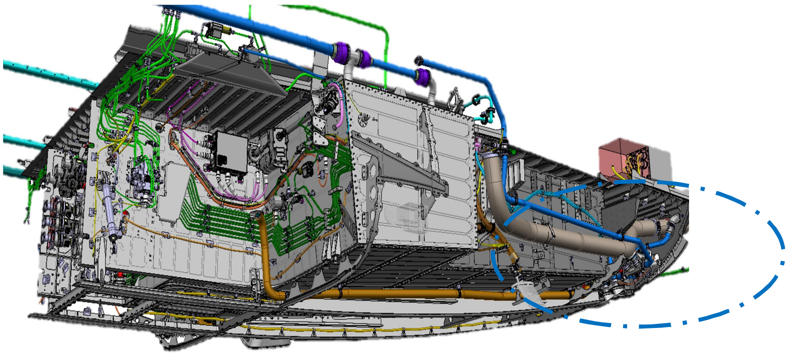

Figure 1-10: Location of the system support structure in aeroplane

The existing structural part is an assembly made of 11 primary parts produced and bolted together by conventional methods (Figure 1-11). The assembly is produced from aluminium sheet metal (ALU 2024), which is cut and cold formed to the required shape and then assembled using conventional slug rivets. The total weight of the original plate-metal assembly inclusive some floating nuts is 0,386kg.

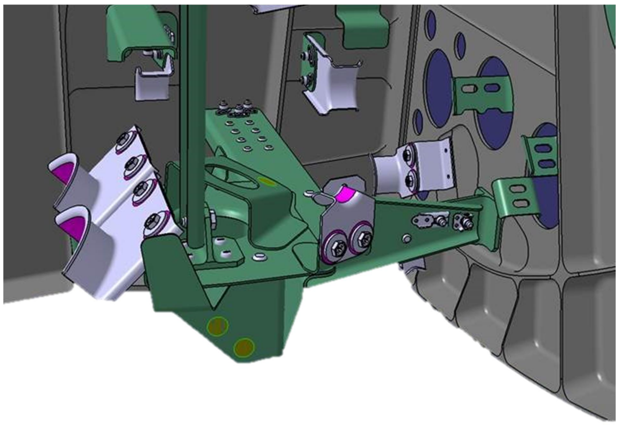

Figure 1-11: Original system support structure

The ultimate goal of this thesis is to design and manufacture a lightweight and one-piece system support structure using the design freedom of additive manufacturing technologies. This alternative structure must perform the same functions as the current structure. The designed piece will exploit the potential of AM fully, but will also take into account the limitations of the process. Lower mass means less fuel consumption. Less fuel consumption in turn means cheaper flights and less pollution. For a passenger airplane, a reduction of 1kg in weight can result in a cost saving of €100 000 over the operational life of the aircraft according to S.A.B.C.A. This shows once again the importance of weight in the aviation industry.

1.4 Requirements

The requirements and conditions will largely determine the shape and appearance of the system support structure. The following sections list all the relevant requirements set by S.A.B.C.A.

1.4.1 Operational

These requirements define the essential capabilities the structure must have. They are related to the maximal stress that may occur. Also durability, guarantee, resonance and safety are covered by these requirements.

- The functional life of the product shall be 20 000 flight cycles
- The supplier shall guarantee a 20 years lifetime of the product.
- The structure has to avoid resonance at windmilling frequency (25Hz)
- The structure shall be sufficiently flexible to allow installation
- The structure shall be earthed to the airframe
- The structure shall be corrosion free over its whole lifetime
- The structure shall be able to withstand inertial loads applied by the equipment that is attached to it during crash landing conditions. Accelerations are expressed in G, this is 9,81m/s². The accelerations during crash landing are as follows:
  - Forward acceleration: -9G
  - Rearward acceleration: +1,5G
  - Sideward acceleration: ±3G
  - Upward acceleration: +3G
  - Downward acceleration: -6G

1.4.2 Environmental

The environmental requirements give the range of the operating specifications where the system can operate reliably. For this support structure only the temperature ranges are specified.

- The product shall be compatible with the temperature range from -100°C to 100°C

1.4.3 Logistic support

These requirements are needed in order to operate efficient and continuously.

- The product shall be marked clearly and unambiguously
- The product shall be maintenance free over its whole lifetime

1.4.4 Physical

These requirements are limited to the weight of the structure and the design space.

- The mass of the product shall not exceed 0,380kg (exclusive paint, support seats and fasteners). This is the weight of the original part.
- The support structure shall not interfere with components already present in the aircraft and be attached at the same interface points as the existing structure.

1.4.5 Production

The production rate of the product shall not be put in danger by the complexity of the product. The optimal orientation has to be determined to ensure a smooth production.

- The product shall be produced at a production rate of one item per month over a period of ten years.

1.4.6 Installation

In addition to the design of the frame, the installation conditions shall be kept in mind. The bracket must be able to be incorporated in the plane. Any mounting tension must be taken into account and may not cause a problem after installation.

- Installation and removal of piping and cabling shall be possible without removal of the frame itself
- The position of the seats for the pressure relief valves and the pipes shall be adjustable so as to fit the valve and pipe positions
- The supporting structure shall be mounted without the use of shimming
- The tolerances and the flexibility of the free structure shall be such that the resulting assembly stresses (residual stresses) shall not exceed 50Mpa
- The support structures shall be designed with flat interfaces to which clamps can be attached
- There must be enough space to be able to install the bolts and the rivets

Most of these requirements are implemented in the topology optimization software. During this thesis *Altair HyperWorks* version 14 was used to generate and validate the outcomes. Some constraints, such as the logistic requirements, are impossible to implement in the software. They have to be checked manually by the designers.

1.5 Work flow

The procedure followed to obtain accurate and good results is based on the method proposed by Alzahrani [1]. This is the general procedure for a topological optimization. This procedure consists of some steps that must be completed. The results generated in one step are the input of the next step. At the end of the cycle, a product is obtained that complies with all constraints and requirements. The workflow is illustrated in Figure 1-12.

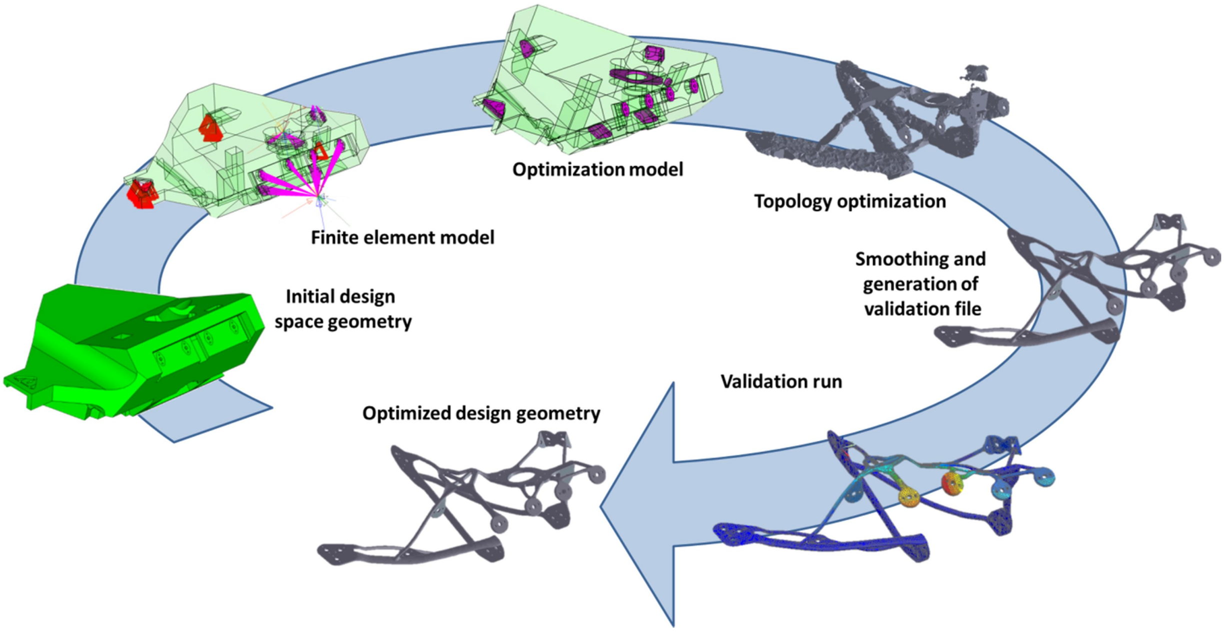

Figure 1-12: Conventional workflow in topology optimization

Topology optimization is very useful in the early phase of the design cycle. The result from the topology optimization gives the load paths of the structure. The final design is based on these load paths.

The results coming out of the optimization software are very rough and unfinished. These parts must be smoothened to reduce stress concentrations and to make them producible. *Geomagic Design X* is the software to smoothen the rough results. The process to obtain a topologically optimized bracket is explained from section 1.5.1 to section 1.5.6.

1.5.1 Initial design and space geometry

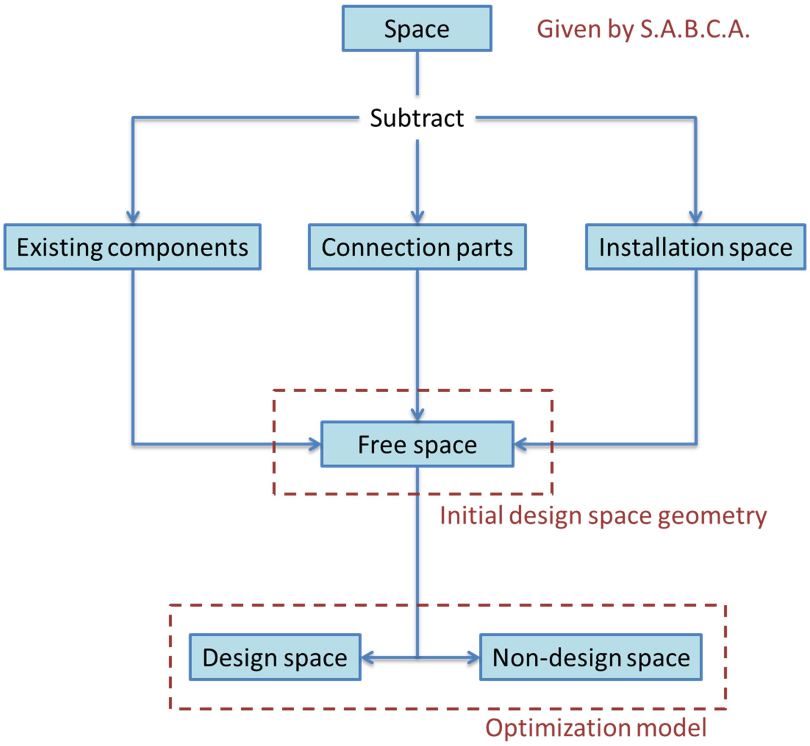

Figure 1-13: Procedure followed to obtain the space geometry

The space that the spider can occupy is given by S.A.B.C.A. (Figure 1-14). However there are still existing components (red parts in Figure 1-15) in this volume. The existing components cannot be modified or moved. The space of these components has to be subtracted from the volume given by S.A.B.C.A.

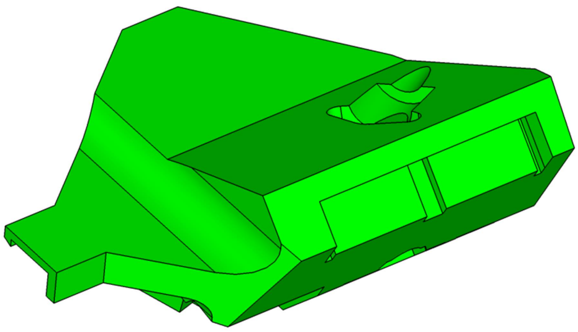

Figure 1-14: Space given by S.A.B.C.A.

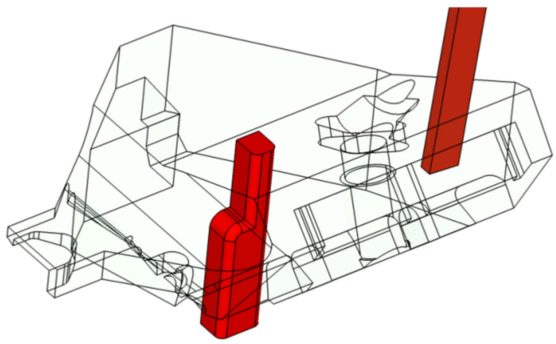

Figure 1-15: Components crossing the volume

Floating nuts, bolts and rivets provide the connection between the spider and the aeroplane. The space necessary for these parts needs to be subtracted from the volume given by S.A.B.C.A. There are four types of floating nuts used in the bracket: MS21061L3, MS21069L3, MS21059L3 and NAS1789-3. Technical drawings of these floating nuts are given in respectively Appendix A, Appendix B, Appendix C and Appendix D. The spider is connected with a bolt, NAS6203-4, in point C. The technical drawing is given in Appendix E. All the connection points are shown in Figure 1-16 and the corresponding connection parts are listed in Table 1-1. Figure 1-18 is an example of the free space removed to accommodate the bolts and rivets of the floating nuts.

Table 1-1: Floating nut types

Connection point	Type of floating nut
A	MS21061L3
B	NAS1789-3
C	NAS6203-4
D	MS21069L3
E	MS21069L3
F	MS21069L3
a	MS21069L3
b	MS21069L3
c	MS21069L3
d	MS21069L3
e	MS21059L3
f	MS21059L3
g	MS21059L3
h	MS21059L3
i	MS21059L3
j	MS21059L3
k	MS21069L3
l	MS21069L3

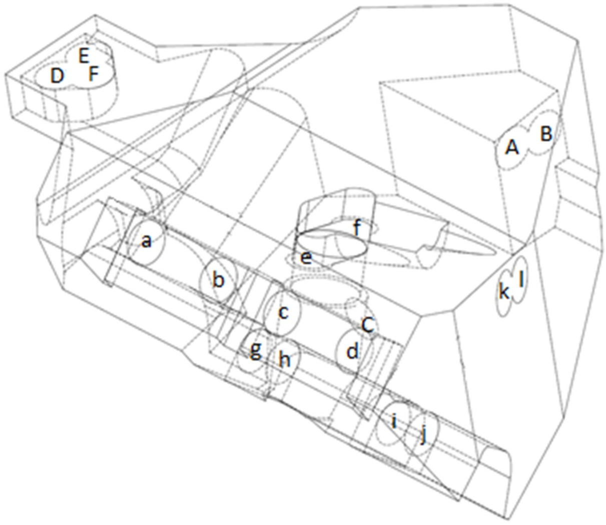

Figure 1-16: Connection points

To install the spider, the bolts and rivets must be accessible with tools. For this tooling an installation space is foreseen. This space is subtracted from the free space. Figure 1-19 is an example of the space removed due to installation constraints.

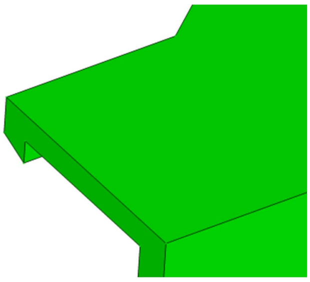

Figure 1-17: Close-up of space given by S.A.B.C.A.

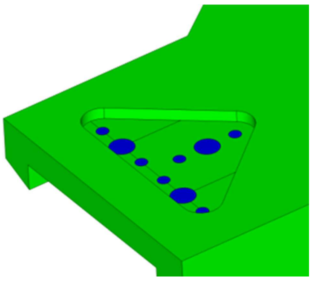

Figure 1-18: Removed space due to connection parts (blue)

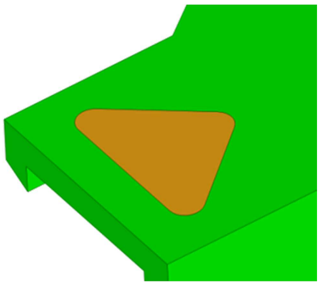

Figure 1-19: Removed installation space (orange)

Figure 1-20 shows the free space (green) and all the space that has to be subtracted (blue, orange and red). The result of this subtraction is shown in Figure 1-21. This is the initial design space geometry. The topology optimization is performed on this space.

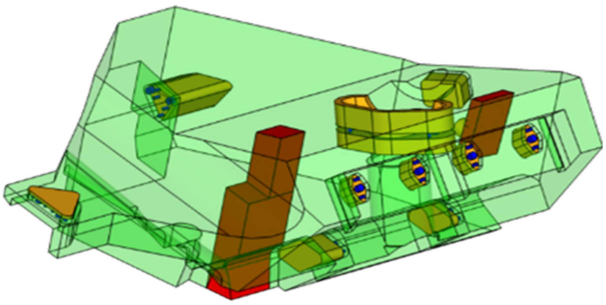

Figure 1-20: Installation constraints

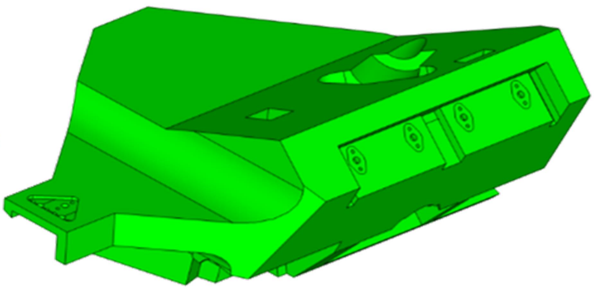

Figure 1-21: Initial design space geometry

1.5.2 Finite element model

When the initial design space geometry is determined, the finite element model can be set up. This model consists of a proper mesh. Because of the irregular shape of the initial design space, a 3D tetrahedral mesh type is the best choice.

A uniform mesh size over the whole volume is an important feature of a good mesh for a topology optimization. When using only the automatic mesh creator, there is a risk of non-uniform mesh, see Figure 1-22. A non-uniform mesh is too coarse, the solver will take away big elements and the results will not be accurate. To create a uniform mesh, the refinement tool in *Altair HyperWorks* is used, see Figure 1-23.

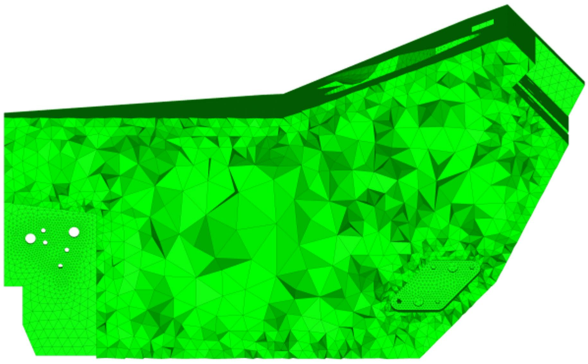

Figure 1-22: Automatically created mesh

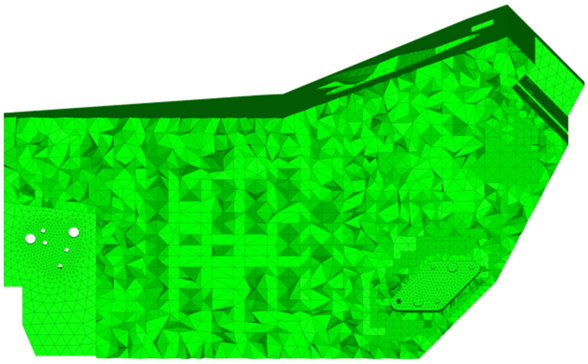

Figure 1-23: Refined mesh

In order to determine the ideal mesh size, a convergence study can be performed. A smaller mesh means intuitively more accurate results, but the CPU-time will increase as well. It is important to carry out a trade-off between these two parameters. The uniform element size for this topology optimization is 5mm.

In the FEM model, the boundary conditions should be assigned properly. The support structure is attached to the surrounding in three places. In these places, a fixed clamping constraint is supposed (red parts in Figure 1-24). These parts of the structure have no degrees of freedom. This assumption is only valid when the structure can be fitted perfectly. When the frame shows some deviations, it should be stretched or compressed in order to fix it correctly. In this case, one of the three fixed clamping will have some degrees of freedom. This is discussed further in section 1.5.6.

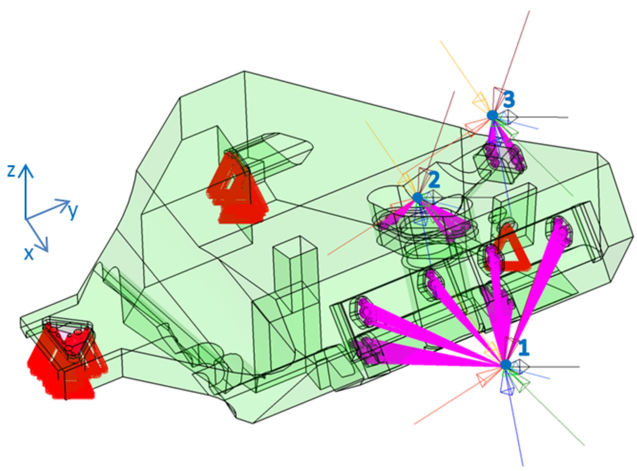

Figure 1-24: Constraints and loads

The sizing load cases for the support structure are the inertial loads due to the accelerations/decelerations generated during crash landing conditions. During a crash, the airplane stops moving, but the pipes and attached components will still move forward. Table 1-2 gives the acceleration at which these parts move forward. This causes forces on the support structure. These forces act at the centre of gravity of the parts. Table 1-3 gives the mass of these parts. The masses of the pipes are represented by point masses and are connected to the support structure using rigid elements. One node is the independent node and here the force will act on. The nodes on the support structure are the dependent nodes and are connected to the independent node using RBE3 elements (purple parts in Figure 1-24).

Table 1-2: Crash landing load cases

Load case	x-direction	y-direction	z-direction
crash landing 1	-9G	3G	-6G
crash landing 2	-9G	3G	3G
crash landing 3	-9G	-3G	-6G
crash landing 4	-9G	-3G	3G
crash landing 5	1,5G	3G	-6G
crash landing 6	1,5G	3G	3G
crash landing 7	1,5G	-3G	-6G
crash landing 8	1,5G	-3G	3G

Table 1-3: Mass of attached components

Point of engagement in Figure 1-24	Attached mass
1	3,484kg
2	0,047kg
3	0,020kg

From the requirements set by S.A.B.C.A., it can be seen that eight different load cases can occur. All these subcases are implemented in the *Altair HyperWorks* software. The advantage of working with multiple load cases is that all loads are taken into account. The optimized structure meets all the requirements of a crash landing.

1.5.3 Optimization model

In this step of the work flow, a finite element model is prepared for the topology optimization. Figure 1-13 shows that the free space is split in design and non-design space. This is necessary for the optimization. Also the objective and the constraints need to be set.

It is important to determine the design space and the non-design space. Without a proper non-design space the topology optimization will fail. The design space is the part of the free space where volume can be optimised. In the end of the topology optimization, it is in the design space that the support structure should appear. The non-design space is the area that remains unaffected during the optimization run. For the spider this is the area where it is attached to the plane and other components. The boundary conditions (loads and displacements) are acting on these parts of the structure. If the boundary conditions act on the design space, the solver gets confused because elements where forces are acting on, are taken away during optimization. The separation of design space and non-design space is shown in Figure 1-25.

Initially, the non-design space represents 0,41% of the total volume. The mass of the non-design space is 0,053kg. The mass of the initial design space is 13,28kg.

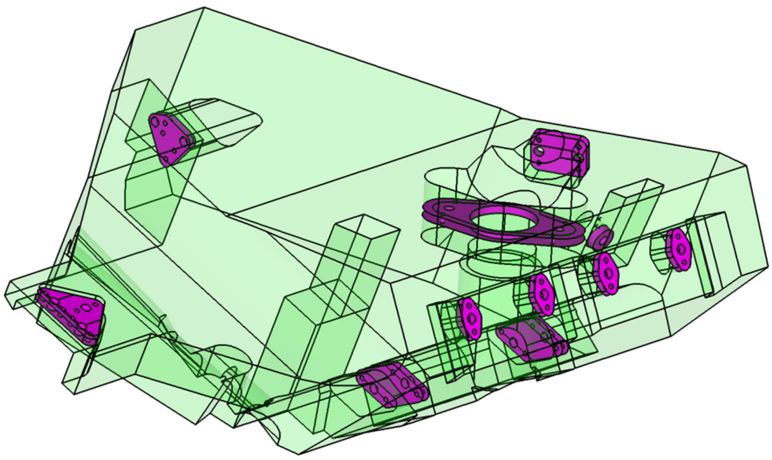

Figure 1-25: Design space (green) and non-design space (purple)

The objective and constraint(s) have to be determined to run a topology optimization. The objective is the property of the structure that is minimized or maximized. During optimization, the solver will distribute the material in such a way that the objective function is fulfilled as much as possible.

Due to the lack of computational power, not every requirement can be translated to a constraint. To minimize the mass of the structure, the stresses due to crash landing are the constraints. The natural frequency and stresses due to the installation are checked afterwards. However only stress as constraint result in a failed optimization. All the design space will be removed. A stiffness constraint is required to leave some material in the design space.

According to the advice of Dr. Christoph Katzenschwanz, expert in the *Altair HyperWorks* software, the weighted compliance is minimized and a volume fraction is one of the constraints. This gives a first view on the resulting design and an idea of the magnitude of the compliance.

In the first performed topology optimization the minimizing of the weighted compliance is the objective. Compliance is the recursive of stiffness. Minimizing the compliance is therefore the same as maximizing the stiffness. Highly compliant materials are easily stretched or distended. Compliance is used because stiffness is not a feature in *Altair HyperWorks.*

$$k = \frac{F}{\delta} \rightarrow k^{-1} = \frac{\delta}{F}$$

With:
k=stiffness [N/m]
F= Force [N]
δ = Displacement [m]

The weighted compliance is a method used to consider multiple subcases in a classical topology optimization. The response is the weighted sum of the compliance of each individual subcase. A weight factor for each individual subcase is given at the start. This factor is then multiplied with the individual compliances of each subcase. This product is added together to form the overall weighted compliance. [8]

The constraints limit the ability to achieve the objective. In other words, these conditions must be satisfied for sure. The more constraints are defined, the better the structure is adapted to the requirements. The constraints for the first optimization are the maximal stress and the maximum volume fraction.

During crash landing, the bracket will deform. Plastic deformation is allowed in so far that it is only local. Large deformations are not allowed as these can cause rupture of fuel pipes. The spider is made of AlSi10Mg. Figure 1-26 [9] gives the stress-strain curve of AlSi10Mg.

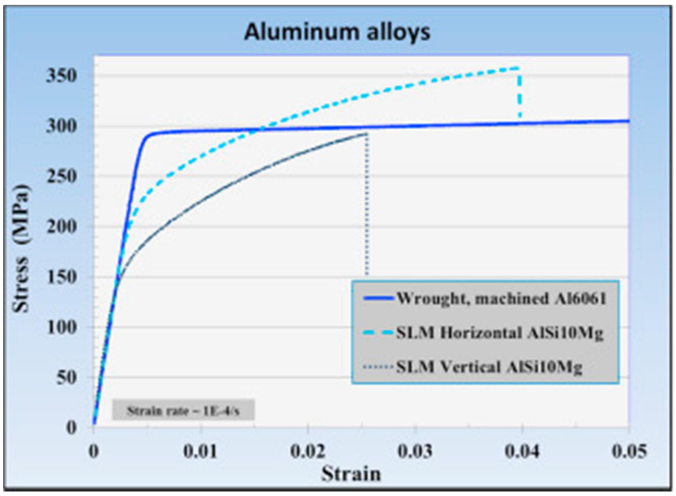

Figure 1-26: Stress-strain curve of AlSi10Mg

SLM-printing is a layered based production method. The products therefore have an anisotropic character. The properties are different from direction to direction. Table 1-4 [9] shows an overview of the differences between the properties depending on the direction. To make sure that the designed spider will be strong enough, the lowest yield strength, 172MPa, is chosen. This yield stress value will be used as the allowable stress for the applied crash load conditions. By doing so, no plastic deformation will occur during crash landing.

Table 1-4: Material properties of AlSi10Mg

Material	Orientation	Young's modulus (GPa)	Yield strength (MPa)	Ultimate strength (MPa)	Failure strain	Density (g/cm³)	Poison coefficient
SLM AlSi10Mg	Horizontal	65,5	227	358	0,039	2,68	0,33
SLM AlSi10Mg	Vertical	75,4	172	289	0,026	2,68	0,33

Also volume fraction is defined as a constraint. The volume fraction defines the fraction of the total volume that has to be left at the end of an optimization run. In fact it gives the same results as a mass constraint. The value of the volume fraction is changed in an iterative way until the lightest possible structure is reached.

After these iterations the structure becomes visible and the obtained compliance of this structure can serve as guidance. The results and corresponding values are given in 1.5.4 Topology optimization.

In the second topology optimization, the minimizing of the mass is the objective. The constraints are the stress due to the crash landing and the weighted compliance based on the previous found values. The outcome of this topology optimization is the structure that is used to work with in the following steps. The results and corresponding values are given in 1.5.4 Topology optimization

The struts generated in the support structure must have a minimum diameter. This constraint has two reasons. The first reason is that smaller struts are too fragile. Accidental contact during installation may cause fracture of the struts. The minimal diameter to prevent accidental damage was defined as 4mm. This limit is somewhat arbitrary and must be regarded as a rule of thumb that may be reviewed later. The second reason is the risk of buckling. Slender struts will easily buckle under compressive loads so a minimum diameter has to be defined. This constraint can be fulfilled using the minimum member size command. A member size of 4mm is sufficient to overcome above-mentioned problems. *Altair HyperWorks* has a feature to set this constraint. A minimal member size of 4mm is used for every optimization.

1.5.4 Topology optimization

In this step of the workflow, the software of *Altair HyperWorks* calculates the topology optimized structure based on the parameters set in 1.5.3 Optimization model.

Firstly the importance of a minimal member size is discussed. The minimal member size used is 4mm. Adding a minimal member size in *Altair HyperWorks* results in load paths without any interruptions. The improvement of the struts is clearly visible in the comparison of Figure 1-27 and Figure 1-28. Figure 1-27 is a topology optimization without a minimal member size. Between low stressed elements are discontinuities visible. This problem is solved by adding a minimal member size as is shown in Figure 1-28. The settings for obtaining Figure 1-27 and Figure 1-28 are:

Objective:	Minimize weighted compliance	
Constraints:	Volume Fraction:	<9%
	Static stress:	<172Mpa
	Member size:	>4mm (only for Figure 1-28)

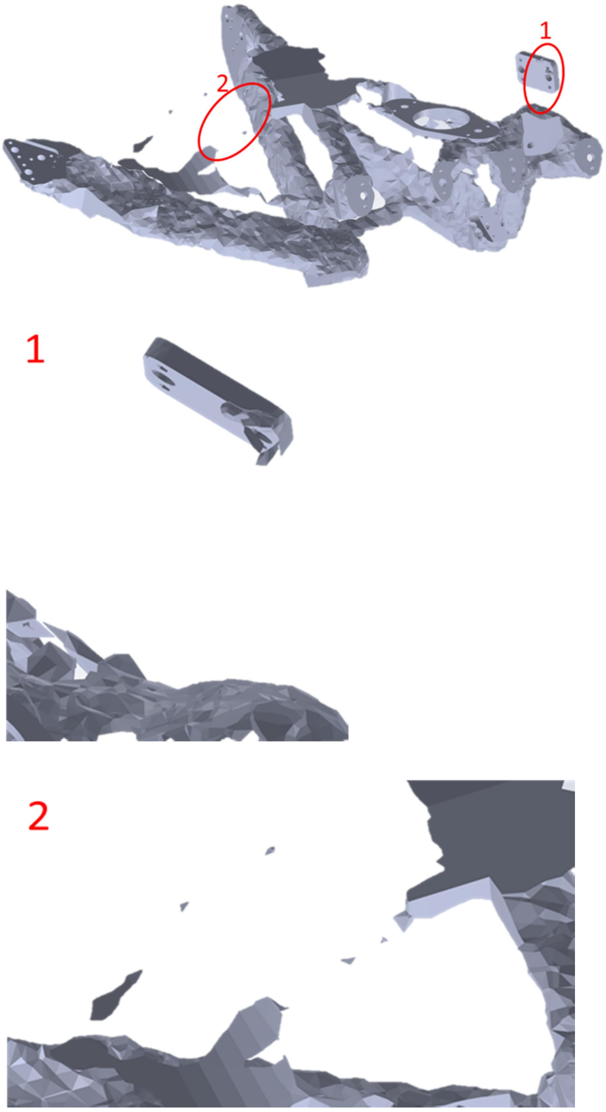

Figure 1-27: Optimization without minimal member size

Figure 1-28: Optimization with minimal member size

The first topology optimization is run according to the theory discussed in section 1.5.3 Optimization model. The goal of this optimization is to give a first impression of the optimized structure. Also a value for the weighted compliance can be derived from this process. The topology optimization is performed with following parameters:

Objective: Minimize weighted compliance

Constraints:

Volume Fraction: <25% (for Figure 1-29)
Volume Fraction: <15% (for Figure 1-30)
Volume Fraction: <7% (for Figure 1-31)
Static stress: <172Mpa
Member size: >4mm

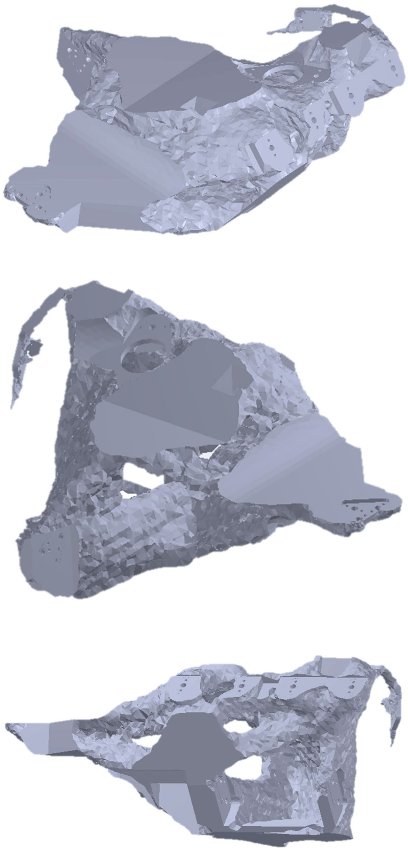

Figure 1-29: Volfrac 25%

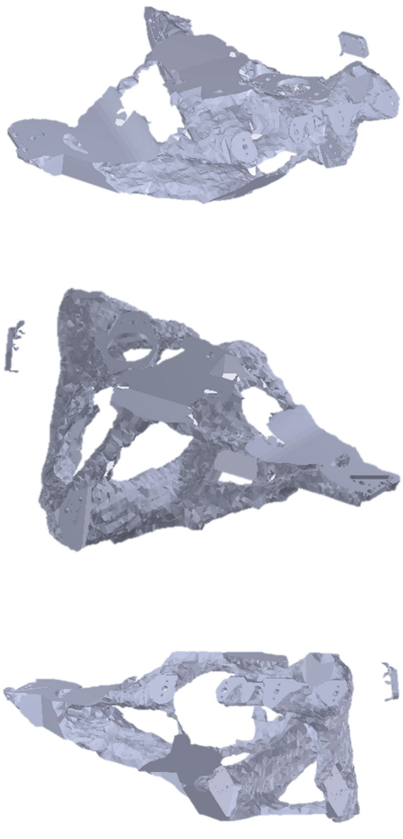

Figure 1-30: Volfrac 15%

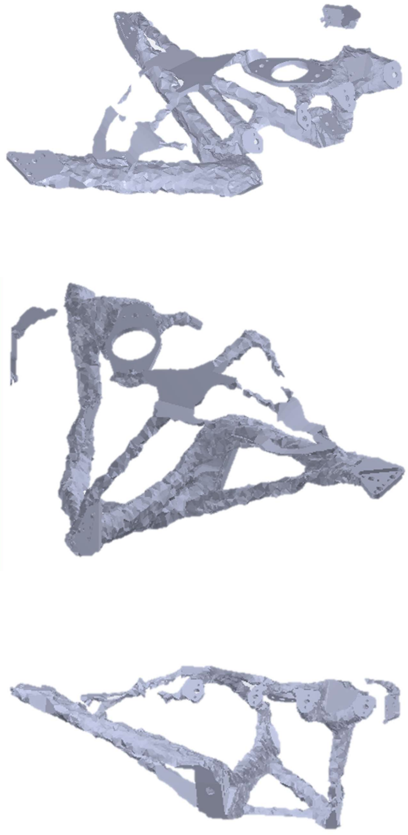

Figure 1-31: Volfrac 7%

When 25% of the original volume is kept, it is not yet possible to distinguish a realistic bracket. When lowering the volume fraction, the structure becomes more visible. With a volume fraction of 7% the struts become discontinued, even with the use of a minimal member size. At this point it is no longer useful to lower the volume fraction. The obtained structure gives a reference for the next optimization. The objective, the weighted compliance for this topology optimization, is 4,4mm/N after the last iteration.

The second topology optimization is run in order to minimize the mass. The weighted compliance is the constraint. The value of this constraint varies around the value found in the first topology optimization.

Objective: Minimize mass

Constraints:
Weighted compliance: <10mm/N (for Figure 1-32)
Weighted compliance: <6,5mm/N (for Figure 1-33)
Weighted compliance: <4,4mm/N (for Figure 1-34)
Static stress: <172Mpa
Member size: >4mm

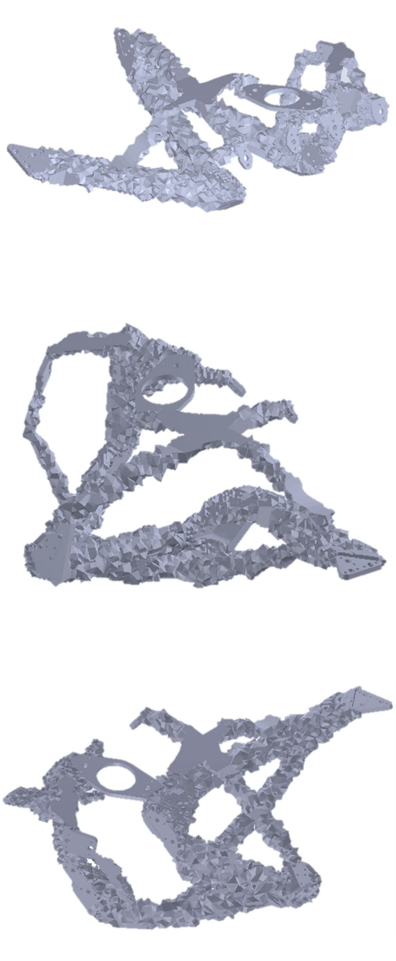

Figure 1-32: Weighted compliance 10mm/N

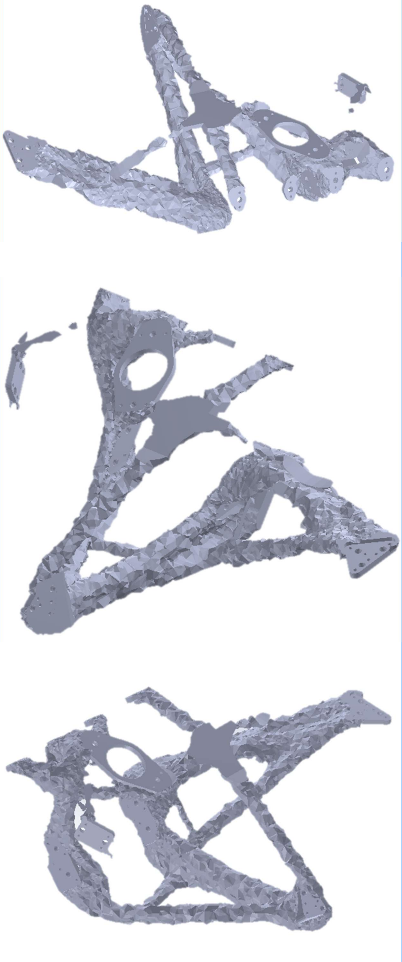

Figure 1-33: Weighted compliance 6,5mm/N

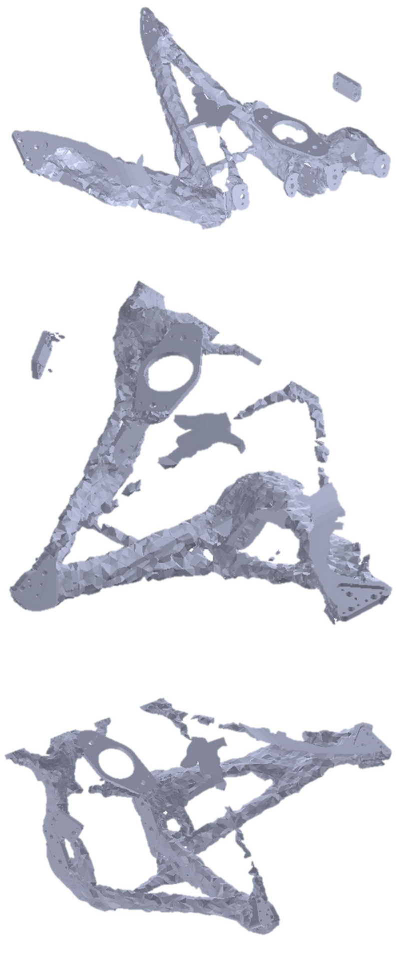

Figure 1-34: Weighted compliance 4,4mm/N

With a weighted compliance of 10mm/N and 6,5mm/N, the structure of the first topology optimization with a volume fraction of 7% is recognisable. The topology optimization with a weighted compliance of 4,4mm/N shows discontinuities in the struts. This result is not useable. This is remarkable because the weighted compliance has the value found in the first topology optimization. Changing the objective and the constraint results in a different solution.

The load paths of the topology optimization performed with a weighted compliance with 10mm/N and 6,5mm/N are the same. But the contours are more visible with a weighted compliance of 6,5mm/N. Therefore this topology optimization is chosen to work with in the next step. The topology optimization has following parameters:

Objective:	Minimize mass	
Constraints:	Weighted compliance:	<6,5mm/N
	Static stress:	<172Mpa
	Member size:	>4mm

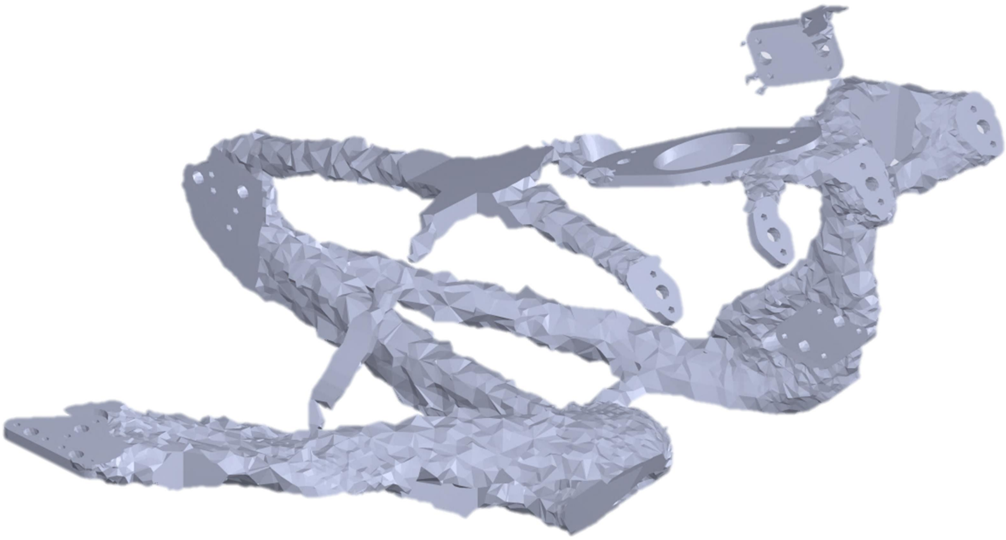

Figure 1-35: Topology optimized structure

1.5.5 Smoothing and generation of validation file

The rough structure is now visible in the software. *Altair HyperWorks*, however, does not take into account any limitations associated with the production process used to manufacture the part. The limitations of the SLM-technique will have to be entered manually.

1.5.5.1 Generating the validation file

Geomagic Design X is the software used in this step of the design process to smoothen the rough mesh structure. A 3D CAD model is designed using the mesh data that comes out of *Altair HyperWorks*. Figure 1-36 shows the topology optimized rough mesh data.

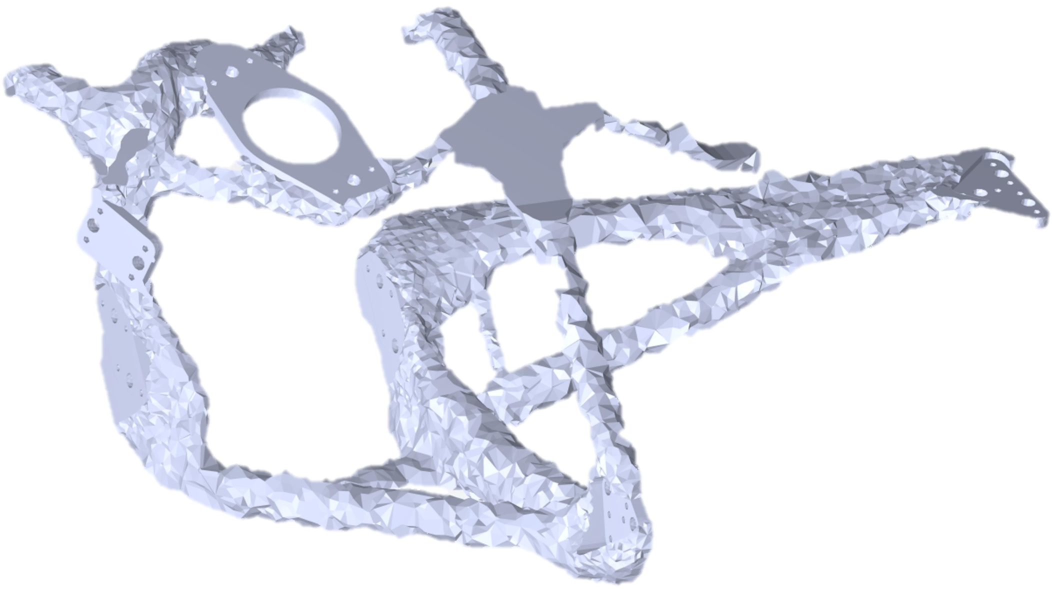

Figure 1-36: Rough mesh structure

The optimized structure from *Altair HyperWorks* is still oversized. This means that the diameter of the struts can be reduced in order to save weight. The mesh data only gives an idea of how the final structure should look like. It gives the force lines in the structure. Modifications to the proposed structure from Figure 1-36 may still be provided, but will have an effect on the ultimate stiffness and mass of the product. The only requirements which always have to be respected are to stay within the given free space and have a minimal strut diameter of 4mm to avoid fractures during installation or buckling.

The best way to design the spider as light as possible is to start from the thinnest possible structure. Therefore all possible struts are set at 4mm diameter. Where the mesh indicates a larger diameter, the diameter of the strut is also chosen to be larger. This reasoning is the same for the shape of the struts. Not all struts of the spider are perfectly circular. This means that some of the rods will be more elliptical than circular.

To ensure that no stress concentrations occur in the spider, all corners and edges are rounded using fillets. Where it is expected that the stress will not be high, material can be cut away in order to save as much weight as possible.

The structure must be stiff to have a natural frequency above 25Hz. But the structure must be flexible to avoid internal stress when installing it in the airframe without the use of shims to take up tolerance gaps. Figure 1-37 shows a comparison between the mesh and the smoothened spider.

It can be clearly seen that one strut has been omitted at point A in Figure 1-37. This has two reasons. First, it provides a weight saving. Second, it gives the structure more flexibility. The natural frequency of the spider will decrease, but is expected to be sufficiently high. The additional flexibility that is achieved, will lead to lower stresses when the spider is installed.

The structure shown on the right is much finer than the mesh. All sharp edges and corners are rounded to avoid stress concentrations. The total weight of the smoothened structure is 0,189kg. The original rough mesh structure had a weight of 0,616kg. This gives a weight reduction of 0,427kg.

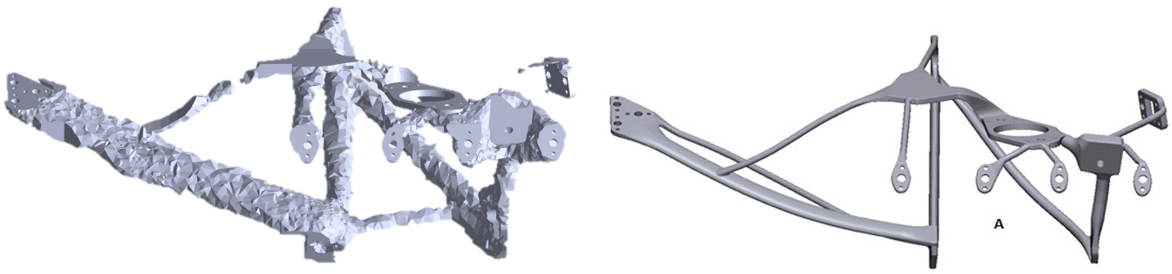

Figure 1-37: Left) Rough mesh structure Right) Smoothened 3D-file

1.5.5.2 Orientation of the spider

The next step in the design is to determine the print orientation of the spider. As stated in 1.2 Selective laser melting, it is intended to use the minimal amount of support structures to reduce the cost. Figure 1-38 shows the best orientation for the designed spider. The build-up direction is the z-axis.

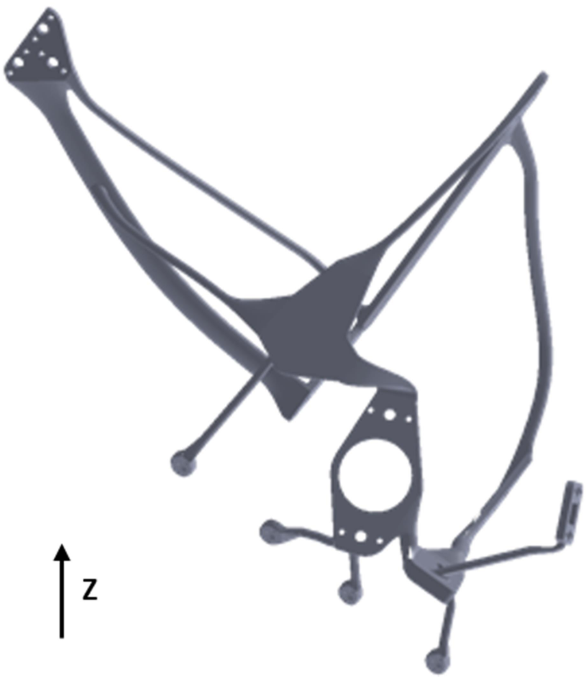

Figure 1-38: Orientation of the spider

The parts of the spider that need supports, are indicated in orange and red in Figure 1-39. They make an angle of 45° or less with the horizontal plane.

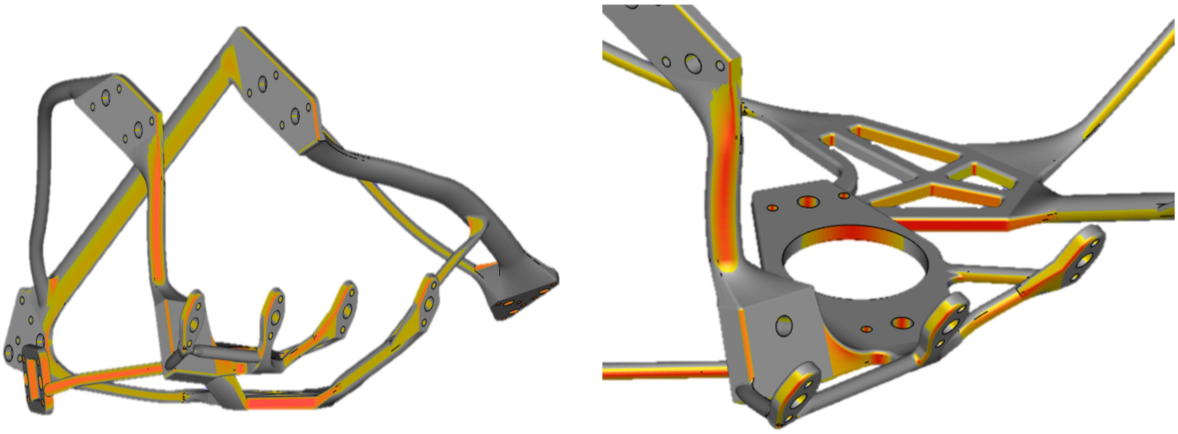

Figure 1-39: Down facing surfaces

The holes for the floating nuts cannot be placed too close to the edge. In combination with a down-facing region, they can cause problems to the accuracy during production. Normally the distance to the board is 1,5 to 2 times the diameter of the hole. This is shown in Figure 1-40. At a smaller distance, the allowable bearing pressure is much lower.

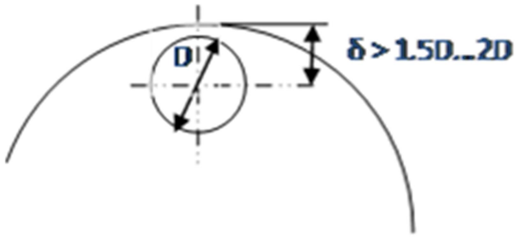

Figure 1-40: Distance to the board

To ensure the most accurate result, the holes in the structure are not printed to final size. After the production, the holes are drilled at the appropriate size. This structure has three sizes of holes:

- The holes for the floating nuts are 4,8mm. They are printed with a size of 3,3mm.
- The holes for the electric cable support part are 3,3mm and they are printed with a size of 2,2mm.
- The holes for the rivets are 2,49mm. They are not printed. During drilling, they can be put in the desired position.

A strut which connects the rear entity with the front may be provided with a permanent or by means of support ring to remove, in order to improve the rigidity of the assembly during the production. The extra strut is shown in red in Figure 1-41.

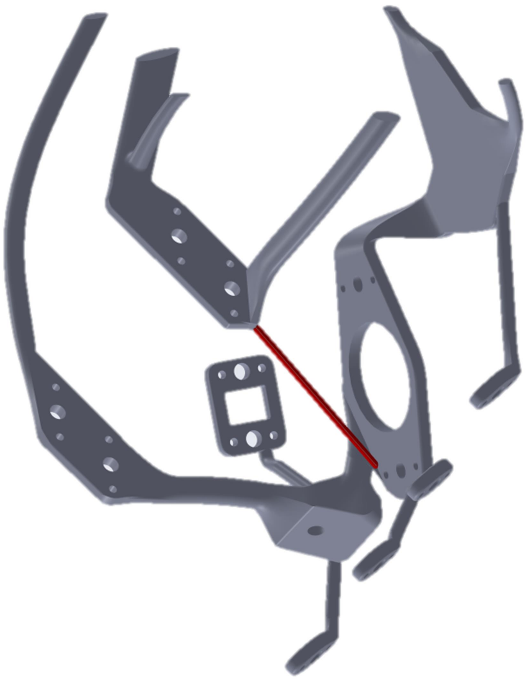

Figure 1-41: Extra strut to increase the stiffness of the spider during production

The structure, coming out of the printer, is different from the spider which will be incorporated in the airplane. A number of steps need to be taken to obtain the final structure. First, there is a stress relieve heat treatment to eliminate the stress between the base plate and the structure. Next, the bracket is removed from the base plate. This can be done manually or by means of wire EDM or milling techniques. Next, the supports need to be removed and all the supported surfaces are manually smoothened. Superfluous powder is removed by means of shot peening. The holes are drilled to the correct size and the structure is cleaned afterwards. Optionally, the structure can be anodised to protect it against corrosion. After completing all these steps, the spider can be fitted in the aeroplane.

1.5.6 Validation run

After the design of the refined structure, the spider has to be validated once again. A new finite element analysis can reveal the weak spots of the structure. These weak parts have to be adjusted until all requirements are met. This step is very important in the overall design process. For this part of the design process, the software *Siemens NX 10* is used.

The spider structure is refined in the previous step to save weight. Therefore it is important to validate if the internal stresses are not too high in the spider. This is among other the case in the connection between a strut and the mounting plates of the structure. If the stress becomes too high, a fillet radius has to be placed to reduce the problem. Another possible solution is increasing the diameter of the struts.

An analysis of the natural frequency of the spider is carried out additional to a strength calculation. This is important in a possible windmilling situation. Windmilling occurs when one of the engines fails. Due to the incoming wind, the rotor blades of the motor keep on turning and as a result, the whole structure will vibrate at 25Hz. Consequently the natural frequency of the spider must always be higher than this value.

The same constraints as during the topological optimization in step 1.5.3 are applied. In Table 1-5 they are listed:

Table 1-5 : Overview of the requirements

Requirement	Maximal/minimal value
Natural frequency	>25Hz
Allowable stress during crash landing	<172MPa
Clamp stress	<50Mpa

1.5.6.1 Internal stresses

There are two possible load cases that have to be validated. In both scenarios the stresses will appear in the spider. The validation of both load cases is discussed in this section.

The crash landing is the first load case. The attached tubes and pipes exert an acceleration force on the spider. As a result, stresses develop in the support structure. However, these should not be higher than the yield strength of the material used. This is 172MPa. It is allowed that the spider deforms plastically, but it should never break. Locally slightly higher stresses than the yield strength are admitted. For safety reasons these high stresses are restricted as much as possible and the yield strength will determine the allowable upper bound.

The spider is a relatively thin structure with a very irregular shape and thickness. Therefore it is necessary to choose a 3D mesh. The choice is made for a CTETRA(10) element type. The next step is the determination of the mesh size. A compromise between accuracy and CPU-time must be found. A size of 3mm provides accurate and fast results.

Accelerations are working on the structure, with a certain direction and size. There are nine possibilities, but the first load case in Table 1-2 is the critical one.

The magnitude of the acceleration is -88,29m/s² in the x-direction, -29,43m/s² in the y-direction and -58,86m/s² in the z-direction and are indicated in orange in Figure 1-42. All these parameters are given by S.A.B.C.A. and are identical as described in section 1.5.2. The accelerations are working at the centre of mass of the pipes and tubes. Therefore they are connected through RBE3 elements. These elements are indicated in purple in Figure 1-42. The red parts in Figure 1-42 are the connections to the aeroplane.

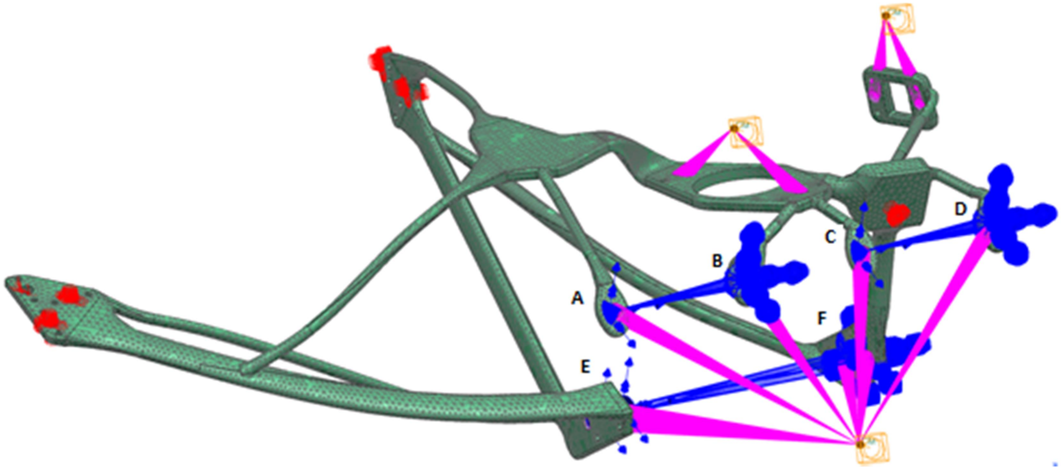

Figure 1-42: Loads and constraints on the spider

The interfaces A, B, C and D in Figure 1-42 support some pipes using two small clamps. The brackets are placed respectively between A, B, C and D. It can be assumed that these clamps are infinitely stiff compared to the support structure. This inherently means that the interfaces A and B are located at a fixed distance from each other. The same applies to interfaces C and D. Interfaces E and F in Figure 1-42 support the manifold. This manifold can also be modelled as infinitely stiff so that the distance between the interfaces E and F is fixed. The spider is validated with and without this coupling between the interfaces to investigate its effect. The Von Mises-stresses are the relevant stresses in the validations and are used to draw conclusions about the stress situations.

The finite element analysis in Figure 1-43 indicates that in parts of the structure the stress exceeds the allowable value of 172Mpa. This is for example the case in strut 1 leading to interface A in the front of the spider. The interfaces A, B, C and D are not coupled in this analysis.

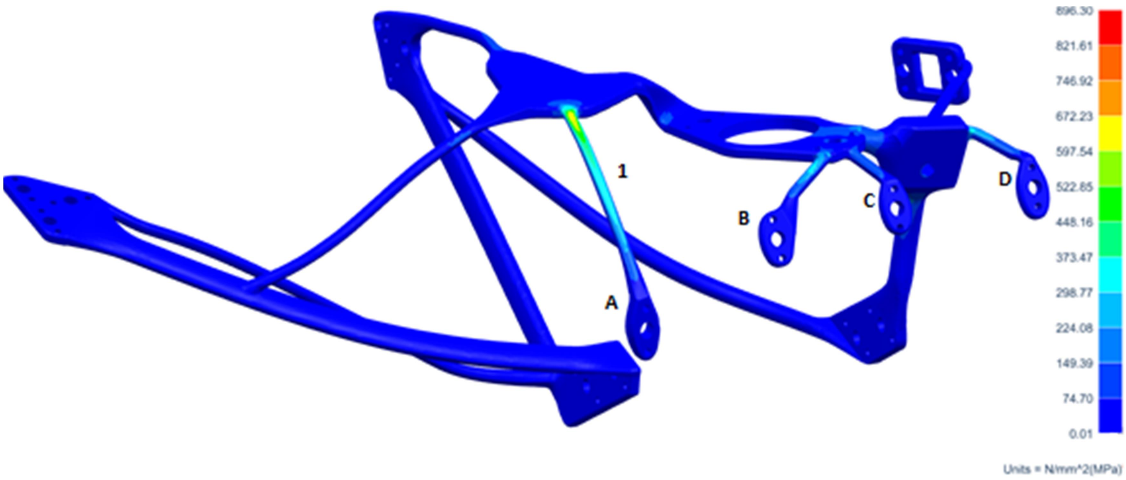

Figure 1-43: Stress in the non-coupled spider during crash landing

Figure 1-44 shows all the parts of the support structure where the internal stress exceeds the allowable limit of 172MPa. Most of the problems occur in the struts leading to the four interfaces A, B, C and D in the front.

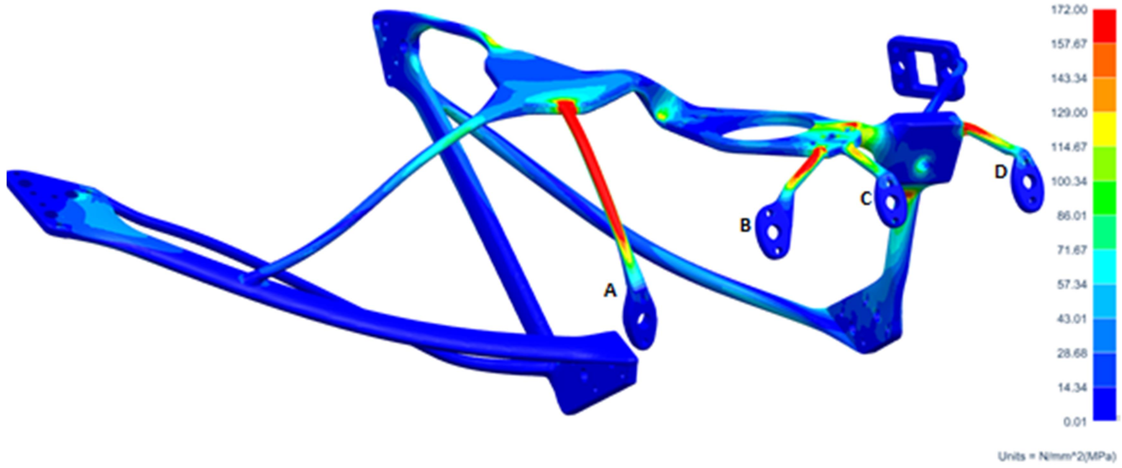

Figure 1-44: Red parts indicate a stress value greater than 172MPa

The previous FEM model is extended with a coupling constraint between interfaces A, B, C, D, E and F from Figure 1-42. Figure 1-45 indicates that the stress distribution looks different in comparison with previous analyzes. Only in struts 2 and 4 appear stresses that exceed the allowable stress value.

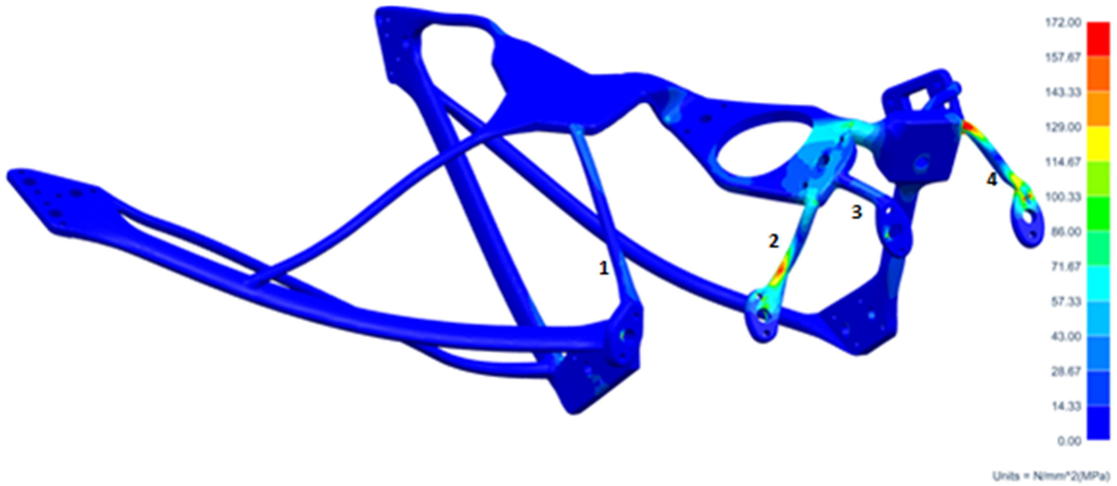

Figure 1-45: The stress distribution in the spider with a manual coupling between the interfaces.

The main goals of the design of the spider is to keep the weight as low as possible and ensure a safe support structure in all possible circumstances. Therefore it is important to look at both the coupled and non-coupled case. From the non-coupled case can be concluded that some parts need to be reinforced. The diameter of strut 1 in Figure 1-44 is increased from 4mm to 6,5mm. The connection of strut 1 with the rest of the spider is also reinforced. Moreover, at interfaces B, C and D are two struts added which will absorb some of the stress. These struts do have a minimum diameter of 4mm to save weight.

The preceding finite element analyses have shown that the stresses in the interface plates are low. The plates, which are reserved to tighten the bolts, are reduced from 4mm thickness to 2mm thickness. Parts are cut away in the plates where possible. The weight gain of the additional struts for reinforcement is partly compensated by this. All the changes in the spider are visible in Figure 1-46.

Additionally, there are two small interfaces and two holes added to the spider. The two interfaces are used to connect passing pipes to the spider. The two holes in the structure are meant to attach the support for an electric cable which ensures an equal electric potential between all the parts of the fuel system. All these additional features have no effect on the finite element analysis.

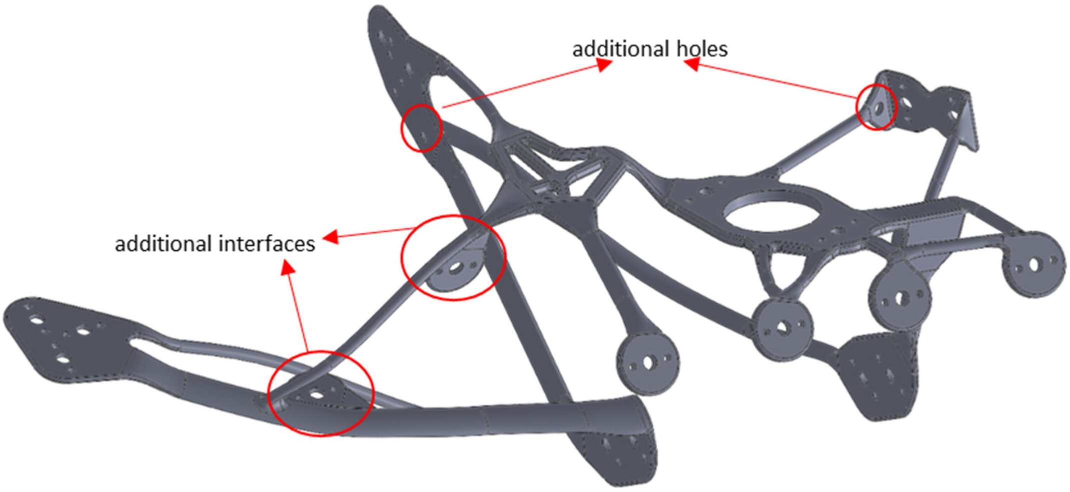

Figure 1-46: Reinforced spider with additional features

The finite element analysis of the new spider without coupled interfaces in Figure 1-47 shows that the stresses are reduced. The problems with the previous spider are largely solved. The overall stress value is lower and the struts 1, 2, 3 and 4 do not exhibit too high stresses. Only the strut 5 is experiencing more than the allowable stress. A possible reinforcement will be apparent from the analysis with the coupled interfaces.

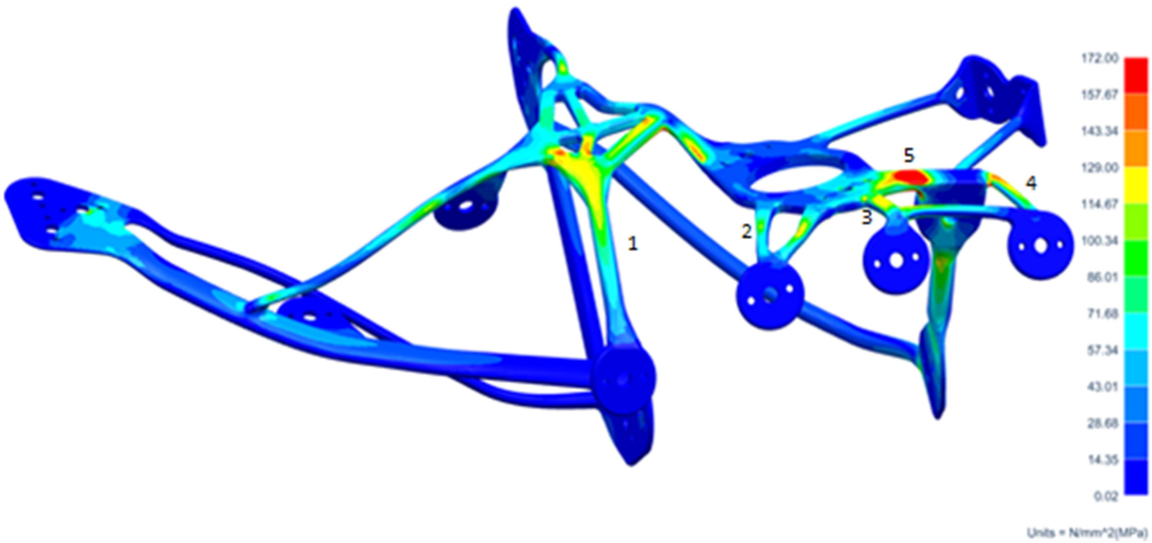

Figure 1-47: Stress distribution without a coupling constraint

If the coupling constraint is implied on the spider, like in Figure 1-36, the stresses are lower. No part of the structure shows too high stresses. This support structure meets all the requirements related to crash landing and is approved.

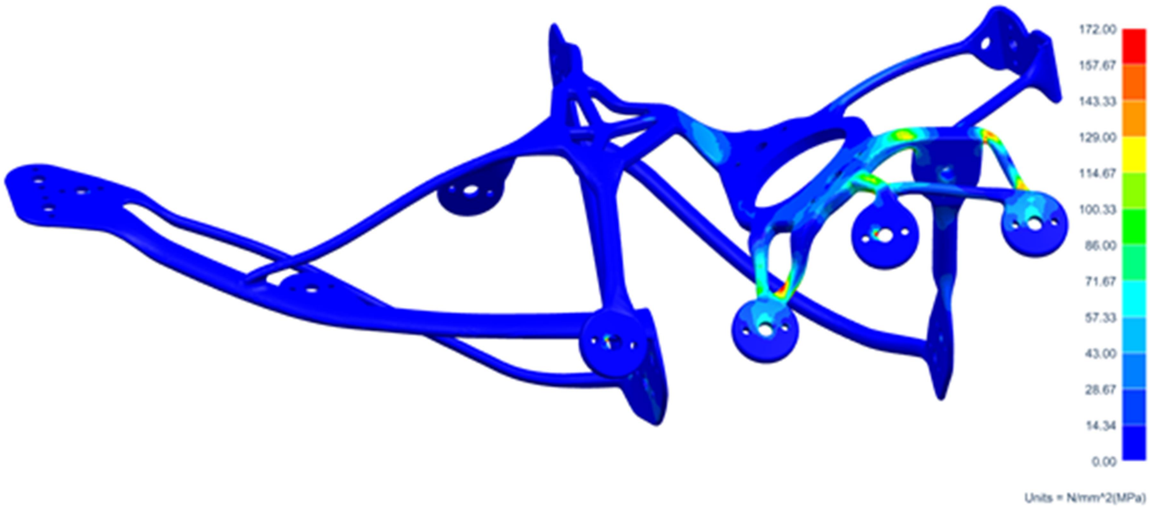

Figure 1-48: Stress distribution with a coupling constraint

The mass of the final spider is 0,189kg. This is about the same as the first spider. The reinforcements have not caused a weight increase. This design of the spider will be used to do the other validations.

1.5.6.2 Clamping stress

The next validation to be carried out is the clamping stress during installation. Since it is impossible to make the spider perfectly, the structure will be stretched to fit in the aeroplane. Therefore, stresses will occur in the structure. The permissible value is 50MPa and is given by Airbus. When this value is exceeded, shims must be used. They pick up the backlash between the structure and the aeroplane. In this way, the stresses will disappear in the structure. It is preferable not to use the shims because they can be forgotten to reinstall during maintenance.

As shown in Figure 1-49, the spider is fixed in points A, B and C to the aeroplane. An analysis of the clamping stresses can be done by fixing two of this three interfaces. A given displacement is imposed on the third interface. From optical measurements, given by 3D systems, it can be seen that a tolerance of 0,3mm is the standard in SLM printing. A displacement of this order is imposed on the third interface.

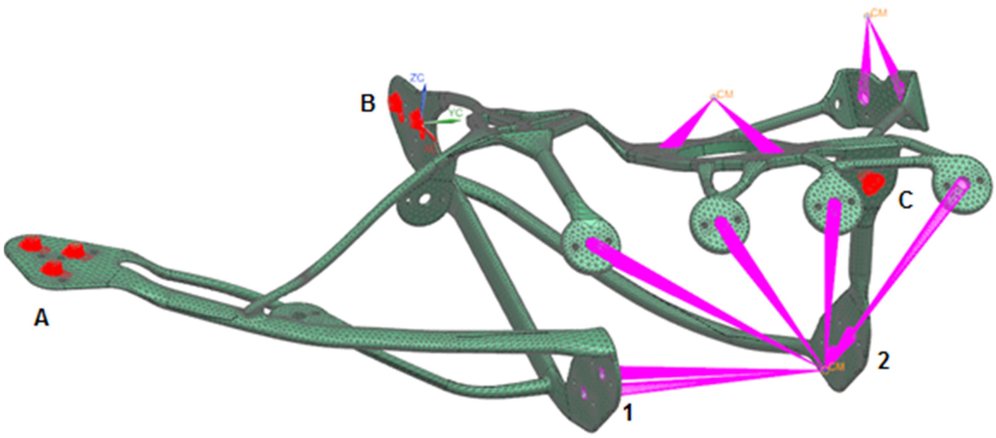

Figure 1-49: Setup validation clamping stresses

It is quite natural that the clamping C with the long rod is always managed at first. The long rod has some moving space in the aeroplane and can accommodate a small deviation. Point A lies further away from the rest of the structure. Therefore it is the most suitable to implement a displacement in this point.

The spider is validated similarly to the analysis of the crash landing, this means that both the coupled interfaces and non-coupled interfaces are investigated. A deviation of 0,3mm is given to interface A of Figure 1-49. Figure 1-50 shows the resulting stresses in the structure. The original, undeformed structure is shown in gray in Figure 1-50.

No coupled interfaces	**Coupled interfaces**

0,3mm displacement in x-direction

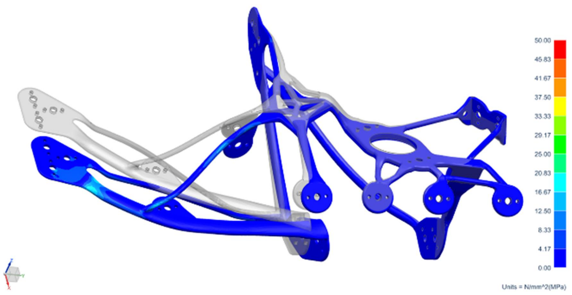

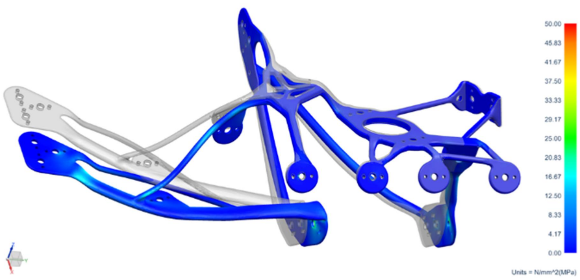

Max. stress: 22,728MPa	Max. stress: 25,740Mpa

0,3mm displacement in y-direction

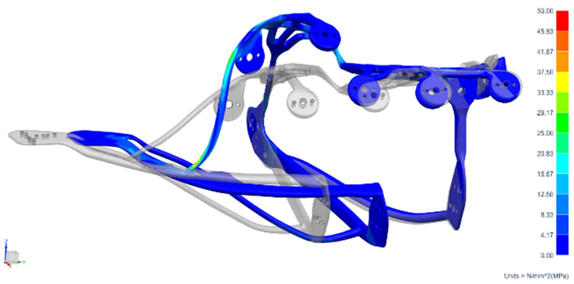

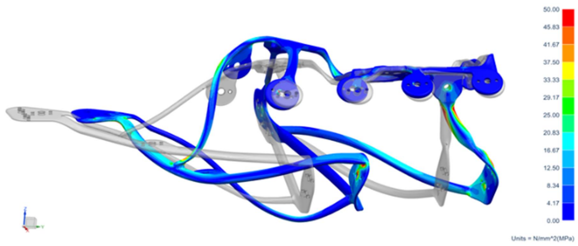

Max. stress: 40,385MPa	Max. stress: 59.595Mpa

0,3mm displacement in z-direction

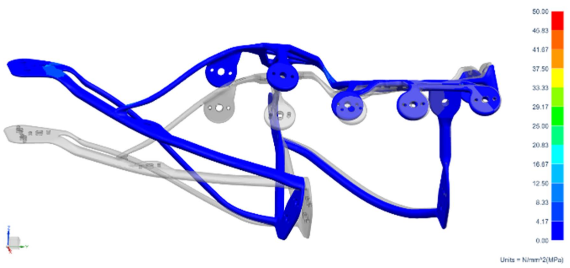

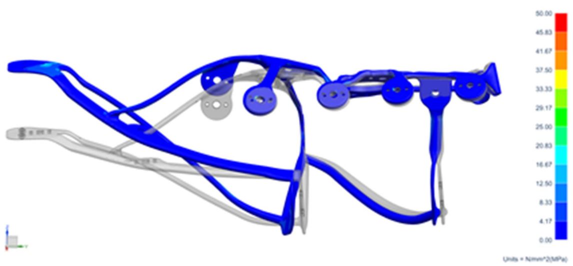

Max. stress: 8,269MPa	Max. stress: 13.932MPa

Figure 1-50: Overview of the clamping stresses in the spider with different displacements.

Only displacements of 0,3mm in the y-direction causes stresses higher than 50MPa in the spider. This means that the structure must be produced within this tolerance in the y-direction. The x-direction and the z-direction are less critical and have more freedom. Furthermore, the maximum stress at the coupled interface is higher than in the uncoupled case. The structure is stiffer due to the coupling of the interfaces. This reduction in freedom of movement results in higher stresses in the structure.

Figure 1-51 shows the stresses in the spider resulting from the combination of a crashlanding and clamping. Figure 1-52 gives the results with non-coupled interfaces. The effect of clamping stresses is negligible compared to crashlanding-stresses when both arises in the structure. The stress distribution during crashlanding is once again shown in Figure 1-53 and Figure 1-54.

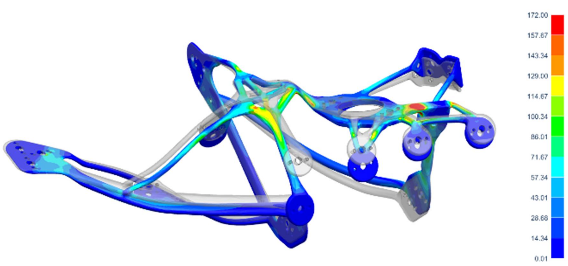

Figure 1-51: Crashlanding and clamping stresses without coupled interfaces

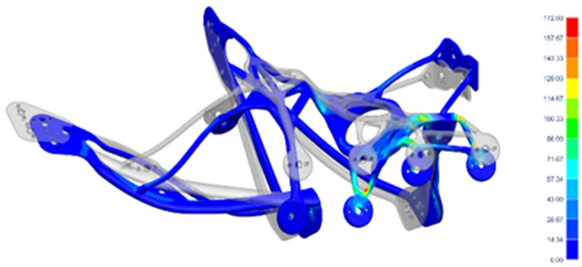

Figure 1-52: Crashlanding and clamping stresses with coupled interfaces.

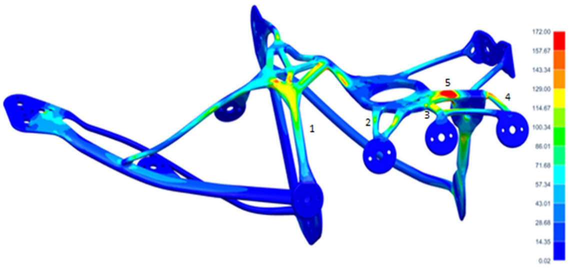

Figure 1-53: Stress distribution during crashlanding without coupled interfaces

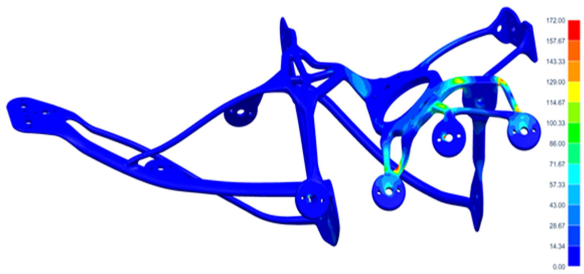

Figure 1-54: Stress distribution during crashlanding with coupled interfaces

A last possible scenario arises when the interfaces 1 and 2 from Figure 1-49 are not at a perfect distance from each other. This will give problems when connecting the manifold and the spider in interfaces 1 and 2. The interfaces must be pulled apart or together in order to fit the manifold. A displacement of 0,3mm is imposed on both interfaces in this validation.

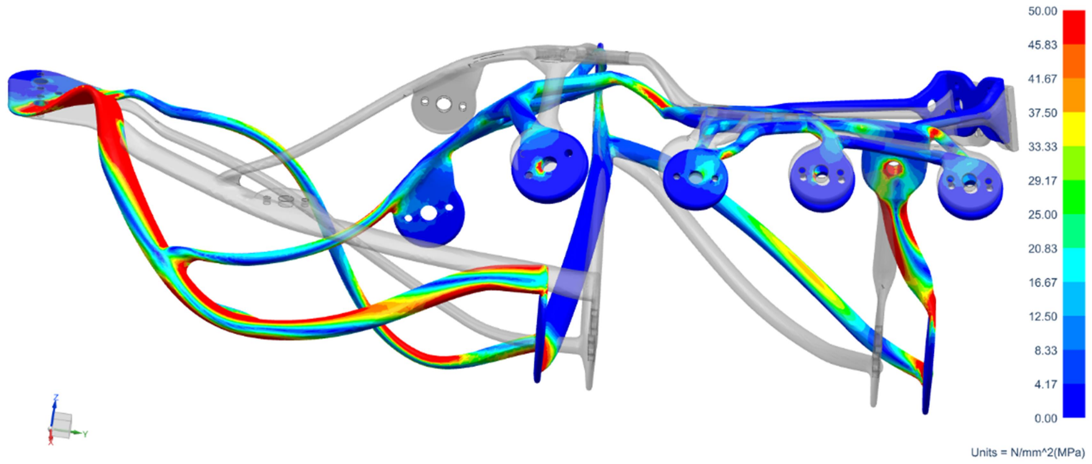

Figure 1-55: Stresses as a result of a non-fitting manifold

It can be deduced from Figure 1-55 that the stresses in this scenario are much higher than allowable. The average stresses in the red struts are about 100MPa. The interfaces for the manifold must be manufactured with the necessary precision to meet all requirements. The fitting of the spider is strongly dependent on the accuracy capabilities of the SLM printing process. If the tolerances of the resulting spider are within the limits of 0,3mm, no shims will be needed. Otherwise the use of shims is unavoidable.

1.5.6.3 Natural frequency

Figure 1-56 shows the complete setup for a frequency analysis. The analysis is done on the spider that meets the requirements for crash landing. In order to find the natural frequency, the spider is clamped the same way as it is in the aeroplane. The weights of the pipes and tubes that are supported, are applied on the structure and are indicated in orange in Figure 1-56. They should be included in the FEM-model since they are also present in a potential windmilling scenario. RBE3 elements ensure the connection between the weights and the spider and are highlighted in purple in Figure 1-56.

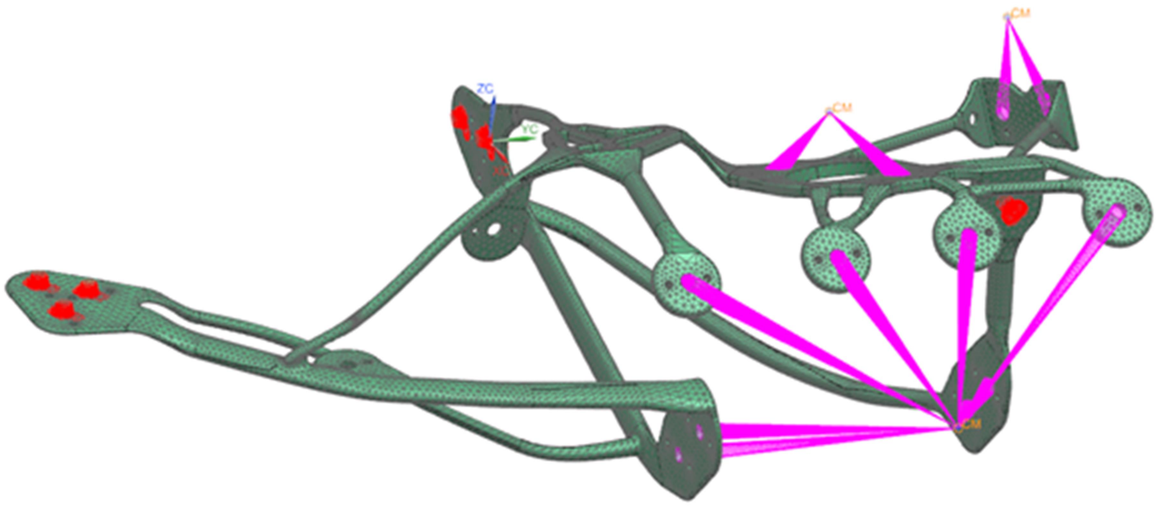

Figure 1-56: Setup natural frequency

Similar to the validation of the crash landing, two possible scenarios are discussed. The difference between the two scenarios is the presence of the coupling constraint between the adjacent interfaces in the front and at the bottom of the structure.

Figure 1-57 to Figure 1-60 show the development of the first three modes and the maximal displacement in two different structures. The first structure has an upper plate thickness of 2mm and the second one has a thickness of 4mm. For both spiders the coupled and the uncoupled natural frequency are illustrated.

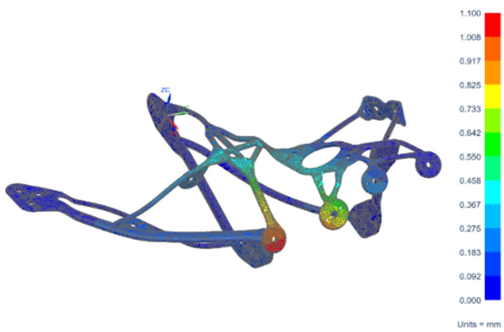

Figure 1-57: 2mm uncoupled spider

Mode 1: 17,936Hz
Mode 2: 52,688Hz
Mode 3: 102,288Hz
Max. displacement: 1,069mm

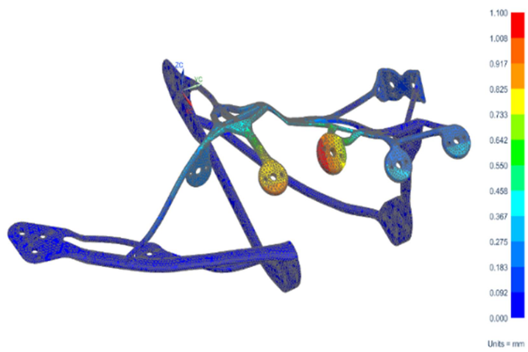

Figure 1-58: 2mm coupled spider

Mode 1: 21,026Hz
Mode 2: 71,854Hz
Mode 3: 99,738Hz
Max. displacement: 1,091mm

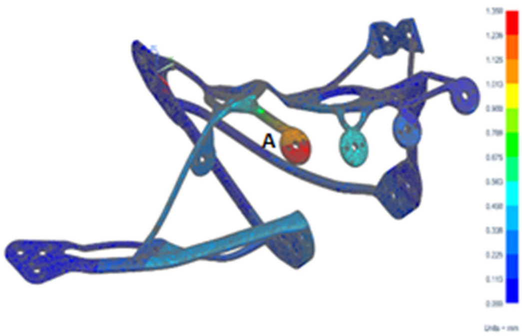

Figure 1-59: 4mm uncoupled spider

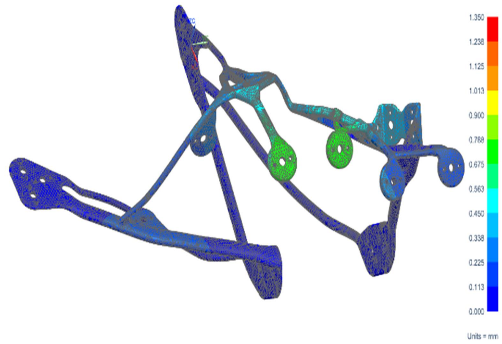

Figure 1-60: 4mm coupled spider

Mode 1: 25,102Hz
Mode 2: 56,042Hz
Mode 3: 116,141Hz
Max. displacement: 1,352mm

Mode 1: 55,049Hz
Mode 2: 116,353Hz
Mode 3: 147,048Hz
Max. displacement: 0,757mm

Figure 1-57 to Figure 1-60 clearly indicate that changes in the geometry affect the natural frequency of the spider. By enlarging the thickness of the struts and interface plates, the structure becomes stiffer and the Eigen frequency increases. The reinforcements set in the crash landing case are also required to meet the requirements related to the natural frequency.

The first mode of the uncoupled 4mm spider is 25,1Hz. This is above the desired value of 25Hz. The structure will not excessively excite at windmilling frequency. Resonance is avoided. On Figure 1-59, it is noticeable that, in this first mode, only interface A will vibrate. This is mainly due to the fact that the designed spider has an open structure. Topology optimized structures are often characterised by this feature. Interface A is only at one place connected to the rest of the spider. This weak connection causes the low natural frequency of the structure.

Therefore it is important to look at the mode where the whole spider vibrates. This is the case at mode 3, thus a frequency of 116Hz. Only at this applied frequency, the whole structure starts to vibrate. At 116Hz, the entire structure can break by resonance. In all of the foregoing cases, only a small interface will break.

The coupled case is less critical than the uncoupled one. Figure 1-60 indicates that the 4mm coupled structure has a first mode of 55,049Hz. This is far above the desired value of 25Hz. The first natural frequency of 55Hz is only valid when it is assumed that the couplings between the interfaces are infinitely stiff.

The 4mm spider is stiff enough. The natural frequency is higher than 25Hz. This condition is always met. The designed system support structure has all requirements met and is now ready to be built into the aeroplane.

2 TRADE-OFF STUDY

While the first part of the thesis discussed the design of the support structure, this part focuses on the financial side of the support structure. The economic potential of selective laser melting is investigated in the trade-off study. The production cost of the designed bracket is calculated followed by a financial comparison of the designed structure and the original structure. All the numbers used in this chapter are provided by S.A.B.C.A. and 3D Systems, unless otherwise mentioned.

2.1 Cost of a topology optimized bracket

To calculate the cost of one topology optimized bracket, the method described by Jason T. Ray [10] is followed. The design engineer of the spider must have had a training in *Altair HyperWorks* and *Geomagic Design X.* The designer must have some experience because a topology optimization requires insight in the design problem. The cost for a company to pay a design engineer varies from 80 to 125 euro per hour. An engineer with the required profile costs 110 euro per hour, more than the average. The experienced design engineer can design the spider in 2 months. This makes a total time of 288 hours.

$$Labour\ cost = 110\frac{€}{hour}\ 288\ hours = €31\ 680$$

The company must pay the licenses for the software used in the design process. The license of *Altair HyperWorks* and *Geomagic Design X* costs respectively €25 000 per year and €19 000 per year. It is assumed that the software is used for two months for this design. The license can be used for other projects during the rest of the year. In the most expensive scenario, only one design project at the time is executed and the cost cannot be divided over multiple parts

$$License\ cost\ Altair\ HyperWorks = 25\ 000\frac{€}{year}\frac{2}{12}year = €4\ 166{,}67$$

$$License\ cost\ Geomagic\ Design\ X = 19\ 000\frac{€}{year}\frac{2}{12}year = €3\ 166{,}67$$

The support structure is produced at a production rate of one item per month for a period of ten years. This means that a total of 120 brackets will be produced. With this information the design cost per bracket can be calculated.

$$Labour\ cost\ per\ bracket = \frac{€31\ 680}{120\ brackets} = 264\frac{€}{bracket}$$

$$Licen\quad cost\ Altair\ HyperWorks\ per\ bracket = \frac{€4\ 166{,}66}{120\ brackets} = 34{,}72\frac{€}{bracket}$$

$$License\ cost\ Geomagic\ Design\ X\ per\ bracket = \frac{€3\ 166{,}67}{120\ brackets} = 26{,}39\frac{€}{bracket}$$

$$Total\ design\ cost = (264 + 34{,}72 +\ 26{,}39)\frac{€}{bracket} = 325{,}11\ \frac{€}{bracket}$$

The production cost of the designed structure consists of multiple costs: material, setup, machine run time and support removal.

The price of AlSi10Mg varies a lot, from 40€/kg to 100€/kg. To calculate the cost, an average of 70€/kg is taken. The topology optimized structure weighs 0,189kg. Due to the complex shape and the relatively large size, there is a lot of support needed. This results in a higher scrap rate than usual. The assumed scrap rate is 25%.

$$Material\ cost\ per\ bracket = 70\frac{€}{kg}\ 0{,}189\frac{kg}{bracket}\ 1{,}25 = 16{,}54\frac{€}{bracket}$$

The setup cost includes the file preparation. The support for the designed structure are created by software in this step. This will take 8 hours for this structure and it is a non-recurring cost. For the production of the following brackets, the file preparation will take half an hour. During the setup machine time, the settings are set and the machine is filled up with the right metal powder. The setup machine time will take 2 hours including the time to recycle metal powder. The labour cost of the operator to do this job is 40€/hour.

$$File\ preparation\ per\ bracket = \frac{8\ hours}{120\ brackets} + 0{,}5\frac{hours}{bracket} = 0{,}56\frac{hour}{bracket}$$

$$Setup\ cost\ per\ bracket = (2 + 0{,}56)\frac{hours}{brackets}\ 40\frac{€}{hour} = 102{,}4\frac{€}{bracket}$$

The calculation of the machine run time depends on confidential information of 3D Systems. Values for the deprecation period, asset utilization and hurdle rate come from the article of Jason T. Ray [10]. The deprecation period is 2 years. This is the period that a SLM printer remains competitive with the new technologies. The asset utilization is 80%. This means that the SLM printer is almost all the time in use, knowing that there is a maintenance period. The hurdle rate is 5% and is dependent on the company. According to 3D Systems, the purchase cost of a new machine is between €300 000 and €700 000. The average of €500 000 is taken as purchase cost. Yearly 10% of this cost goes to maintenance. With a simplified net present value calculation the monthly machine cost can be calculated:

$$Monthly\ machine\ cost = \frac{(purchase\ cost \cdot (1 + hurdle\ cost \cdot deprecation\ time) + maintenance\ )}{deprecation\ time}$$

$$Monthly\ machine\ cost = \frac{\left(€500\,000\left(1 + \frac{5\%}{year}\ 2years\right) + €500\,000\ \frac{10\%}{year}\ 2years\ \right)}{2years\ 12\frac{months}{years}} = 27\,083\frac{€}{month}$$

The SLM printer is available every day except when maintenance is occurring. The print process cannot suddenly be stopped when the weekend begins. The process continues during the weekend until it is finished.

$$Monthly\ available\ time = 30\frac{days}{month}24\frac{hours}{days}80\% = 576\frac{hours}{month}$$

$$Machine\ run\ time\ cost = 27\,083\frac{€}{month}\frac{1}{576}\ \frac{month}{hours} = 47{,}02\frac{€}{hour}$$

The SLM printer can produce 2 brackets in one run. The printing of these 2 brackets takes 80 hours. The machine run time for one bracket in this situation is 40 hours.

$$Machine\ run\ time\ cost\ per\ bracket = 47{,}02\frac{€}{hour}\ 40\frac{hours}{bracket} = \ 1\ 881\frac{€}{bracket}$$

After the bracket is printed, the supports need to be removed. The support removal will take the operator 3 hours.

$$Removal\ cost = 3\frac{hours}{bracket}\ 40\frac{€}{hour} = 120\frac{€}{bracket}$$

The time to recover the metal powder is been charged in the setup cost. The production cost of the bracket is the sum of the previous calculated costs.

$$Production\ per\ bracket = \frac{Material\ cost +\ \ setup\ cost + machine\ run\ time\ cost + removal\ cost}{bracket}$$

$$Production\ cost\ per\ bracket = (16{,}54 + 102{,}4 + 1881 + 120)\frac{€}{bracket} = 2\ 120\frac{€}{bracket}$$

The fail rate of the production is maximally 5% according to 3D Systems. The total production cost can be calculated if the fail rate is brought into account. The profit from the recycle of the broken component is negligible.

$$Total\ production\ cost\ per\ bracket = 1{,}05 \cdot 2\ 120\frac{€}{bracket} = \ 2\ 226\frac{€}{bracket}$$

It is possible to post-process the bracket after the production. Post-processes are meant to modify the mechanical properties of the produced structure. The only post-processing process of the spider is a heat treatment. This costs €200 for 2 brackets.

$$Post - processing\ cost\ per\ bracket = \ 200\frac{€}{2\ brackets} = 100\frac{€}{bracket}$$

Every 20 brackets, 1 bracket is optically measured. An optical scan costs €300 per brackets. For a total of 120 brackets, 6 brackets are measured. The qualification cost can be divided over all the brackets.

$$Qualification\ cost\ per\ bracket = 6\ brackets\ 300\frac{€}{bracket}\frac{1}{120\ brackets} = 15\frac{€}{bracket}$$

$$Total\ post - processing\ cost\ per\ bracket = (100 + 15)\frac{€}{bracket} = 115\frac{€}{brack}$$

With an overhead of 10%, the cost per bracket can be calculated. This is the price that will be used in the comparison with the original structure.

$$Cost\ per\ bracket = (total\ design\ cost + total\ production\ cost + total\ post - processing\ cost)(1 + overhead)$$

$$Cost\ per\ bracket = (325{,}11 + 2\ 226 + 115)1{,}1\ \frac{€}{bracket} = 2\ 932{,}72\frac{€}{bracket}$$

Figure 2-1 shows the cost distribution of the bracket. The production cost is 76% of the total cost and is the most determining factor for the final price of the bracket. To lower the price of the bracket, it is best to focus on lowering the production cost. Figure 2-2 gives the cost distribution of the production cost.

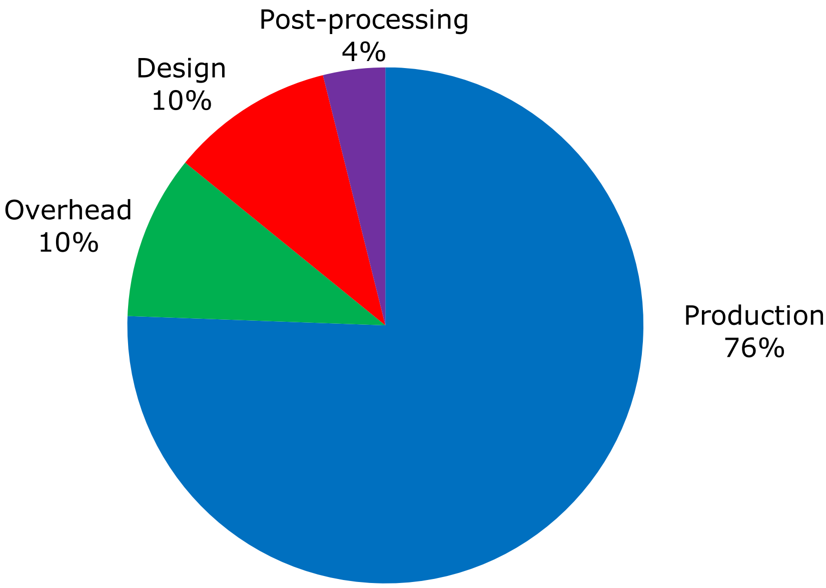

Figure 2-1: Cost distribution of bracket

The production consists almost completely of the machine run time cost. The machine run time cost is 88% of the total production cost. A lowering of this cost can lower the final price drastically. This can be achieved by extending the deprecation time. If the technology of the SLM printer is longer competitive with new models, the machine run time will lower inversely proportional with the deprecation time. By way of example if the deprecation time doubles to 4 years, the machine run time cost is lower. This results in a saving of €760 with the overhead and failure included.

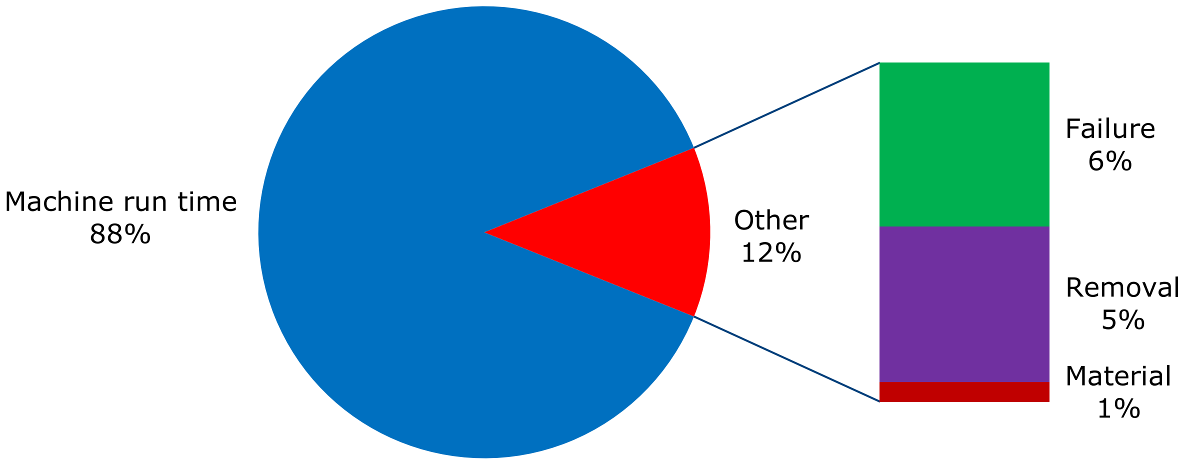

Figure 2-2: Cost distribution of production cost

2.2 Comparison

If S.A.B.C.A. buys the original structure from a subcontractor, they pay around €400 per bracket. In aviation every component has to be electrically connected with each other. This is to avoid a difference in the electrical potential between the components. Since the spider supports fuel pipes it is important to avoid sparks. The SLM produced structure consists of a single part while the original structure is made up of of 11 different parts. All these different parts are connected with electrical wiring. This wiring costs €50/bracket more than the SLM produced bracket.

Extra components like floating nuts, rivets and bolts, cost around €100 for both structures. The assembly time is the time to assemble the extra components on the structure and to install the structure. The assembly time for the SLM produced bracket is 1,5 hour. The assembly time for the original bracket is half an hour longer because there are more components to install. The technician to install the structure costs the company around €30 per hour.

$$Assembly\ cost\ for\ original\ bracket = 2hours\ 30\frac{€}{hour} = €60$$

$$Assembly\ cost\ for\ SLM\ produced\ bracket = 1{,}5hours\ 30\frac{€}{hour} = €45$$

With this information the cost of the bracket as installed in the plane can be calculated.

Table 2-1: Installation cost of the structures

	Original bracket	SLM produced bracket
Purchase cost	€400	€2 933
Extra components	€150	€100
Assembly cost	€60	€45
The cost of the bracket as installed	€610	€3 078

The spider has also a lifetime cost. Because the plane moves, every component has a cost on fuel. The specifications of the Falcon 5x, a similar business jet, are used to calculate the fuel consumption. [11]. The method used is according to the method of Jason T. Ray [12].

Fully tanked the business jet can fly maximum 9 630km. The maximum amount of fuel is 12 791kg. Since kerosene has a density of 0,80kg/l, the total volume of the fuel is 15 988l. This gives:

$$Fuel\ consumption = \frac{15\ 988l}{9\ 630km} = 1{,}66\frac{l}{km}$$

The fuel price of kerosene at the stock market in New York on 11 April 2017 is 310,6 cents per gallon. This is 0,756 €/l.

$$Fuel\ cost\ per\ km = 0{,}76\frac{€}{l}\ 1{,}66\frac{l}{km} = 1{,}26\frac{€}{km}$$

The maximal zero fuel weight of the plane is 19 731kg.

$$Fuel\ cost\ per\ km\ per\ kg = 1{,}26\frac{€}{km}\ \frac{1}{19\ 731\ kg} = 6{,}36\ 10^{-5}\frac{€}{km\ kg}$$

The business jet will accomplish 20 000 flight cycles. An average flight cycle is 40% of the range of the plane. The support structure must be replaced after 20 years.

$$Flown\ distance\ = 20\,000\ flight\ cycles\ 3852\frac{km}{flight\ cycle} = 7\,704\ 10^4 km$$

With this information the cost on fuel consumption per kg can be calculated.

$$Cost\ per\ kg = \ Fuel\ cost\ per\ km\ per\ kg \cdot Flown\ distance$$

$$Cost\ per\ kg = \ 6{,}36\ 10^{-5}\frac{€}{km\ kg}\ \ 7\,704\ 10^4 km = 4\,900\frac{€}{kg}$$

The mass of the original structure is 0,380kg. The SLM produced structure weighs 0,189kg.

$$Fuel\ cost\ for\ original\ structure = 0{,}380 kg\ 4\,900\frac{€}{kg} = €1\,862$$

$$Fuel\ cost\ for\ SLM\ produced\ bracket = 0{,}189 kg\ 4\,900\frac{€}{kg} = €926{,}10$$

The maintenance cost is included in the lifetime cost of the structure. This cost is the same for both structures. The structure is yearly inspected. The inspection time is 5 minutes. This job is performed by an engineer who is paid €80 per hour.

$$Yearly\ maintenance\ cost\ = 5\frac{minutes}{year}\ \frac{hour}{60\ minutes}\ 80\frac{€}{hour} = 6{,}67\frac{€}{year}$$

A bracket has a lifetime of 20years.

$$Total\ maintenance\ cost = 6{,}67\frac{€}{year} 20\frac{years}{lifetime}\ = 133{,}33\frac{€}{lifetime}$$

Both structures are designed to be used for the entire lifetime of the plane. Statistical information about failure is not available. The replacement cost of the structure and its extra components is assumed to be zero. Also the cost or earnings of the decomposition and recycling of the structure is unknown. This is not included in the cost calculation.

Table 2-2: Total cost of the structures with comparison

	Original bracket	SLM produced bracket	Profit/Loss
Cost bracket as installed	€610	€3 078	-€2 468
Fuel cost	€1 862	€926,10	€935,90
Total maintenance cost	€133,33	€133,33	€0
Total cost	€2 605,33	€4 137,43	-€1 532,1

Table 2-2 gives the cost comparison between the two brackets. Over the whole lifetime of the plane the SLM produced bracket costs €1 532,1 more than the original bracket. Figure 2-3 gives a break-even analysis. The fixed costs for a bracket over its lifetime are the installation and maintenance cost. The variable cost is the fuel cost. This analysis proves that it is impossible to make profit in the current situation. The break-even point is when the plane travels 202 10^6km or 104% of its maximum range per flight cycle. The bracket has to weigh less than 0,179kg to have a break-even point before 100%.

At the end of section 2.1 a possibility to save money on production cost was discussed. If this saving is included in the break-even analysis with a bracket weight of 0,189kg, the break-even point is 127,93 10^6km. This is 66,4% of the maximum range per flight cycle. The SLM produced bracket becomes profitable if the purchase cost of the bracket lowers. Extending the deprecation time of the SLM printer have to be considered.

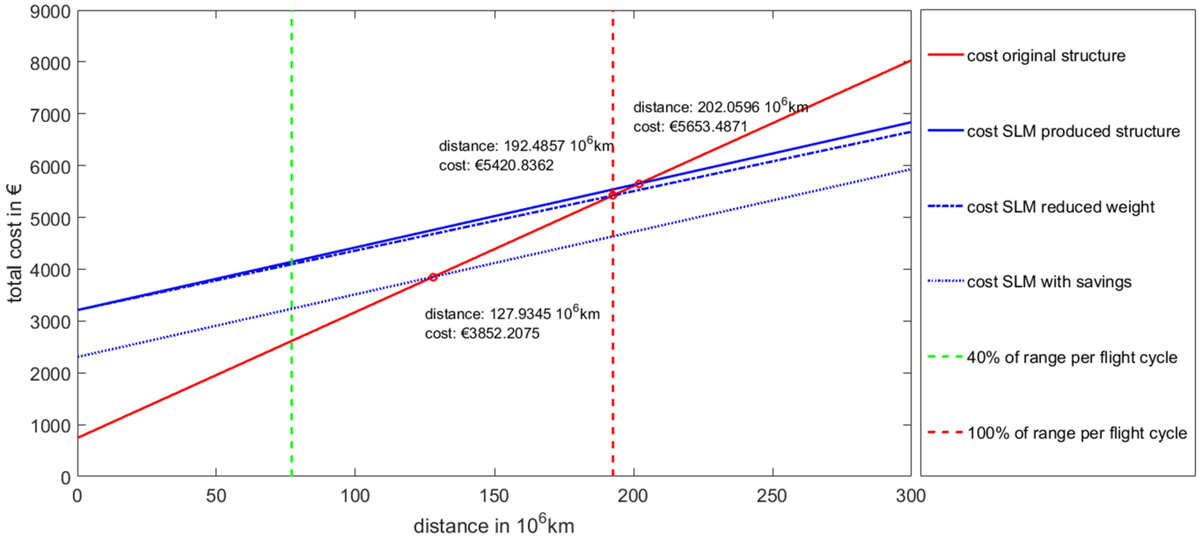

Figure 2-3: Break-even analysis

It is important to notice that in the previous calculation the fuel price is considered constant over the years. In reality this is not the case. Figure 2-4 shows the kerosene price over the last two years. The price has increased with 6,43% over two years. This is an average annual increase of 3,22%. [13]

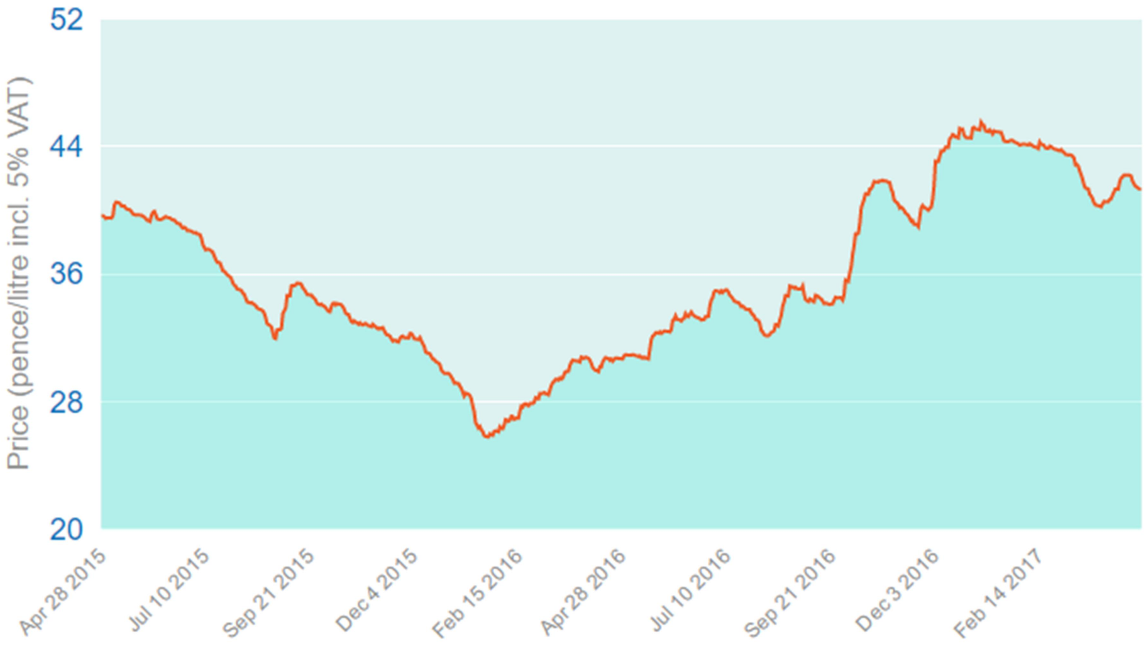

Figure 2-4: Average kerosene price in the UK over the past two years

Figure 2-5 is the break-even analysis with an increasing fuel price. It is assumed that the flown time is evenly distributed over the lifetime of the plane. The fuel price has a constant increase of 3,22% per year. Figure 2-5 points out that there is no break-even point in the lifetime of the plane if 40% of the maximum range is travelled per flight cycle. To obtain a break-even point in the lifetime of the bracket, 55,6% of the range must be travelled per flight cycle. When flying at 100%, the break-even point is reached after 13,618 years.

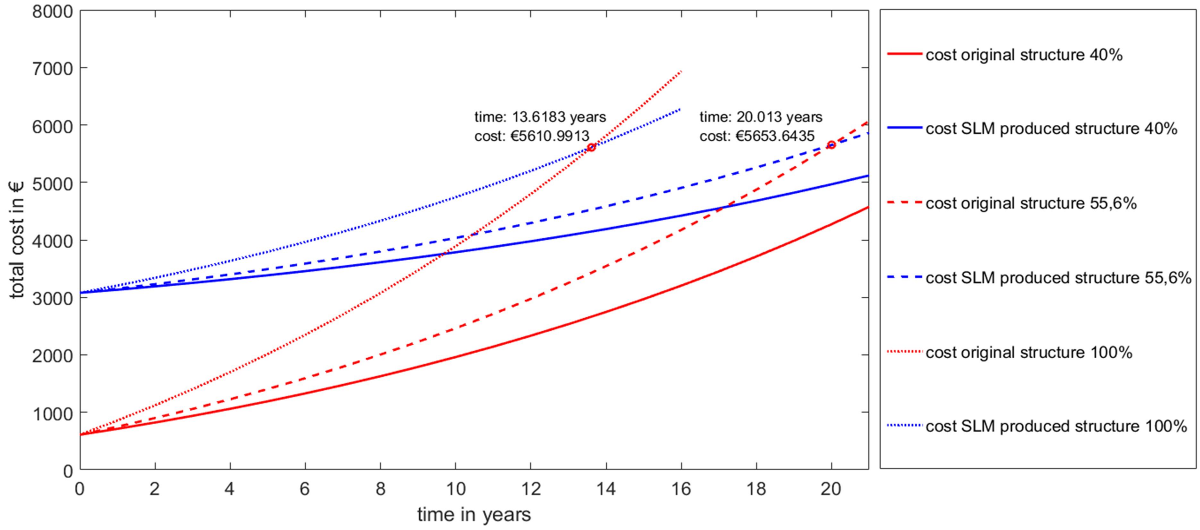

Figure 2-5: Break-even analysis with variable fuel price

Figure 2-3 and Figure 2-5 show that it is possible to reach a break-even point. Figure 2-6 shows the cost distribution of the two brackets. The cost distribution is based on the values of Table 2-1. The total cost of the SLM produced bracket is mainly determined by the cost of the bracket as installed. Figure 2-3 proves that reducing this cost gives a break-even point. Figure 2-5 shows that the break-even point is reached when the fuel price increases and the plane travels more than 55,6% of its range per flight cycle. The cost distribution shows that the total price of the original structure is strongly influenced by the fuel cost. As previously mentioned, the fuel cost increases with the years. This means that a low weight support structure becomes more and more profitable.

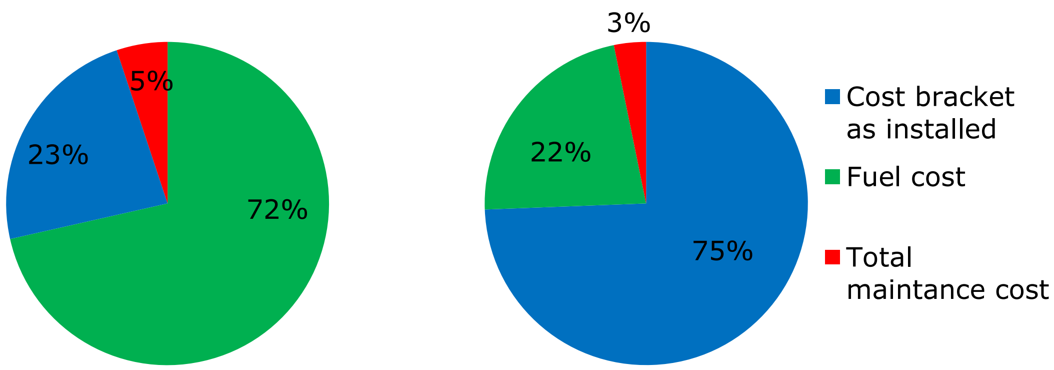

Figure 2-6: Left) Cost distribution of original bracket Right) SLM produced bracket

The break-even analyses show that it is important to investigate and make hypotheses of the future fuel prices and the expected usage of the customer. These factors determine wheter the original or SLM produced bracket is more profitable or not.

CONCLUSION

The aim of this thesis is to investigate the feasibility of AM as a manufacturing method for system support brackets in aircraft. This investigation includes the design, testing and producibility of a system support bracket. The additive manufactured structure, named 'spider', will serve as a technology demonstrator. The technology demonstrator exhibits the possibilities of AM to replace the current system support bracket.

The resulting topology optimized structure has a weight of 0,189kg. The mass of the original structure is 0,380kg. A weight reduction of 50% is accomplished using the techniques of topology optimization. Since fuel cost is related to the mass of the aeroplane, one can derive that the savings on this part of the total cost is significant.The topology optimized 'spider' suffices all requirements set by S.A.B.C.A. and 3D Systems. These requirements are related to operational circumstances as well as installation circumstances. All the requirements were individually tested using the appropriate tools. When the structure fails to fulfil one of the requirements, it has to be redesigned and the validations should be repeated.

The installation requirements are implemented in the design of the spider based on knowledge and experience. These cannot be validated with a software program. The stress related requirements are validated using a finite element package namely the *Siemens NX* software. Three different scenarios were simulated and tested.

First the crash-landing is discussed. During this load case, the spider preferably does not undergo any plastic deformation. This means that the internal stresses have to be under the yield strength of the used material. The results of the simulation indicates that the topology optimized structure showed excessive internal stresses. The spider had to be redesigned to meet the requirement. The stresses in the second structure were under the allowable limit.

The next validation is the clamping stress requirement. The spider will always have to be stretched to fit in the aeroplane due to production tolerances. From the results of the finite element analysis, it can be concluded that the spider is really sensitive to deviations in the y-direction, but less sensitive in the other two directions. A deviation of 0,3mm is the maximum in order to stay within the limits.

Finally a frequency analysis is carried out on the structure. This is important in a windmilling scenario. Here, the structure will vibrate at a frequency of 25Hz. The designed support structure has a natural frequency of 55Hz. This indicates that the structure will not resonate at windmilling frequency.

In addition to all the technical related issues, the economic side has also been studied to fully answer the research question. The total cost to produce and install the bracket is €3078. The total cost for the original bracket is €610. The fuel saving with the SLM structure is €935,90. This proves that it is presently impossible to achieve a cost saving over the operational life of the aircraft, unless the weight of the structure is reduced, the deprecation time of the SLM printer is extended or the increasing fuel prices are taken into account.

This thesis indicates that additive manufacturing has a lot of opportunities in the aerospace industry, but it is still too early to speak of a real breakthrough. At the technical level, there are no significant problems but there are still some issues to overcome on the economic side. The total cost of production should decrease to commercialize the spider. All factors of the AM process must evolve to realize this decline. The technology is currently too expensive to replace conventional techniques. However, if the technology continues on evolving as in the previous years, it will not take long before the transition takes place.

REFERENCES

[1] M. Alzahrani, "Design of truss-like cellular structures using density information from topology optimization," Georgia Institute of Technology, Georgia, 2014.

[2] H. A. Eschenauer and O. Niels, "Topology optimization of continuum structures: a review," American Society of Mechanical Engineers, Siegen, 2001.

[3] M. Bendsoe and O. Sigmund, Topology Optimization: Theory, Methods and Applications, Berlin: Springer, 2003.

[4] A. Gebhardt, Rapid Prototyping, Munich: Hanser Publishers, 2003.

[5] J. Van Humbeek, "KU Leuven," 2016. [Online]. Available: https://www.mtm.kuleuven.be/Onderzoek/Ceramics/research/additive-manufacturing. [Accessed 2 February 2017].

[6] D. Thomas, "The Development of Design Rules for Selective Laser Melting," University of Wales Institute, Cardiff, 2009.

[7] D. Paramita, C. Ramya, S. Rutuja and A. Sam, "Optimum Part Build Orientation in Additive Manufacturing for Minimizing Part Errors and Support Structures," Elsevier, Amsterdam, 2015.

[8] R. Ponginan, "Meaning of compliance," Altair HyperWorks, 16 September 2014. [Online]. Available: http://forum.altairhyperworks.com/index.php?/topic/13591-meaning-of-compliance/. [Accessed 17 February 2017].

[9] M. T.M. and L. M.J., "Mechanical Behaviour of Additive Manufactured, Powder-bed Laser-fused Materials, Material Science and Engineering," Elsevier, Amsterdam, 2016.

[10] J. T. Ray, "Calculating the cost of additive manufacturing," paperlessPARTS, 6 December 2016. [Online]. Available: https://www.linkedin.com/pulse/calculating-cost-additive-manufacturing-jason-t-ray?trk=hp-feed-article-title-ppl-follow. [Accessed 18 April 2017].

[11] Dassault, "Dassault Falcon 5X," Dassault Aviation, [Online]. Available: http://www.dassaultfalcon.com/en/Aircraft/Models/5X/Pages/overview.aspx. [Accessed 23 April 2017].

[12] J. T. Ray, "Economic Benefits of Additive Manufacturing in Aerospace," paperlessPARTS, 30 November 2016. [Online]. Available: https://www.linkedin.com/pulse/economic-benefits-additive-manufacturing-aerospace-jason-t-ray. [Accessed 23 April 2017].

[13] Boilerjuice.com, Artist, *Kerosene Prices in the UK.* [Art]. Boilerjuice, 2017.

APPENDIX A

Form Approved
OMB No 0704-0188

CONFIGURATION OF NUT OPTIONAL WITHIN THE LIMITATIONS IMPOSED BY DIM'S, AND REQUIREMENTS AS SPECIFIED HEREIN

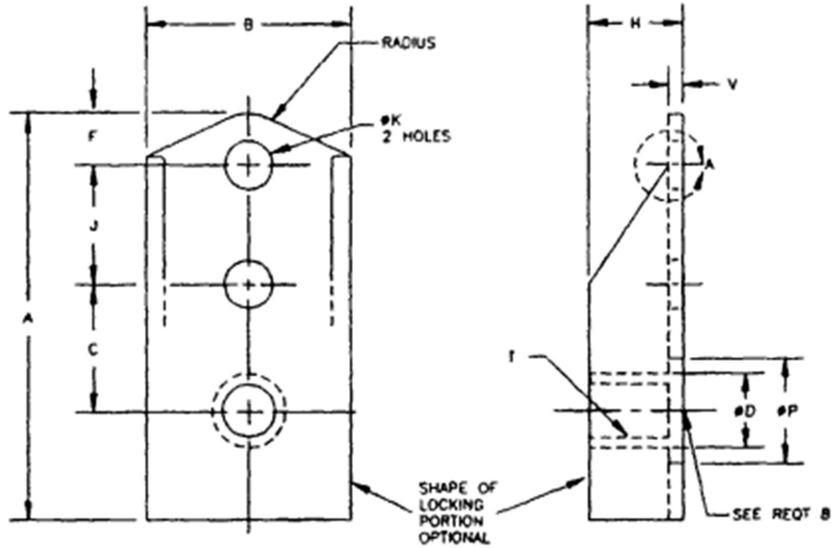

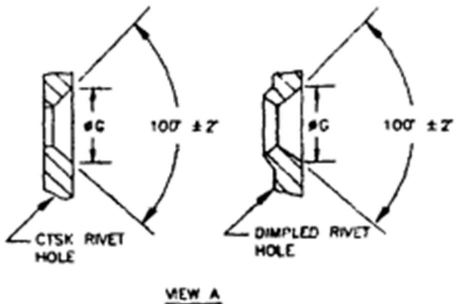

VIEW A

TABLE I DASH NUMBERS AND DIMENSIONS

DASH NUMBERS																			
PLAIN RIVET HOLES		COUNTERSUNK OR DIMPLED RIVET HOLES																	
NON-DRY FILM LUBRICANT	DRY FILM LUBRICANT	NON-DRY FILM LUBRICANT	DRY FILM LUBRICANT	T THREAD SIZES	A MAX	B MAX	B MIN	C ± 005	⌀D MIN	F MIN	⌀G ± 010	H 1/ MAX	J ± 002	⌀K 2/ + 005 − 000	⌀P MAX	⌀P MIN	V MAX	AXIAL STRENGTH LBS/MIN	WEIGHT LBS/100
-04	L04	-04K	L04K	112-40UNJC-3B	1 051	422	290	344	–	100	200	175	312	098	270	172	032	750	52
-06	L06	-06K	L06K	138-32UNJC-3B	1 051	422	290	344	–	100	200	203	312	098	270	198	032	1,130	53
-08	L08	-08K	L08K	164-32UNJC-3B	1 051	422	290	344	168	100	200	250	312	098	270	224	032	1,720	54
-3	L3	-3K	L3K	190-32UNJF-3B	1 051	422	290	344	194	100	200	250	312	098	270	250	032	2,460	56
-4	L4	-4K	L4K	250-28UNJF-3B	1 308	531	350	500	254	100	.200	281	312	098	330	310	032	4,580	93
-5	L5	-5K	L5K	3125-24UNJF-3B	1 398	641	412	500	317	125	230	328	312	130	392	372	045	7,390	1 44
-6	L6	-	-	375-24UNJF-3B	1 422	703	656	500	380	125	230	479	312	130	487	438	075	11,450	2 00
-8	L8	-	-	500-20UNJF 3B	1 800	859	796	625	504	125	230	595	500	161	550	500	075	15,450	2 50

1/ MINIMUM "H" NOT SPECIFIED LIMITED ONLY BY STRENGTH REQUIREMENTS OF SPECIFICATION
2/ DIMPLED RIVET HOLE TOLERANCE FOR "⌀K" IS + 015 − 000

(G) DENOTES CHANGES

INCH-POUND

PREPARING ACTIVITY DLA-IS
CUSTODIANS ARMY- AV NAVY- AS
AIR FORCE- 11 DLA-
REVIEW
USER CR, MI
PROJECT NUMBER 5310-1950

MILITARY SPECIFICATION SHEET

TITLE

NUT, SELF-LOCKING, PLATE, ONE LUG, FLOATING, LOW HEIGHT, STEEL, 125 KSI Ftu 450° F

SPECIFICATION SHEET NUMBER
MS21061 1 FEB 94 REV C

SUPERSEDING
MS21061F 30 SEP 87 (SEE NOTE 5)

AMSC- N/A FSC 5310

DISTRIBUTION STATEMENT
A. Approved for public release distribution is unlimited

Form Approved
OMB No. 0704-0188

REQUIREMENTS

(G) 1 MATERIAL. CARBON STEEL COMPOSITIONS 1035 (UNS G10350) 1040 (UNS G10400) AND 1050 (UNS G10500) IN ACCORDANCE WITH ASTM A827 OR QQ-S-700 1042 (UNS G10420) IN ACCORDANCE WITH ASTM A29 ALLOY STEEL GRADES 4130 (UNS G41300) 4340 (UNS G43400) AND 8740 (UNS G87400) IN ACCORDANCE WITH ASTM A29

2 FINISH. CADMIUM PLATE IN ACCORDANCE WITH QQ-P-416 TYPE II CLASS 2 FOR DRY FILM LUBRICATED NUTS THE TYPE AND CLASS ARE OPTIONAL IF THE NUTS MEET THE SALT SPRAY REQUIREMENTS OF QQ-P-416 TYPE II

3 DIMENSIONING AND TOLERANCING. DIMENSIONING AND TOLERANCING SHALL BE IN ACCORDANCE WITH ANSI Y14 5M

4 HARDNESS. 49HRC, MAX

5 THREADS. THREADS BEFORE LUBRICATION IN ACCORDANCE WITH MIL-S-8879

6 SURFACE TEXTURE. SURFACE TEXTURE UNLESS OTHERWISE SPECIFIED SHALL NOT EXCEED 125 MICROINCHES IN ACCORDANCE WITH ANSI/ASME B46 1

7 LUBRICANT. DRY FILM LUBRICANT APPROVED IN ACCORDANCE WITH MIL-N-25027 NON-DRY FILM LUBRICANTS SHALL BE SOLUBLE IN THE CLEANER SPECIFIED IN MIL-S-8802

8 COUNTERBORE/COUNTERSINK. ON SIZE 164 AND LARGER THREAD RELIEF SHALL BE 062 MINIMUM, ON SIZE 138 AND SMALLER, COUNTERSINK OR RADIUSED WITHIN "P" DIAMETER

9 FLOAT OF NUT PORTION. FLOAT OF NUT PORTION OF ASSEMBLY SHALL NOT BE LESS THAN 030 RADIALLY FROM CENTERED POSITION NUT ELEMENT SHALL BE CAPABLE OF ENGAGEMENT WITH BOLT IN THE MAXIMUM MISALIGNED POSITION

10 PART NUMBER. THE PART NUMBER SHALL CONSIST OF THE BASIC MS NUMBER FOLLOWED BY A DASH NUMBER FROM TABLE I

EXAMPLE. MS21061L4K

- L4K — DASH NUMBER
- MS21061 — BASIC MS NUMBER

MS21061L4K INDICATES NUT, SELF-LOCKING PLATE ONE LUG FLOATING LOW HEIGHT, STEEL, 125 KSI Ftu, 450° F, 250-28 UNJF-3B DRY FILM LUBRICANT, COUNTERSUNK OR DIMPLED HOLES

NOTES

1 ALL DIMENSIONS ARE IN INCHES

2 IN THE EVENT OF A CONFLICT BETWEEN THE TEXT OF THIS STANDARD AND THE REFERENCES CITED HEREIN THE TEXT OF THIS STANDARD SHALL TAKE PRECEDENCE

3 REFERENCED GOVERNMENT (OR NON-GOVERNMENT) DOCUMENTS OF THE ISSUE LISTED IN THAT ISSUE OF THE DEPARTMENT OF DEFENSE INDEX OF SPECIFICATIONS AND STANDARDS (DODISS) SPECIFIED IN THE SOLICITATION FORM A PART OF THIS STANDARD TO THE EXTENT SPECIFIED HEREIN

4 DESIGN AND USAGE LIMITATIONS THESE NUTS ARE DESIGNED TO DEVELOP THE TENSILE STRENGTH OF BOLTS AND SCREWS WITH AN ULTIMATE TENSILE STRENGTH OF 125 KSI BASED ON THE CROSS SECTION AREA AT THE BASIC ROOT DIAMETER OF THE THREADS THESE NUTS ARE DESIGNED TO BE USED ON A 3A EXTERNAL THREADS THESE NUTS SHALL BE USED IN ACCORDANCE WITH THE LIMITATIONS OF MS33588 ONLY NUTS FOR WHICH THERE ARE QUALIFIED PRODUCTS LISTED ON QPL 25027 SHALL BE USED

5 MS21061 SUPERSEDES NAS 687, NAS 1032 (IN PART)

PREPARING ACTIVITY DLA-IS CUSTODIANS ARMY- AV NAVY- AS AIR FORCE- 11 DLA- REVIEW USER CR MI PROJECT NUMBER 5310-1950	MILITARY SPECIFICATION SHEET TITLE NUT, SELF-LOCKING, PLATE, ONE LUG, FLOATING, LOW HEIGHT STEEL, 125 KSI Ftu, 450° F	SPECIFICATION SHEET NUMBER MS21061 1 FEB 94 REV G SUPERSEDING MS21061F 30 SEP 87 (SEE NOTE 5) AMSC- N/A FSC 5310

DISTRIBUTION STATEMENT
A. Approved for public release, distribution is unlimited

Form Approved
OMB No 0704-0188

INTERCHANGEABILITY RELATIONSHIP

MS21061 NUTS CAN UNIVERSALLY REPLACE NAS687 AND NAS1032 NUTS OF ALL LIKE MATERIAL, THREAD SIZE LUBRICANT (DRY FILM OR NON-DRY FILM LUBRICANT) FASTENING METHOD (PLAIN RIVET HOLES DIMPLED OR COUNTERSUNK RIVET HOLES) BUT THESE NAS687 AND NAS1032 NUTS CAN NOT UNIVERSALLY REPLACE MS21061 NUTS

INTERCHANGEABILITY TABLE

CANCELLED PART NUMBERS		SUBSTITUTIVE PART NUMBERS
NAS687X04	---	MS21061-04
NAS687X04K	---	MS21061-04K
NAS687A04	NAS1032A04	MS21061L04
NAS687A04K	---	MS21061L04K
NAS687X06	---	MS21061-06
NAS687X06K	---	MS21061-06K
NAS687A06	NAS1032A06	MS21061L06
NAS687A06K	---	MS21061L06K
NAS687X08	---	MS21061-08
NAS687X08K	---	MS21061-08K
NAS687A08	NAS1032A08	MS21061L08
NAS687A08K	---	MS21061L08K
NAS687X3	---	MS21061-3
NAS687X3K	---	MS21061-3K
NAS687A3	NAS1032A3	MS21061L3
NAS687A3K	---	MS21061L3K
NAS687X4	---	MS21061-4
NAS687X4K	---	MS21061-4K
NAS687A4	NAS1032A4	MS21061L4
NAS687A4K	---	MS21061L4K
NAS687X5	---	MS21061-5
NAS687X5K	---	MS21061-5K
NAS687A5	NAS1032A5	MS21061L5
NAS687A5K	---	MS21061L5K
---	---	MS21061-6
---	NAS1032A6	MS21061L6
---	---	MS21061-8
---	NAS1032A8	MS21061L8

PREPARING ACTIVITY DLA-IS
CUSTODIANS ARMY- AV NAVY- AS
AIR FORCE- 11 DLA-
REVIEW
USER CR, MI
PROJECT NUMBER 5310-1950

MILITARY SPECIFICATION SHEET

TITLE

NUT, SELF-LOCKING, PLATE, ONE LUG, FLOATING, LOW HEIGHT, STEEL 125 KSI Ftu 450° F

SPECIFICATION SHEET NUMBER
MS21061 1 FEB 94 REV G

SUPERSEDING
MS21061F 30 SEP 87 (SEE NOTE 5)

AMSC- N/A FSC 5310

DISTRIBUTION STATEMENT
A Approved for public release distribution is unlimited

APPENDIX B

Form Approved
OMB No 0704-0185

CONFIGURATION OF NUT OPTIONAL WITHIN THE LIMITATIONS IMPOSED BY DIMENSIONS AND REQUIREMENTS AS SPECIFIED HEREIN

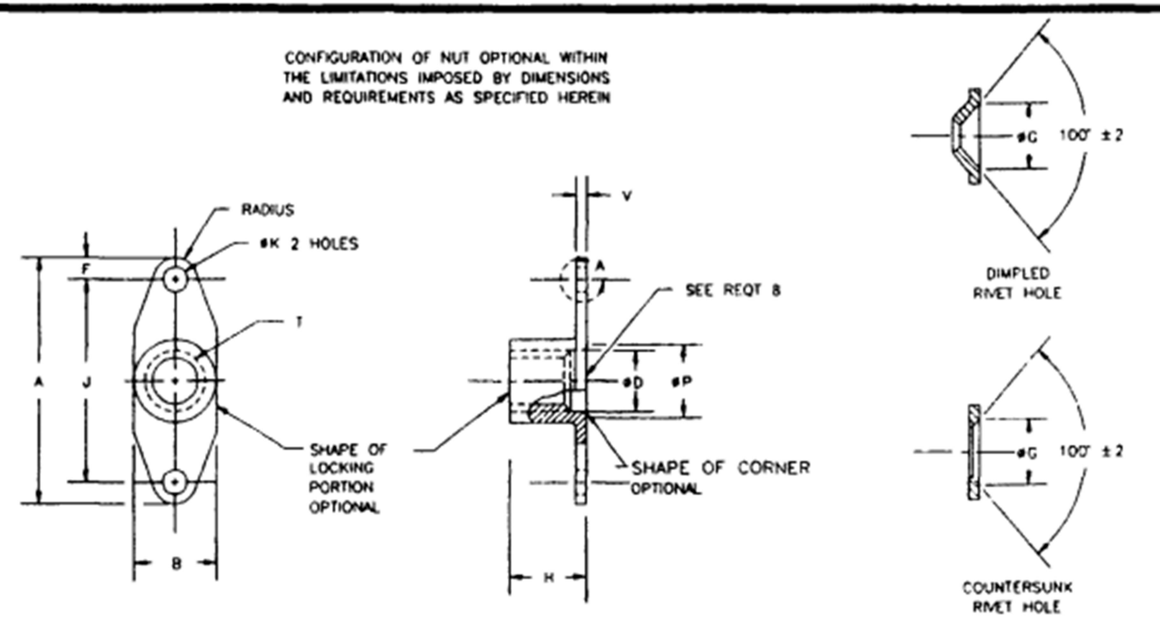

TABLE I DASH NUMBERS AND DIMENSIONS

DASH NUMBERS: PLAIN RIVET HOLES, NON-DRY FILM LUBRICANT	DASH NUMBERS: PLAIN RIVET HOLES, DRY FILM LUBRICANT	DASH NUMBERS: COUNTERSUNK OR DIMPLED RIVET HOLES, NON-DRY FILM LUBRICANT	DASH NUMBERS: COUNTERSUNK OR DIMPLED RIVET HOLES, DRY FILM LUBRICANT	T THREAD SIZES	A MAX	B MAX	B MIN	øD MIN	F MIN	øG ± 010	H 1/ MAX	J 2/ ± 002	øK 3/ + 005 - 000	øP MAX	V MAX	AXIAL STRENGTH LBS/MIN	WEIGHT LBS/100
-02	L02	–	–	086-56UNJC-3B	410	162	140	–	071	4/	110	250	066	130	035	440	05
-03	L03	–	–	099-48UNJC-3B	425	184	140	–	071	4/	125	265	066	143	035	550	08
-04	L04	-04K	L04K	112-40UNJC-3B	630	260	140	–	089	200	143	406	098	166	040	750	11
-06	L06	-06K	L06K	138-32UNJC-3B	661	265	195	–	089	200	171	437	098	206	047	1,130	14
-08	L08	-08K	L08K	164-32UNJC-3B	692	297	230	168	100	200	250	468	098	248	047	1,720	18
-3	L3	-3K	L3K	190-32UNJF-3B	724	328	298	194	100	200	250	500	098	274	047	2 460	26
-4	L4	-4K	L4K	250-28UNJF-3B	786	414	380	254	100	200	281	562	098	344	055	4 580	40
-5	L5	-5K	L5K	3125-24UNJF-3B	1 006	505	475	317	125	230	328	718	130	417	065	7 390	77
-6	L6	–	–	375-24UNJF-3B	1 116	614	580	379	125	230	344	828	130	505	075	11,450	1 86

1/ MINIMUM "H" NOT SPECIFIED LIMITED ONLY BY STRENGTH REQUIREMENTS OF SPECIFICATION
2/ CENTER OF THE TAPPED HOLE SHALL NOT DEVIATE IN ANY DIRECTION FROM THE CENTER OF THE PLATE NUT AS DETERMINED BY THE RIVET HOLES BY MORE THAN 005
3/ DIMPLED RIVET HOLE TOLERANCE FOR "øK" IS + 015 - 000
4/ SPACE WILL NOT PERMIT COUNTERSINK

INCH-POUND

(G) DENOTES CHANGE(S)

PREPARING ACTIVITY DLA-IS
CUSTODIANS ARMY- AV NAVY- AS
AIR FORCE- 11 DLA-
REVIEW 82
USER CR MI
PROJECT NUMBER 5310-1955

MILITARY SPECIFICATION SHEET

TITLE

NUT, SELF-LOCKING PLATE, TWO-LUG, REDUCED RIVET SPACING, LOW HEIGHT, STEEL, 125 KSI Ftu, 450°F

SPECIFICATION SHEET NUMBER
MS21069 1 FEB 94 REV G
SUPERSEDING
MS21069 F 30 SEPT 87 (SEE NOTE 5)
AMSC- N/A FSC 5310

DISTRIBUTION STATEMENT
A. Approved for public release distribution is unlimited

Page 1 of 2

REQUIREMENTS

Form Approved
OMB No 0704-0188

(G) 1 MATERIAL. CARBON STEEL COMPOSITIONS 1035 (UNS G10350) 1040 (UNS G10400) AND 1050 (UNS G10500) IN ACCORDANCE WITH ASTM A827 OR QQ-S-700 1042 (UNS G10420) IN ACCORDANCE WITH ASTM A29 ALLOY STEEL GRADES 4130 (UNS G41300) 4340 (UNS G43400) AND 8740 (UNS G87400) IN ACCORDANCE WITH ASTM A29

2 FINISH. CADMIUM PLATE IN ACCORDANCE WITH QQ-P-416 TYPE II CLASS 3 FOR DRY FILM LUBRICATED NUTS THE TYPE AND CLASS ARE OPTIONAL IF THE NUTS MEET THE SALT SPRAY REQUIREMENTS OF QQ-P-416 TYPE II

3 DIMENSIONING AND TOLERANCING. DIMENSIONING AND TOLERANCING SHALL BE IN ACCORDANCE WITH ANSI Y14.5M

4 HARDNESS. 49 HRC MAX

5 THREADS. THREADS BEFORE LUBRICATION IN ACCORDANCE WITH MIL-S-8879

6 SURFACE TEXTURE. SURFACE TEXTURE UNLESS OTHERWISE SPECIFIED SHALL NOT EXCEED 125 MICROINCHES IN ACCORDANCE WITH ANSI/ASME B46.1

7 LUBRICANT. DRY FILM LUBRICANT APPROVED IN ACCORDANCE WITH MIL-N-25027 NON-DRY FILM LUBRICANTS SHALL BE SOLUBLE IN THE CLEANER SPECIFIED IN MIL-S-8802

(G) 8 EDGES BREAK ALL SHARP EDGES AND REMOVE ALL BURRS

9 COUNTERBORE/COUNTERSINK. ON SIZE .164 AND LARGER THREAD RELIEF SHALL BE .062 MINIMUM ON SIZE .138 AND SMALLER COUNTERSINK TO "P" DIAMETER

10 PART NUMBER THE PART NUMBER SHALL CONSIST OF THE BASIC MS NUMBER FOLLOWED BY A DASH NUMBER FROM TABLE I

EXAMPLE MS21069L4K
- L4K — DASH NUMBER
- MS21069 — BASIC MS NUMBER

MS21069L4K INDICATES NUT SELF-LOCKING PLATE TWO LUG REDUCED RIVET SPACING LOW HEIGHT STEEL 125 KSI Ftu 450°F .250-28UNJF-3B, DRY FILM LUBRICATION COUNTERSUNK OR DIMPLED RIVET HOLES

NOTES

1 ALL DIMENSIONS ARE IN INCHES

2 IN THE EVENT OF A CONFLICT BETWEEN THE TEXT OF THIS STANDARD AND THE REFERENCES CITED HEREIN THE TEXT OF STANDARD SHALL TAKE PRECEDENCE

3 REFERENCED GOVERNMENT (OR NON-GOVERNMENT) DOCUMENTS OF THE ISSUE LISTED IN THAT ISSUE OF THE DEPARTMENT OF DEFENSE INDEX OF SPECIFICATIONS AND STANDARDS (DODISS) SPECIFIED IN THE SOLICITATION FORM A PART OF THIS STANDARD TO THE EXTENT SPECIFIED HEREIN

4 DESIGN AND USAGE LIMITATIONS THESE NUTS ARE DESIGNED TO DEVELOP THE TENSILE STRENGTH OF BOLTS AND SCREWS WITH AN ULTIMATE TENSILE STRENGTH OF 125 KSI BASED ON THE CROSS SECTION AREA AT THE BASIC ROOT DIAMETER OF THE THREADS THESE NUTS ARE DESIGNED TO BE USED ON 3A EXTERNAL THREADS THESE NUTS SHALL BE USED IN ACCORDANCE WITH THE LIMITATIONS OF MS33588 ONLY NUTS FOR WHICH THERE ARE QUALIFIED PRODUCTS LISTED ON QPL 25027 SHALL BE USED

5 MS21069 SUPERSEDES NAS697

INTERCHANGEABILITY RELATIONSHIP

MS21069 NUTS CAN UNIVERSALLY REPLACE NAS697 NUTS OF LIKE MATERIAL THREAD SIZE LUBRICANT (DRY FILM OR NON-DRY FILM LUBRICANT) AND FASTENING METHOD (PLAIN RIVET HOLES DIMPLED OR COUNTERSUNK RIVET HOLES) BUT THESE NAS697 NUTS CANNOT UNIVERSALLY REPLACE MS21069 NUTS

INTERCHANGEABILITY TABLE

CANCELLED PART NUMBERS	SUBSTITUTIVE PART NUMBERS	CANCELLED PART NUMBERS	SUBSTITUTIVE PART NUMBERS
NAS697X02	MS21069-02	NAS697X3K	MS21069-3K
NAS697A02	MS21069L02	NAS697A3K	MS21069L3K
NAS697X03	MS21069-03	NAS697X4	MS21069-4
NAS697A03	MS21069L03	NAS697A4	MS21069L4
NAS697X04L	MS21069-04	NAS697X4K	MS21069-4K
NAS697A04L	MS21069L04	NAS697A4K	MS21069L4K
NAS697X04LK	MS21069-04K	NAS697X5	MS21069-6
NAS697A04LK	MS21069L04K	NAS697A5	MS21069L6
NAS697X06L	MS21069-06	NAS697X5K	MS21069-6K
NAS697A06L	MS21069L06	NAS697A5K	MS21069L6K
NAS697X06LK	MS21069-06K	NAS697X6	MS21069-6
NAS697A06LK	MS21069L06K	NAS697A6	MS21069L6
NAS697X08	MS21069-08		
NAS697A08	MS21069L08		
NAS697X08K	MS21069-08K		
NAS697A08K	MS21069L08K		
NAS697X3	MS21069-3		
NAS697A3	MS21069L3		

PREPARING ACTIVITY DLA-IS
CUSTODIANS ARMY- AV NAVY- AS
AIR FORCE- 11 DLA-
REVIEW 82
USER CR, MI
PROJECT NUMBER 5310-1955

MILITARY SPECIFICATION SHEET

TITLE
NUT, SELF-LOCKING, PLATE TWO LUG, REDUCED RIVET SPACING LOW HEIGHT STEEL, 125 KSI Ftu, 450°F

SPECIFICATION SHEET NUMBER
MS21069 1 FEB 94 REV G

SUPERSEDING
MS21069 F 30 SEPT 87 (SEE NOTE 5)

AMSC- N/A FSC 5310

DISTRIBUTION STATEMENT
A. Approved for public release distribution is unlimited

APPENDIX C

Form Approved
OMB No 0704-0188

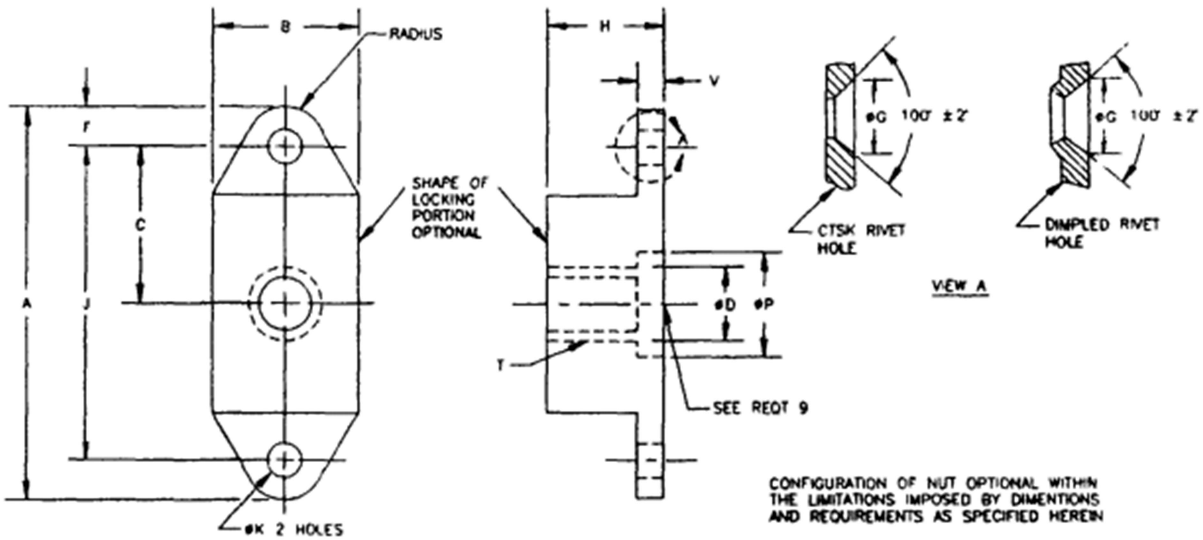

CONFIGURATION OF NUT OPTIONAL WITHIN THE LIMITATIONS IMPOSED BY DIMENTIONS AND REQUIREMENTS AS SPECIFIED HEREIN

TABLE I DASH NUMBERS AND DIMENSIONS

DASH NUMBERS																			
PLAIN RIVET HOLES		COUNTERSUNK OR DIMPLED RIVET HOLES																	
NON-DRY FILM LUBRICANT	DRY FILM LUBRICANT	NON-DRY FILM LUBRICANT	DRY FILM LUBRICANT	T THREAD SIZES	A MAX	B MAX	B MIN	C ± 005	ϕD MIN	ϕP MIN	ϕG ± 010	1/ H MAX	J ± 002	2/ ϕK + 005 − 000	ϕP MAX	ϕP MIN	V MAX	AXIAL STRENGTH LBS/MIN	WEIGHT LBS/100
-04	L04	-04K	L04K	112-40 UNJC-3B	948	416	290	344	–	100	200	175	688	098	270	172	032	750	38
-06	L06	-06K	L06K	138-32 UNJC-3B	948	416	290	344	–	100	200	203	688	098	270	198	032	1 130	39
-08	L08	-08K	L08K	164-32 UNJC-3B	948	416	290	344	168	100	200	250	688	098	270	224	032	1 720	40
-3	L3	-3K	L3K	190-32 UNJF-3B	948	416	290	344	194	100	200	250	688	098	270	250	.032	2,460	41
-4	L4	-4K	L4K	250-28 UNJF-3B	1 292	516	350	500	254	100	200	281	1 000	098	330	310	032	4 580	90
-5	L5	-5K	L5K	3125-24 UNJF-3B	1 292	609	412	500	317	125	230	328	1 000	130	392	372	045	7 390	1 26
-6	L6	–	–	375-24 UNJF-3B	1 292	680	475	500	379	125	230	344	1 000	130	455	435	055	11 450	1 55
-7	L7	–	–	4375-20 UNJF-3B	1 477	719	672	562	442	146	230	504	1 125	161	517	497	115	15 450	3 30
-8	L8	–	–	500-20 UNJF-3B	1 602	859	796	625	504	146	230	630	1 250	161	580	560	115	21 110	4 00

1/ MINIMUM "H" NOT SPECIFIED, LIMITED ONLY BY STRENGTH REQUIREMENTS OF SPECIFICATION
2/ DIMPLED RIVET HOLE TOLERANCE FOR "ϕK" IS + 015 − 000

(J) DENOTES CHANGE(S)

INCH–POUND

PREPARING ACTIVITY DLA-IS
CUSTODIANS ARMY- AV NAVY- AS
AIR FORCE- 11 DLA-
REVIEW
USER CR, MI
PROJECT NUMBER 5310-1949

MILITARY SPECIFICATION SHEET
TITLE
NUT, SELF-LOCKING, PLATE, TWO LUG, FLOATING, LOW HEIGHT STEEL, 125 KSI Ftu, 450° F

SPECIFICATION SHEET NUMBER
MS21059 1 FEB 94 REV J
SUPERSEDING
MS21059H 30 OCT 89 (SEE NOTE 5)
AMSC- N/A FSC 5310

DISTRIBUTION STATEMENT
A. Approved for public release distribution is unlimited

Page 1 of 3

Form Approved
OMB No 0704-0188

REQUIREMENTS

1 MATERIAL

(J) NUT - CARBON STEEL COMPOSITIONS 1035 (UNS G10350) 1040 (UNS G10400) AND 1050 (UNS G10500), IN ACCORDANCE WITH ASTM A827 OR QQ-S-700 1042 (UNS G10420) IN ACCORDANCE WITH ASTM A29 ALLOY STEEL GRADES 4130 (UNS G41300) 4340 (UNS G43400) AND 8740 (UNS G87400) IN ACCORDANCE WITH ASTM A29

(J) RETAINER (IF APPLICABLE) - CARBON STEEL COMPOSITIONS 1035 (UNS G10350) AND 1050 (UNS G10500), IN ACCORDANCE WITH ASTM A827 OR QQ-S-700 1042 (UNS G10420) AND ALLOY STEEL GRADE 4130 (UNS G41300) IN ACCORDANCE WITH ASTM A29

2 FINISH. CADIUM PLATE IN ACCORDANCE WITH QQ-P-416 TYPE II CLASS 2 FOR DRY FILM LUBRICATED NUTS THE TYPE AND CLASS ARE OPTIONAL IF THE NUTS MEET THE SALT SPRAY REQUIREMENTS OF QQ-P-416 TYPE II

3 DIMENSIONING AND TOLERANCING. DIMENSIONING AND TOLERANCING SHALL BE IN ACCORDANCE WITH ANSI Y14 5M

4 HARDNESS. 49HRC MAX

5 THREADS. THREADS BEFORE LUBRICATION IN ACCORDANCE WITH MIL-S-8879

6 SURFACE TEXTURE. SURFACE TEXTURE, UNLESS OTHERWISE SPECIFIED SHALL NOT EXCEED 125 MICROINCHES IN ACCORDANCE WITH ANSI/ASME B46 1

7 LUBRICANT. DRY FILM LUBRICANT APPROVED IN ACCORDANCE WITH MIL-N-25027 NON-DRY LUBRICANTS SHALL BE SOLUBLE IN THE CLEANER SPECIFIED IN MIL-S-8802

8 COUNTERBORE/COUNTERSINK. ON SIZE 164 AND LARGER THREAD RELIEF SHALL BE 062 MINIMUM, ON SIZE 138 AND SMALLER, COUNTERSINK OR RADIUSED WITHIN "P" DIAMETER

(J) 9 FLOAT. FLOAT OF NUT ELEMENT PORTION OF ASSEMBLY SHALL NOT BE LESS THAN 030 LATERALLY AND LONGITUDINALLY FROM CENTERED POSITION NUT BODY SHALL BE CAPABLE OF ENGAGEMENT WITH A BOLT IN THE MAXIMUM MISALIGNED POSITION MAXIMUM AXIAL FLOAT 020 INCHES FOR 190 AND SMALLER, 030 FOR 250 AND LARGER NUT MISALIGNMENT SHALL NOT EXCEED DIMENSION "B" THE NUT AND BASE PORTION OF THE ASSEMBLY SHALL FORM ONE INTEGRAL UNIT AND THE SURFACE ASSEMBLY SHALL PROVIDE A BEARING FOR THE NUT

10 PART NUMBER. THE PART NUMBER SHALL CONSIST OF THE BASIC MS NUMBER FOLLOWED BY A DASH NUMBER FROM TABLE I

EXAMPLE. MS21059L4K

- L4K — DASH NUMBER
- MS21059 — BASIC MS NUMBER

MS21059L4K INDICATES NUT SELF-LOCKING, PLATE, TWO LUG, FLOATING LOW HEIGHT STEEL 125 KSI Ftu 450° F 250-28 UNJF-3B DRY FILM LUBRICANT COUNTERSUNK OR DIMPLED HOLES

NOTES

1 ALL DIMENSIONS ARE IN INCHES

2 IN THE EVENT OF A CONFLICT BETWEEN THE TEXT OF THIS STANDARD AND THE REFERENCES CITED HEREIN THE TEXT OF THIS STANDARD SHALL TAKE PRECEDENCE

3 REFERENCED GOVERNMENT (OR NON-GOVERNMENT) DOCUMENTS OF THE ISSUE LISTED IN THAT ISSUE OF THE DEPARTMENT OF DEFENSE INDEX OF SPECIFICATIONS AND STANDARDS (DODISS) SPECIFIED IN THE SOLICITATION FORM A PART OF THIS STANDARD TO THE EXTENT SPECIFIED HEREIN

4 DESIGN AND USAGE LIMITATIONS THESE NUTS ARE DESIGNED TO DEVELOP THE TENSILE STRENGTH OF BOLTS AND SCREWS WITH AN ULTIMATE TENSILE STRENGTH OF 125 KSI BASED ON THE CROSS SECTION AREA AT THE BASIC ROOT DIAMETER OF THE THREADS THESE NUTS ARE DESIGNED TO BE USED ON 3A EXTERNAL THREADS THESE NUTS SHALL BE USED IN ACCORDANCE WITH THE LIMITATIONS OF MS33588 ONLY NUTS FOR WHICH THERE ARE QUALIFIED PRODUCTS LISTED ON QPL 25027 SHALL BE USED

5 MS21059 SUPERSEDES NAS686 NAS1031

PREPARING ACTIVITY DLA-IS CUSTODIANS ARMY- AV NAVY- AS AIR FORCE- 11 DLA- REVIEW USER CR, MI PROJECT NUMBER 5310-1949	MILITARY SPECIFICATION SHEET TITLE NUT, SELF-LOCKING PLATE TWO LUG, FLOATING, LOW HEIGHT STEEL 125 KSI Ftu, 450° F	SPECIFICATION SHEET NUMBER MS21059 1 FEB 94 REV J SUPERSEDING MS21059H 30 OCT 89 (SEE NOTE 5) AMSC- N/A FSC 5310
DISTRIBUTION STATEMENT A. Approved for public release, distribution is unlimited		Page 2 of 3

Form Approved
OMB No 0704-0188

INTERCHANGEABILITY RELATIONSHIP

MS21059 NUTS CAN UNIVERSALLY REPLACE NAS686 AND NAS1031 NUTS OF LIKE MATERIAL, THREAD SIZE, LUBRICANT (DRY FILM OR NON-DRY FILM), RIVET SPACING AND FASTENING METHOD (PLAIN RIVET HOLES, DIMPLED OR COUNTERSUNK RIVET HOLES), BUT THESE NAS686 AND NAS1031 NUTS CANNOT UNIVERSALLY REPLACE MS21059 NUTS.

INTERCHANGEABILITY TABLE

CANCELLED PART NUMBERS	SUBSTITUTIVE PART NUMBERS	CANCELLED PART NUMBERS	SUBSTITUTIVE PART NUMBERS	CANCELLED PART NUMBERS	SUBSTITUTIVE PART NUMBERS
NAS686X04	MS21059-04	NAS1031X04	MS21059-04	NAS1031A3	MS21059L3
NAS686X04K	MS21059-04K	NAS1031X04K	MS21059-04K	NAS1031A3K	MS21059L3K
NAS686A04	MS21059L04	NAS1031A04	MS21059L04	NAS1031X4	MS21059-4
NAS686A04K	MS21059L04K	NAS1031A04K	MS21059L04K	NAS1031X4K	MS21059-4K
NAS686X06	MS21059-06	NAS1031X06	MS21059-06	NAS1031A4	MS21059L4
NAS686X06K	MS21059-06K	NAS1031X06K	MS21059-06K	NAS1031A4K	MS21059L4K
NAS686A06	MS21059L06	NAS1031A06	MS21059L06	NAS1031X5	MS21059-5
NAS686A06K	MS21059L06K	NAS1031A06K	MS21059L06K	NAS1031X5K	MS21059-5K
NAS686X08	MS21059-08	NAS1031X08	MS21059-08	NAS1031A5	MS21059L5
NAS686X08K	MS21059-08K	NAS1031X08K	MS21059-08K	NAS1031A5K	MS21059L5K
NAS686A08	MS21059L08	NAS1031A08	MS21059L08	NAS1031X6	MS21059-6
NAS686A08K	MS21059L08K	NAS1031A08K	MS21059L08K	NAS1031A6	MS21059L6
NAS686X3	MS21059-3	NAS1031X3	MS21059-3	NAS1031X7	MS21059-7
NAS686X3K	MS21059-3K	NAS1031X3K	MS21059-3K	NAS1031A7	MS21059L7
NAS686A3	MS21059L3			NAS1031X8	MS21059-8
NAS686A3K	MS21059L3K			NAS1031A8	MS21059L8
NAS686X4	MS21059-4				
NAS686X4K	MS21059-4K				
NAS686A4	MS21059L4				
NAS686A4K	MS21059L4K				
NAS686X5	MS21059-5				
NAS686X5K	MS21059-5K				
NAS686A5	MS21059L5				
NAS686A5K	MS21059L5K				
NAS686X6	MS21059-6				
NAS686A6	MS21059L6				

PREPARING ACTIVITY DLA-IS CUSTODIANS ARMY- AV NAVY- AS AIR FORCE- 11 DLA- REVIEW USER CR, MI PROJECT NUMBER 5310-1949	MILITARY SPECIFICATION SHEET TITLE NUT, SELF-LOCKING, PLATE, TWO LUG, FLOATING, LOW HEIGHT STEEL, 125 KSI Ftu, 450° F	SPECIFICATION SHEET NUMBER MS21059 1 FEB 94 REV J SUPERSEDING MS21059H 30 OCT 89 (SEE NOTE 5) AMSC- N/A FSC 5310
DISTRIBUTION STATEMENT A Approved for public release distribution is unlimited		Page 3 of 3

APPENDIX D

FED.SUPPLY CLASS
5310

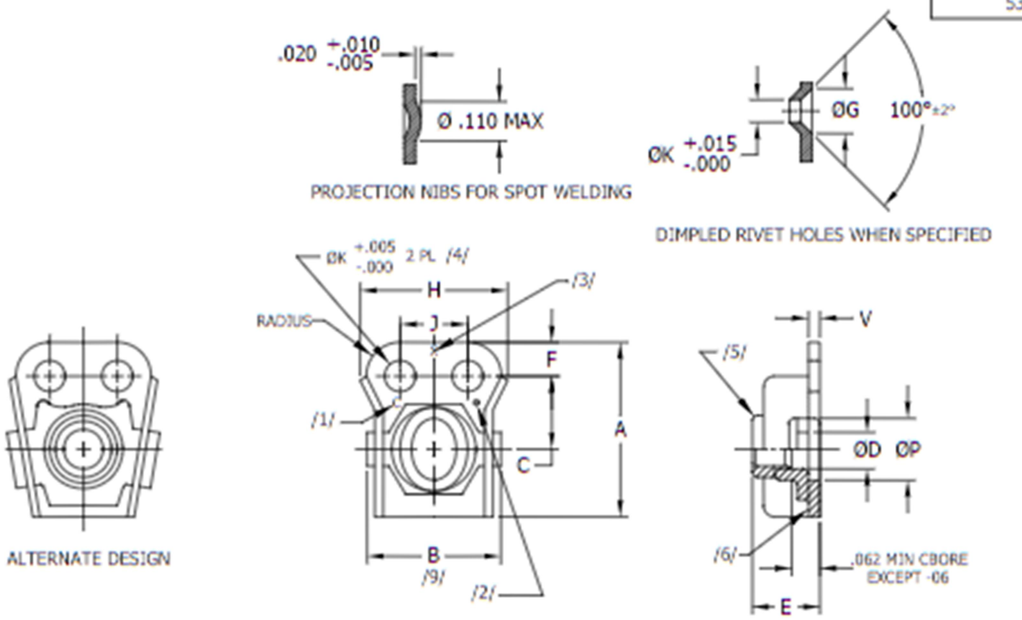

③ TABLE I – DIMENSIONS AND STRENGTH VALUES

DASH NUMBER				T	A	B	C	ØD	E	F	ØG	H	J	ØK	~~H~~	P	V	AXIAL
STEEL		CRES		THREAD /11/	MAX	+.000 −.050 /9/		MIN	MAX /10/	MIN	±.010	MAX	±.002	+.005 −.000	~~MAX~~	MAX	MAX	TENSILE STRENGTH LBF
CAD+ MoS_2 450 °F	CAD W/O MoS_2 450 °F	SILVER PLATE 800 °F	MoS_2 450 °F															
-06	X06	C06	C06M	.1380-32 UNJC-3B	.525	.440	.250	–	.203	.100	.200	.490	.219	.098	~~.409~~	.232	.035	1,600
-08	X08	C08	C08M	.1640-32 UNJC-3B	.525	.440	.250	.168	.250	.100	.200	.490	.219	.098	~~.409~~	.232	.035	2,500
-3	X3	C3	C3M	.1900-32 UNJF-3B	.525	.440	.250	.194	.250	.100	.200	.490	.219	.098	~~.409~~	.232	.035	3,620
-4	X4	C4	C4M	.2500-28 UNJF-3B	.617	.557	.281	.254	.281	.100	.200	.502	.219	.098	~~.526~~	.300	.035	6,470
-5	X5	C5	C5M	.3125-24 UNJF-3B	.767	.619	.359	.317	.328	.125	.230	.609	.269	.130	~~.588~~	.357	.045	10,200
-6	X6	C6	C6M	.3750-24 UNJF-3B	.876	.682	.414	.379	.344	.125	.230	.629	.269	.130	~~.651~~	.420	.055	15,200

MATERIAL:

STEEL - CARBON OR ALLOY HEAT TREATED SAE1030 OR BETTER; NEITHER THE SULFUR NOR PHOSPHORUS CONTENT SHALL EXCEED .050% BY WEIGHT.
CRES - A286 PER AMS5525, AMS5732, ~~AMS5735~~, AMS5737 OR AMS5853. /7/

FINISH:

STEEL - CADMIUM PLATE PER AMS-QQ-P-416, TYPE II, CLASS 2.
CRES - SILVER PLATE FOR 800 °F USE PER AMS2410 TO A .0002 MIN THICKNESS ON SURFACE WHICH CAN BE TOUCHED BY A .750 DIAMETER BALL. THREADS SHALL SHOW COMPLETE COVERAGE, BUT THICKNESS REQUIREMENTS ON THREADS IS WAIVED.
③ PASSIVATE ALL CRES PARTS PER AMS2700, METHOD 1, CLASS 4 BEFORE THE APPLICATION OF DRY FILM LUBRICANT.

THIRD ANGLE PROJECTION	CUSTODIAN NATIONAL AEROSPACE STANDARDS COMMITTEE	REVISION 3
PROCUREMENT SPECIFICATION NOTED	TITLE **NUT, SELF-LOCKING, PLATE, SIDE BY SIDE, FLOATING, LOW HEIGHT, REDUCED RIVET SPACING, CBORED, 160 KSI, 450 °F, 800 °F**	CLASSIFICATION PART STANDARD **NAS1789** SHEET 1 OF 3

LUBRICANT:

MOLYDISULFIDE (MoS_2) DRY FILM LUBRICANT PER NASM25027. THE INCLUSION OF A LUBRICANT ON THE BASKETS OF DRY FILM LUBRICATED NUTS IS OPTIONAL.

CODE:

"-" STEEL, CADMIUM PLATED WITH DRY FILM LUBRICANT.
"C" IN PLACE OF DASH INDICATES CRES NUTS WITH SILVER PLATE.
"K" SUFFIXED TO THE DASH NUMBER INDICATES DIMPLED RIVET HOLES.
"M" SUFFIXED TO THE DASH NUMBER INDICATES CRES NUTS, WITHOUT SILVER PLATE, WITH DRY FILM LUBRICANT.
"W" SUFFIXED TO THE DASH NUMBER INDICATES PROJECT WELD NIBS FOR CRES SILVER PLATED PARTS ONLY (NO SILVER PLATE ON WELD NIBS).
"X" IN PLACE OF DASH INDICATES CADMIUM PLATED NUTS WITHOUT DRY FILM LUBRICANT.

EXAMPLES OF PART NUMBERS:

STEEL

NAS1789-4	=	.2500-28 UNJF-3B THREAD, PLAIN RIVET HOLES, CADMIUM PLATED WITH DRY FILM LUBRICANT.
NAS1789-4K	=	.2500-28 UNJF-3B THREAD, DIMPLED RIVET HOLES, CADMIUM PLATED WITH DRY FILM LUBRICANT.
NAS1789X4	=	.2500-28 UNJF-3B THREAD, PLAIN RIVET HOLES, CADMIUM PLATED AND WITHOUT DRY FILM LUBRICANT.
NAS1789X4K	=	.2500-28 UNJF-3B THREAD, DIMPLED RIVET HOLES, CADMIUM PLATED AND WITHOUT DRY FILM LUBRICANT.

CRES

NAS1789C4	=	.2500-28 UNJF-3B THREAD, PLAIN RIVET HOLES, SILVER PLATED.
NAS1789C4K	=	.2500-28 UNJF-3B THREAD, DIMPLED RIVET HOLES, SILVER PLATED.
NAS1789C4W	=	.2500-28 UNJF-3B THREAD, WELD NIBS, SILVER PLATED.
NAS1789C4M	=	.2500-28 UNJF-3B THREAD, PLAIN RIVET HOLES, DRY FILM LUBRICATED.
NAS1789C4MK	=	.2500-28 UNJF-3B THREAD, DIMPLED RIVET HOLES, DRY FILM LUBRICATED.

NOTES:

/1/ MARK "C" ON CRES PARTS, LOCATION OPTIONAL.

/2/ RAISED OR DEPRESSED DOT FOR 160 KSI IDENTIFICATION, LOCATION OPTIONAL.

(3) /3/ MANUFACTURER'S ID, LOCATION OPTIONAL.

/4/ 2K MINIMUM DIAMETER CLEARANCE FOR ATTACHING RIVETS.

/5/ FLOAT OF NUT PORTION OF ASSEMBLY SHALL NOT BE LESS THAN .020 INCHES LATERALLY AND LONGITUDINALLY FROM CENTERED POSITION. NUT BODY SHALL BE CAPABLE OF ENGAGEMENT WITH A BOLT IN THE MAXIMUM MISALIGNED POSITION.

/6/ THE ASSEMBLY SHALL PROVIDE A BEARING SURFACE FOR THE NUT, AND THE NUT AND BASE PORTION OF THE ASSEMBLY SHALL FORM ONE INTEGRAL UNIT.

/7/ FOR CRES ONLY, MAGNETIC PERMEABILITY SHALL BE LESS THAN 2.0 (AIR = 1.0) FOR A FIELD STRENGTH H = 200 OERSTEDS USING A MAGNETIC PERMEABILITY INDICATOR PER ASTM A342/A342M, TEST METHOD 3.

REVISION
3

NAS1789
SHEET 2

(3) (8) UNLESS OTHERWISE SPECIFIED HEREIN, REFERENCED DOCUMENTS SHALL BE THE ISSUE IN EFFECT ON DATE OF MANUFACTURE. HOWEVER, EXISTING MATERIAL INVENTORY CERTIFIED TO A PREVIOUS REVISION OF THE APPLICABLE MATERIAL SPECIFICATION(S) IS ACCEPTABLE FOR USE UNTIL DEPLETION.

/9/ INCLUDES FLOAT OF NUT ELEMENT.

/10/ MINIMUM "E" LIMITED ONLY BY STRENGTH REQUIREMENTS OF SPECIFICATION.

/11/ THREADS IN ACCORDANCE WITH AS8879 BEFORE LUBRICATION.

(12) DIMENSIONS IN INCHES.

(13) THIS STANDARD TAKES PRECEDENCE OVER DOCUMENTS REFERENCED HEREIN.

(14) REMOVE ALL BURRS AND SHARP EDGES.

(15) DIMENSIONING AND TOLERANCING PER ANSI Y14.5M-1982.

(16) UNLESS OTHERWISE SPECIFIED, PART INVENTORY MANUFACTURED TO PREVIOUS REVISIONS OF THE APPLICABLE DRAWING OR SPECIFICATION MAY BE PROCURED AND USED UNTIL STOCK IS DEPLETED.

PROCUREMENT SPECIFICATION:

STEEL NUTS - NAS3350, CLASS II.

CRES NUTS - NASM25027 EXCEPT MINIMUM TENSILE STRENGTH SHALL BE AS TABULATED. TEST BOLTS FOR CRES NUTS SHALL BE 180 KSI MINIMUM.

ALL PARTS MUST MEET QUALIFICATION AND INSPECTION REQUIREMENTS. MANUFACTURERS SHALL PROVIDE EVIDENCE OF QUALIFICATION WHEN REQUIRED. TESTING SHALL BE PERFORMED BY MANUFACTURER OR INDEPENDENT LABORATORY. PROCURING AGENCY MAY CONDUCT CONFIRMING QUALIFICATION TESTS. NO QPL SHALL BE ESTABLISHED.

APPENDIX E

FED. SUPPLY CLASS
5306

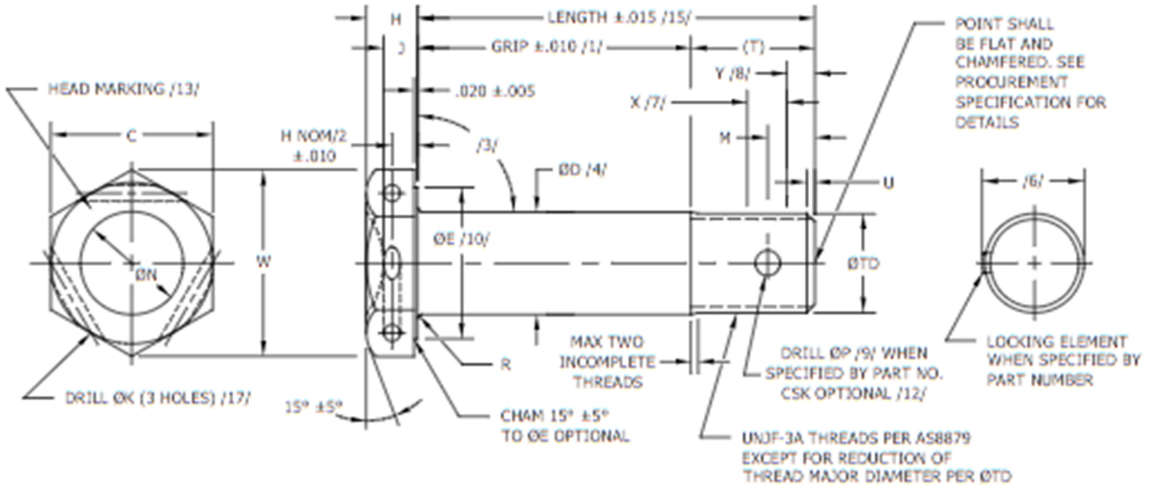

FIGURE 1 – BOLT CONFIGURATION

TABLE I – DIMENSIONS

BASIC NUMBER	THREAD UNJF-3A	C		ØD		ØE MIN /10/	H +.015 –.000	J +.015 –.000	ØK /17/	M ±.010
		MAX	MIN	MAX	MIN					
NAS6203	.1900-32	.376	.367	.1895	.1885	.335	.110	.073	.056	.164
NAS6204	.2500-28	.439	.429	.2495	.2485	.398	.125	.083	.046	.170
NAS6205	.3125-24	.502	.492	.3120	.3110	.460	.156	.104		.182
NAS6206	.3750-24	.564	.554	.3745	.3735	.523	.188	.125		.183
NAS6207	.4375-20	.690	.678	.4370	.4360	.648	.219	.146		.199
NAS6208	.5000-20	.752	.741	.4995	.4985	.710	.250	.167		.198
NAS6209	.5625-18	.877	.865	.5615	.5605	.835	.281	.188	.080	.207
NAS6210	.6250-18	.940	.928	.6240	.6230	.898	.312	.208	.070	.207
NAS6212	.7500-16	1.065	1.052	.7490	.7480	1.023	.375	.250		.222
NAS6214	.8750-14	1.252	1.239	.8740	.8730	1.210	.438	.292		.241
NAS6216	1.0000-12	1.440	1.427	.9990	.9980	1.398	.500	.333		.264
NAS6218	1.1250-12	1.627	1.614	1.1240	1.1225	1.585	.562	.375		.295
NAS6220	1.2500-12	1.814	1.801	1.2490	1.2475	1.772	.625	.417		.295

THIRD ANGLE PROJECTION	CUSTODIAN: NATIONAL AEROSPACE STANDARDS COMMITTEE	REVISION: **11**
PROCUREMENT SPECIFICATION: NOTED	TITLE: **BOLT, TENSION, HEX HEAD, CLOSE TOLERANCE, ALLOY STEEL, SHORT THREAD, REDUCED MAJOR THREAD DIA., SELF-LOCKING AND NONLOCKING, 160 KSI Ftu**	CLASSIFICATION: PART STANDARD **NAS6203 THRU NAS6220** SHEET 1 OF 7

TABLE I – DIMENSIONS (CONTINUED)

BASIC NUMBER	ØN ±.01	ØP ±.005 /9/	R RAD		(T) /2/	ØTD		U MAX	W MIN	X /7/	Y /8/	INSPECTION DATA		
			MAX	MIN		MAX	MIN					AA /4/	BB /5/	CC /4/
NAS6203	.19	.075	.020	.010	.323	.1840	.1810	.039	.410	.156	.094	.0045	.0040	.005
NAS6204	.25	.081	.020	.010	.370	.2440	.2410	.045	.480	.179	.107	.0045	.0030	.006
NAS6205	.31	.081	.020	.010	.438	.3060	.3020	.052	.552	.208	.125	.0045	.0030	.008
NAS6206	.38	.111	.025	.015	.454	.3680	.3640	.052	.623	.208	.125	.0045	.0025	.009
NAS6207	.44	.111	.025	.015	.528	.4310	.4260	.062	.764	.250	.150	.0060	.0025	.010
NAS6208	.50	.111	.030	.020	.528	.4930	.4880	.062	.836	.250	.150	.0060	.0020	.011
NAS6209	.56	.146	.035	.020	.594	.5550	.5500	.068	.978	.278	.167	.0060	.0020	.012
NAS6210	.62	.146	.040	.025	.626	.6180	.6120	.068	1.050	.278	.167	.0060	.0020	.015
NAS6212	.75	.146	.045	.030	.666	.7430	.7370	.078	1.191	.312	.188	.0060	.0020	.018
NAS6214	.88	.146	.050	.035	.759	.8680	.8610	.089	1.405	.357	.214	.0090	.0020	.020
NAS6216	1.00	.146	.060	.045	.895	.9930	.9860	.104	1.619	.417	.250	.0090	.0020	.022
NAS6218	1.12	.146	.070	.055	.989	1.1180	1.1110	.104	1.832	.417	.250	.0090	.0020	.025
NAS6220	1.25	.146	.075	.060	1.083	1.2430	1.2360	.104	2.046	.417	.250	.0090	.0020	.028

MATERIAL: ALLOY STEEL – 4140 (UNS G41400) PER AMS6349 OR AMS6382, 4340 (UNS G43406) PER AMS6415 OR AMS6484 OR 8740 (UNS G87400) PER AMS6322 ~~OR MIL-S-6049~~, AMS6325 OR AMS6327.
LOCKING ELEMENT – NYLON OR EQUIVALENT PER MIL-DTL-18240 AND QPL-18240.

HEAT TREAT: DEVELOP BASIC MATERIAL PROPERTIES AS FOLLOWS, WITH CONTROLS PER ~~AMS-H-6875 OR~~ AMS2759:
160 – 180 KSI Ftu

FINISH: CADMIUM PLATED BOLTS - CADMIUM PLATE PER AMS-QQ-P-416, TYPE II, CLASS 2. EMBRITTLEMENT REQUIREMENT PER NAS4002.

CHROMIUM PLATED BOLTS – CHROMIUM PLATE PER AMS-QQ-C-320, CLASS 2 ON SHANK ONLY. ALL OTHER SURFACES CADMIUM PLATED. NO CHROMIUM WITHIN .020 OF LINE OF TANGENCY OF HEAD TO SHANK FILLET. CHROMIUM IN THREAD RUNOUT PERMITTED. CHROMIUM PLATED BOLTS NOT AVAILABLE WITH GRIP DASH NUMBER 1 OR NUMBER 2.

CODE: NO FINISH CODE AFTER BASIC NUMBER FOR CADMIUM PLATED BOLTS.
ADD "C" AFTER BASIC NUMBER FOR CHROMIUM PLATED BOLTS.
ADD "L" AFTER BASIC NUMBER FOR SELF-LOCKING BOLT WITH LOCKING ELEMENT TYPE OPTIONAL; SEE PROCUREMENT SPEC BELOW. DO NOT USE "L" WITH "D" OR "P" CODE.
ADD "P" AFTER BASIC NUMBER FOR SELF-LOCKING BOLT WITH PATCH TYPE LOCKING ELEMENT ONLY; SEE PROCUREMENT SPEC BELOW. DO NOT USE "P" WITH "D" OR "L" CODE.
GRIP DASH NUMBER INDICATES GRIP IN .0625 INCREMENTS (CONVERTED TO THREE DECIMAL PLACES PER ANSI Y14.5-1982). SEE TABLE II FOR TABULATIONS OF GRIP AND LENGTH DIMENSIONS. /15/
ADD "D" AFTER GRIP DASH NUMBER FOR DRILLED THREAD BOLTS. DO NOT USE WITH "L" OR "P" CODE. /12/
ADD "H" AFTER GRIP DASH NUMBER FOR BOLT WITH DRILLED HEAD.
CODE LETTER "X" AND "Y" FOLLOWING THE GRIP DASH NUMBER INDICATES REPLACEMENT OVERSIZE REPAIR BOLT. (SEE LAST SHEET)
IF MORE THAN ONE CODE LETTER IS USED IN SEQUENCE, ARRANGE THE LETTERS ALPHABETICALLY.

EXAMPLE OF PART NUMBER: (SEE LAST SHEET FOR OVERSIZE BOLTS.)

NAS6204-10	=	BOLT, .2500-28 THREAD, .625 GRIP, UNDRILLED, NONLOCKING, CADMIUM PLATED.
NAS6204-10D	=	BOLT, .2500-28 THREAD, .625 GRIP, DRILLED THREAD, NONLOCKING, CADMIUM PLATED.
NAS6204-10DH	=	BOLT, .2500-28 THREAD, .625 GRIP, DRILLED THREAD, DRILLED HEAD, NONLOCKING, CADMIUM PLATED.
NAS6204C10H	=	BOLT, .2500-28 THREAD, .625 GRIP, DRILLED HEAD, UNDRILLED THREAD, NONLOCKING, CHROMIUM PLATED.
NAS6204L10	=	BOLT, .2500-28 THREAD, .625 GRIP, UNDRILLED, SELF-LOCKING (LOCKING TYPE OPTIONAL), CADMIUM PLATED.
NAS6204P10	=	BOLT, .2500-28 THREAD, .625 GRIP, UNDRILLED, SELF-LOCKING (PATCH TYPE), CADMIUM PLATED.
NAS6204C10	=	BOLT, .2500-28 THREAD, .625 GRIP, UNDRILLED, NONLOCKING, CHROMIUM PLATED.

NOTES:

/1/ GRIP LENGTH: FROM UNDER SIDE OF HEAD TO END OF FULL CYLINDRICAL PORTION OF SHANK.

/2/ REFERENCE DIMENSIONS ARE FOR DESIGN PURPOSES ONLY AND ARE NOT AN INSPECTION REQUIREMENT.

/3/ BEARING SURFACE SQUARENESS: WITHIN .003 FIM OF "ØD".

/4/ CONCENTRICITY: "ØD" AND MAJOR THREAD DIA WITHIN "AA" VALUES FIM. "ØD" AND "ØE" WITHIN "CC" VALUES FIM.

/5/ SHANK STRAIGHTNESS: WITHIN "BB" VALUES FIM PER INCH OF LENGTH.

/6/ PROTRUSION OF LOCKING ELEMENT SHALL BE CONTROLLED SO THAT IT WILL PASS FREELY, OR WITH FINGER PRESSURE, THROUGH A RING GAGE WITH DIAMETER OF .010 (+.001, -.000) GREATER THAN MAXIMUM MAJOR DIAMETER OF BOLT THREAD.

/7/ "X" MIN (5 THREAD PITCHES) = REGION OF MINIMUM ENGAGEMENT WITH INTERNAL THREAD REQUIRED TO MEET MIL-DTL-18240 REQUIREMENTS. LOCKING ELEMENT WITHIN "X" REGION MUST DEVELOP REQUIRED TORQUE WHEN TESTED PER MIL-DTL-18240.

/8/ FOR EASE IN STARTING, LOCKING ELEMENT SHALL NOT BE EFFECTIVE IN "Y" AREA (3 THREAD PITCHES).

/9/ "ØP" HOLE CENTERLINE WITHIN .010 AND NORMAL WITHIN 2° OF BOLT CENTERLINE.

/10/ "ØE" MAX NOT TO EXCEED ACTUAL WIDTH ACROSS FLATS; MIN AS TABULATED IN TABLE I.

~~(11) PLATING THICKNESS MINIMUM TO BE .0003 PER AMS-QQ-P-416, CLASS 2.~~

/12/ IF REQUIRED, TENSILE TESTING OF BOLTS REQUIRING CROSS-DRILLED THREADS SHALL BE PERFORMED PRIOR TO DRILLING AND THE APPLICATION OF PLATING AND/OR COATINGS. WHEN BOLTS HAVE BEEN DRILLED, STRENGTH MAY BE VERIFIED BY SHEAR TESTING, IN LIEU OF TENSILE TESTING, IN ACCORDANCE WITH NASM1312. USERS SHOULD BE AWARE THAT FASTENERS WITH CROSS-DRILLED THREADS MAY EXHIBIT A REDUCTION IN TENSILE STRENGTH.

/13/ HEAD MARKING: BASIC NUMBER PLUS GRIP DASH NUMBER PLUS "D", "L", OR "P", WHEN APPLICABLE, PLUS MANUFACTURER'S SYMBOL, RAISED OR DEPRESSED .010 MAX. ARRANGEMENT OPTIONAL.
"D" IDENTIFIES BOLT WITH DRILLED THREAD.
"L" IDENTIFIES BOLT WITH LOCKING ELEMENT (OPTIONAL TYPE).
"P" IDENTIFIES BOLT WITH PATCH TYPE LOCKING ELEMENT ONLY.
"C", CHROMIUM PLATED CODE NEED NOT APPEAR ON BOLT HEAD.

(14) SURFACE ROUGHNESS: "ØD", BEARING SURFACE OF HEAD, THREAD FLANKS AND THREAD ROOT: 32 MICROINCHES Ra; ALL OTHER SURFACES: 125 MICROINCHES Ra PER ASME B46.1.

/15/ INTERMEDIATE OR LONGER LENGTHS MAY BE SPECIFIED BY THE USE OF WHOLE GRIP DASH NUMBERS ONLY. NOMINAL LENGTH EQUALS NOMINAL GRIP PLUS "T".

(16) DIMENSIONING AND TOLERANCING PER ANSI Y14.5M-1982.

/17/ LOCKWIRE HOLES SHALL BE DRILLED WITHIN .010 OF CENTER OF HEX FLAT WHEN SPECIFIED BY PART NUMBER.

(18) DIMENSIONS IN INCHES AND APPLY AFTER FINISH UNLESS OTHERWISE SPECIFIED.

(19) REMOVE ALL BURRS AND SHARP EDGES.

(20) THIS STANDARD TAKES PRECEDENCE OVER DOCUMENTS REFERENCED HEREIN.

(21) UNLESS OTHERWISE SPECIFIED HEREIN, REFERENCED DOCUMENTS SHALL BE THE ISSUE IN EFFECT ON DATE OF MANUFACTURE. HOWEVER, EXISTING MATERIAL INVENTORY CERTIFIED TO A PREVIOUS REVISION OF THE APPLICABLE MATERIAL SPECIFICATION(S) IS ACCEPTABLE FOR USE UNTIL DEPLETION.

(22) UNLESS OTHERWISE SPECIFIED, PART INVENTORY MANUFACTURED TO PREVIOUS REVISIONS OF THE APPLICABLE DRAWING OR SPECIFICATION MAY BE PROCURED AND USED UNTIL STOCK IS DEPLETED.

PROCUREMENT SPECIFICATION:

NAS4002, EXCEPT AS NOTED. COLD WORK OF HEAD TO SHANK FILLET RADIUS AND FATIGUE TESTING ARE NOT REQUIRED FOR NAS6203 BOLTS. LOCKING ELEMENT FOR SELF-LOCKING BOLTS: PER NASM15981 AND MIL-DTL-18240. LOCKING ELEMENT TYPE, INCLUDING PATCH TYPE, IS OPTIONAL WHEN "L" CODE IS SPECIFIED. PATCH TYPE LOCKING ELEMENT (WITH NO METAL REMOVED) IS REQUIRED WHEN "P" CODE IS SPECIFIED. LOCKING ELEMENT MUST BE SUPPLIED BY A QUALIFIED SOURCE LISTED IN QPL-18240 OR APPROVED FOR LISTING IN QPL-18240. SHIPPING NOTICE SHOULD IDENTIFY SUPPLIER OF BOLT AND LOCKING ELEMENT SEPARATELY.

TABLE II – GRIP AND LENGTH DIMENSIONS

GRIP DASH NO.	GRIP ±.010	LENGTH ± .015 /15/												
		BASIC NUMBER AND THREAD SIZE												
		NAS6203	NAS6204	NAS6205	NAS6206	NAS6207	NAS6208	NAS6209	NAS6210	NAS6212	NAS6214	NAS6216	NAS6218	NAS6220
		.1900-32	.2500-28	.3125-24	.3750-24	.4375-20	.5000-20	.5625-18	.6250-18	.7500-16	.8750-14	1.0000-12	1.1250-12	1.2500-12
1	.062	.385	.432	.500	.516	.590	.590	.656	.688	.728	.821	.957	1.051	1.145
2	.125	.448	.495	.563	.579	.653	.653	.719	.751	.791	.884	1.020	1.114	1.208
3	.188	.511	.558	.626	.642	.716	.716	.782	.814	.854	.947	1.083	1.177	1.271
4	.250	.573	.620	.688	.704	.778	.778	.844	.876	.916	1.009	1.145	1.239	1.333
5	.312	.635	.682	.750	.766	.840	.840	.906	.938	.978	1.071	1.207	1.301	1.395
6	.375	.698	.745	.813	.829	.903	.903	.969	1.001	1.041	1.134	1.270	1.364	1.458
7	.438	.761	.808	.876	.892	.966	.966	1.032	1.064	1.104	1.197	1.333	1.427	1.521
8	.500	.823	.870	.938	.954	1.028	1.028	1.094	1.126	1.166	1.259	1.395	1.489	1.583
9	.562	.885	.932	1.000	1.016	1.090	1.090	1.156	1.188	1.228	1.321	1.457	1.551	1.645
10	.625	.948	.995	1.063	1.079	1.153	1.153	1.219	1.251	1.291	1.384	1.520	1.614	1.708
11	.688	1.011	1.058	1.126	1.142	1.216	1.216	1.282	1.314	1.354	1.447	1.583	1.677	1.771
12	.750	1.073	1.120	1.188	1.204	1.278	1.278	1.344	1.376	1.416	1.509	1.645	1.739	1.833
13	.812	1.135	1.182	1.250	1.266	1.340	1.340	1.406	1.438	1.478	1.571	1.707	1.801	1.895
14	.875	1.198	1.245	1.313	1.329	1.403	1.403	1.469	1.501	1.541	1.634	1.770	1.864	1.958
15	.938	1.261	1.308	1.376	1.392	1.466	1.466	1.532	1.564	1.604	1.697	1.833	1.927	2.021
16	1.000	1.323	1.370	1.438	1.454	1.528	1.528	1.594	1.626	1.666	1.759	1.895	1.989	2.083
17	1.062	1.385	1.432	1.500	1.516	1.590	1.590	1.656	1.688	1.728	1.821	1.957	2.051	2.145
18	1.125	1.448	1.495	1.563	1.579	1.653	1.653	1.719	1.751	1.791	1.884	2.020	2.114	2.208
19	1.188	1.511	1.558	1.626	1.642	1.716	1.716	1.782	1.814	1.854	1.947	2.083	2.177	2.271
20	1.250	1.573	1.620	1.688	1.704	1.778	1.778	1.844	1.876	1.916	2.009	2.145	2.239	2.333
21	1.312	1.635	1.682	1.750	1.766	1.840	1.840	1.906	1.938	1.978	2.071	2.207	2.301	2.395
22	1.375	1.698	1.745	1.813	1.829	1.903	1.903	1.969	2.001	2.041	2.134	2.270	2.364	2.458
23	1.438	1.761	1.808	1.876	1.892	1.966	1.966	2.032	2.064	2.104	2.197	2.333	2.427	2.521
24	1.500	1.823	1.870	1.938	1.954	2.028	2.028	2.094	2.126	2.166	2.259	2.395	2.489	2.583
25	1.562	1.885	1.932	2.000	2.016	2.090	2.090	2.156	2.188	2.228	2.321	2.457	2.551	2.645
26	1.625	1.948	1.995	2.063	2.079	2.153	2.153	2.219	2.251	2.291	2.384	2.520	2.614	2.708
27	1.688	2.011	2.058	2.126	2.142	2.216	2.216	2.282	2.314	2.354	2.447	2.583	2.677	2.771
28	1.750	2.073	2.120	2.188	2.204	2.278	2.278	2.344	2.376	2.416	2.509	2.645	2.739	2.833
29	1.812	2.135	2.182	2.250	2.266	2.340	2.340	2.406	2.438	2.478	2.571	2.707	2.801	2.895
30	1.875	2.198	2.245	2.313	2.329	2.403	2.403	2.469	2.501	2.541	2.634	2.770	2.864	2.958
31	1.938	2.261	2.308	2.376	2.392	2.466	2.466	2.532	2.564	2.604	2.697	2.833	2.927	3.021
32	2.000	2.323	2.370	2.438	2.454	2.528	2.528	2.594	2.626	2.666	2.759	2.895	2.989	3.083
34	2.125	2.448	2.495	2.563	2.579	2.653	2.653	2.719	2.751	2.791	2.884	3.020	3.114	3.208
36	2.250	2.573	2.620	2.688	2.704	2.778	2.778	2.844	2.876	2.916	3.009	3.145	3.239	3.333

TABLE II – GRIP AND LENGTH DIMENSIONS (CONTINUED)

GRIP DASH NO.	GRIP ±.010	LENGTH ± .015 /15/												
		BASIC NUMBER AND THREAD SIZE												
		NAS6203	NAS6204	NAS6205	NAS6206	NAS6207	NAS6208	NAS6209	NAS6210	NAS6212	NAS6214	NAS6216	NAS6218	NAS6220
		.1900-32	.2500-28	.3125-24	.3750-24	.4375-20	.5000-20	.5625-18	.6250-18	.7500-16	.8750-14	1.0000-12	1.1250-12	1.2500-12
38	2.375	2.698	2.745	2.813	2.829	2.903	2.903	2.969	3.001	3.041	3.134	3.270	3.364	3.458
40	2.500	2.823	2.870	2.938	2.954	3.028	3.028	3.094	3.126	3.166	3.259	3.395	3.489	3.583
42	2.625	2.948	2.995	3.063	3.079	3.153	3.153	3.219	3.251	3.291	3.384	3.520	3.614	3.708
44	2.750	3.073	3.120	3.188	3.204	3.278	3.278	3.344	3.376	3.416	3.509	3.645	3.739	3.833
46	2.875	3.198	3.245	3.313	3.329	3.403	3.403	3.469	3.501	3.541	3.634	3.770	3.864	3.958
48	3.000	3.323	3.370	3.438	3.454	3.528	3.528	3.594	3.626	3.666	3.759	3.895	3.989	4.083
50	3.125	3.448	3.495	3.563	3.579	3.653	3.653	3.719	3.751	3.791	3.884	4.020	4.114	4.208
52	3.250	3.573	3.620	3.688	3.704	3.778	3.778	3.844	3.876	3.916	4.009	4.145	4.239	4.333
54	3.375	3.698	3.745	3.813	3.829	3.903	3.903	3.969	4.001	4.041	4.134	4.270	4.364	4.458
56	3.500	3.823	3.870	3.938	3.954	4.028	4.028	4.094	4.126	4.166	4.259	4.395	4.489	4.583
58	3.625	3.948	3.995	4.063	4.079	4.153	4.153	4.219	4.251	4.291	4.384	4.520	4.614	4.708
60	3.750	4.073	4.120	4.188	4.204	4.278	4.278	4.344	4.376	4.416	4.509	4.645	4.739	4.833
62	3.875	4.198	4.245	4.313	4.329	4.403	4.403	4.469	4.501	4.541	4.634	4.770	4.864	4.958
64	4.000	4.323	4.370	4.438	4.454	4.528	4.528	4.594	4.626	4.666	4.759	4.895	4.989	5.083
66	4.125	4.448	4.495	4.563	4.579	4.653	4.653	4.719	4.751	4.791	4.884	5.020	5.114	5.208
68	4.250	4.573	4.620	4.688	4.704	4.778	4.778	4.844	4.876	4.916	5.009	5.145	5.239	5.333
70	4.375	4.698	4.745	4.813	4.829	4.903	4.903	4.969	5.001	5.041	5.134	5.270	5.364	5.458
72	4.500	4.823	4.870	4.938	4.954	5.028	5.028	5.094	5.126	5.166	5.259	5.395	5.489	5.583
74	4.625	4.948	4.995	5.063	5.079	5.153	5.153	5.219	5.251	5.291	5.384	5.520	5.614	5.708
76	4.750	5.073	5.120	5.188	5.204	5.278	5.278	5.344	5.376	5.416	5.509	5.645	5.739	5.833
78	4.875	5.198	5.245	5.313	5.329	5.403	5.403	5.469	5.501	5.541	5.634	5.770	5.864	5.958
80	5.000	5.323	5.370	5.438	5.454	5.528	5.528	5.594	5.626	5.666	5.759	5.895	5.989	6.083
82	5.125	5.448	5.495	5.563	5.579	5.653	5.653	5.719	5.751	5.791	5.884	6.020	6.114	6.208
84	5.250	5.573	5.620	5.688	5.704	5.778	5.778	5.844	5.876	5.916	6.009	6.145	6.239	6.333
86	5.375	5.698	5.745	5.813	5.829	5.903	5.903	5.969	6.001	6.041	6.134	6.270	6.364	6.458
88	5.500	5.823	5.870	5.938	5.954	6.028	6.028	6.094	6.126	6.166	6.259	6.395	6.489	6.583
90	5.625	5.948	5.995	6.063	6.079	6.153	6.153	6.219	6.251	6.291	6.384	6.520	6.614	6.708
92	5.750	6.073	6.120	6.188	6.204	6.278	6.278	6.344	6.376	6.416	6.509	6.645	6.739	6.833
94	5.875	6.198	6.245	6.313	6.329	6.403	6.403	6.469	6.501	6.541	6.634	6.770	6.864	6.958
96	6.000	6.323	6.370	6.438	6.454	6.528	6.528	6.594	6.626	6.666	6.759	6.895	6.989	7.083

RESTRICTED USAGE: FOR REPAIR WORK ONLY

.0156 AND .0312 OVERSIZE SHANK FOR REPLACEMENT OF BOLTS SHOWN ON SHEET 1

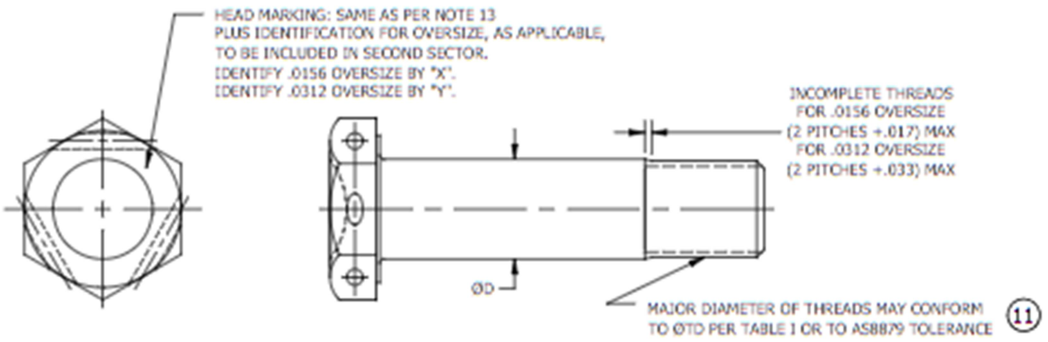

FIGURE 2 – OVERSIZE BOLT CONFIGURATION

(SEE SHEETS 1 THRU 6 FOR MATERIAL, FINISH, PROCUREMENT INFORMATION AND DIMENSIONS NOT SHOWN.)

TABLE III – OVERSIZE PART NUMBERS AND DIMENSIONS

PART NUMBER EXAMPLES (FOR PLATED, NONLOCKING, UNDRILLED THREAD)		NOMINAL THREAD SIZE	ØD .0156 OVERSIZE SHANK	
DRILLED HEAD	UNDRILLED HEAD		MAX	MIN
NAS6203-*HX	NAS6203-*X	.1900-32	.2026	.2016
NAS6204-*HX	NAS6204-*X	.2500-28	.2651	.2641
NAS6205-*HX	NAS6205-*X	.3125-24	.3276	.3266
NAS6206-*HX	NAS6206-*X	.3750-24	.3901	.3891
NAS6207-*HX	NAS6207-*X	.4375-20	.4526	.4516
NAS6208-*HX	NAS6208-*X	.5000-20	.5151	.5141
NAS6209-*HX	NAS6209-*X	.5625-18	.5771	.5761
NAS6210-*HX	NAS6210-*X	.6250-18	.6396	.6386
NAS6212-*HX	NAS6212-*X	.7500-16	.7646	.7636
NAS6214-*HX	NAS6214-*X	.8750-14	.8896	.8886
NAS6216-*HX	NAS6216-*X	1.0000-12	1.0146	1.0136
NAS6218-*HX	NAS6218-*X	1.1250-12	1.1396	1.1381
NAS6220-*HX	NAS6220-*X	1.2500-12	1.2646	1.2631
			ØD .0312 OVERSIZE SHANK	
NAS6203-*HY	NAS6203-*Y	.1900-32	.2182	.2172
NAS6204-*HY	NAS6204-*Y	.2500-28	.2807	.2797
NAS6205-*HY	NAS6205-*Y	.3125-24	.3432	.3422
NAS6206-*HY	NAS6206-*Y	.3750-24	.4057	.4047
NAS6207-*HY	NAS6207-*Y	.4375-20	.4682	.4672
NAS6208-*HY	NAS6208-*Y	.5000-20	.5307	.5297
NAS6209-*HY	NAS6209-*Y	.5625-18	.5927	.5917
NAS6210-*HY	NAS6210-*Y	.6250-18	.6552	.6542
NAS6212-*HY	NAS6212-*Y	.7500-16	.7802	.7792
NAS6214-*HY	NAS6214-*Y	.8750-14	.9052	.9042
NAS6216-*HY	NAS6216-*Y	1.0000-12	1.0302	1.0292
NAS6218-*HY	NAS6218-*Y	1.1250-12	1.1552	1.1537
NAS6220-*HY	NAS6220-*Y	1.2500-12	1.2802	1.2787

* = GRIP DASH NUMBER IN .0625 INCREMENTS.

FACULTY OF ENGINEERING TECHNOLOGY
CAMPUS GROUP T
Andreas Vesaliusstraat 13
3000 LEUVEN, Belgium
tel. + 32 16 30 10 30
iiw.groept@kuleuven.be
iiw.kuleuven.be